Epoxidation of vegetable oils – Process intensification for biomass conversion

Adriana Samantha Freites Aguilera

Laboratory of Industrial Chemistry and Reaction Engineering
Faculty of Science and Engineering / Chemical Engineering
Åbo Akademi University

2019

Adriana Samantha Freites Aguilera

Born 1992, Caracas Venezuela

M. Sc. Chemical Engineering 2015

Universidad Simón Bolívar, Sartenejas, Caracas, Venezuela.

Epoxidation of vegetable oils – process intensification for biomass conversion

Adriana Samantha Freites Aguilera

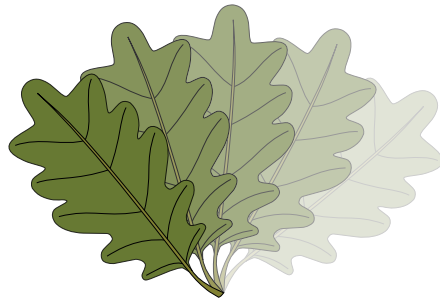

Laboratory of Industrial Chemistry and Reaction Engineering
Johan Gadolin Process Chemistry Centre
Faculty of Science and Engineering / Chemical Engineering
Åbo Akademi University
2019

Supervised by

Academy Professor Tapio O. Salmi
Laboratory of Industrial Chemistry and Reaction Engineering
Johan Gadolin Process Chemistry Centre
Åbo Akademi University
Åbo/Turku, Finland

Docent Pasi Tolvanen
Laboratory of Industrial Chemistry and Reaction Engineering
Johan Gadolin Process Chemistry Centre
Åbo Akademi University
Åbo/Turku, Finland

Professor Sébastien Leveneur
Laboratoire de Sécurité des Procédés Chimiques
Institut National des Sciences Appliquées de Rouen
Normandie Université
Rouen, France

Reviewers

Directrice de recherche Dr Carine Julcour
Laboratoire de Génie Chimique
CNRS
Université de Toulouse
Toulouse, France

Dr Esko Tirronen
Espoo, Finland

Faculty opponent

Dr Carine Julcour
Laboratoire de Génie Chimique
CNRS
Université de Toulouse
Toulouse, France

ISBN 978-952-12-3894-9 (printed version)/ ISBN 978-952-12-3895-6 (electronic version)
ISSN 2669-8315 (*Acta technologiae chemicae Aboensia 2019 A/2*)

Painosalama Oy Turku/Åbo 2019

A mi madre

“My momma always said, ‘Life is like a box of chocolate.
You never know what you’re gonna get’ ”

-Forrest Gump

Preface

Sitting in front of a blank page, I cannot put into words the feelings I have when I think of these past years in Finland. Coming from Venezuela to Finland was a big shock at the beginning. Years later I still feel as grateful and marvelled as I was in the first day I arrived, maybe even more. Living in Turku has given me countless lessons and opportunities that have changed my life, and for that, I will always be grateful. The completion of this thesis has been possible thanks to many people in my life.

Professor Tapio Salmi is the first person I think of when it comes to the realization of my PhD. Professor Tapio has not only 'given me the opportunity to work at Åbo Akademi' but he has also given me a lot more. I am grateful for he has shared so much knowledge, creativity and kindness with me. I must say I am very privileged to have him as a professor, colleague and friend. A day at the lab is never boring when Tapio is around.

I would like to thank Professor Dmitry Murzin as well for always offering the very best scientific advice and inspiring lectures. Dmitry is an example on how high-level research and teaching is done. He has always encouraged us to strive for the very best. Having him in the laboratory is a privilege, too.

Then, someone who has been a fundamental part of my research is Docent Kari Eränen. No doubt the completion of my PhD wouldn't have been possible without his help. Kari helped me with my reactor setup and basically everything that had to do with my work at the lab. Kari has the ability to solve any problem in the most efficient way. Everybody knows that Kari is the most essential member of the lab.

Docent Pasi Tolvanen has been working with me as my closest supervisor in an everyday basis and I cannot thank him enough for all his advice and support since the first day I came to the lab for my master thesis. Besides, Pasi has been a great friend to me and he has made my life in Turku easier. Because of him I never had to learn Finnish.

The supervision of Professor Sébastien Leveneur during these years is greatly appreciated as well as the help of Professor Johan Wärnå in the mathematical modelling. I would also like to thank Professor Timothy Marchant for his supervision during my time in Wollongong.

The environment in the lab was always fantastic and I was honoured to have shared this time with my friends and co-workers. Erfan, Mauricio, Ricardo, Alexey, Cesar, Wander, Cai, Lu, Andrea, Shuyana, Ekaterina, Zuzana, Jussi, Nemanja, Moldir, Anton, Stephanie, Lidia, Imane, Atte, Ole, Pelle, Maria, Sebastien, Ananias and my dearest Soudabeh, Thank you. To Javi, gràcies per tant.

Last but not least, my family. Everything I am today is because of them. Mis hermanos Gonzalo, Virgnia, Raul y Daniel, mi madrina Sonia, mi Momi e Indira siempre han estado para mí y los tengo presentes todos los días. Mariana, Daniela y Edda son lo más importante para mí y les agradezco su apoyo incondicional. Doy gracias a la vida por tenerlos.

Abstract

Epoxidation of vegetable oils – process intensification for biomass conversion

Adriana Samantha Freites Aguilera

Oils extracted from plants, algae, seeds and wood are one of the vast biomass resources which can be used to elaborate a wide range of products. Tall oil obtained from forest biomass is a good source of vegetable oils, because it is a non-edible by-product of Kraft pulping process and it represents an abundant feedstock, particularly in Nordic countries. Epoxidized vegetable oils and fatty acids are used for developing PVC-derived plastic-ware and as intermediates for the synthesis of biolubricants, polyols, glycols, olefinic compounds and stabilizers for polymers. In other words, epoxidized vegetable oils are green platforms by excellence for the development of products and present an alternative to its derivation from non-renewable fossil resources.

This work has focused on the study of the Prilezhaev epoxidation of plant oils as a green process, since it uses renewable raw materials and produces biodegradable products through a non-toxic synthesis route. An important aspect of this thesis was the application of process intensification in the form of microwave irradiation, heterogeneous catalysis and new mixing technology (a rotating bed reactor) for a more energy-efficient process with higher product yields, compared to more conventional approaches.

The reaction was executed by peracetic acid formed in situ from acetic acid and hydrogen peroxide. Epoxidation of oleic acid as a model compound and tall oil mixtures was performed in a batch loop reactor. The core of the reactor system was a vigorously stirred tank which was coupled to a loop with a microwave cavity and a heat exchanger. The microwave effect was compared with the results obtained with conventional heating. The reactor system was equipped with a special mixing device (Spinchem^{TM}), which allowed to immobilize solid resin catalysts and to minimize mass transfer limitations of the oil-aqueous-solid system. An extensive series of kinetic experiments was carried out in the presence and absence of microwave irradiation and heterogeneous catalysts. Typical reaction temperatures were 40-70°C. From the separated aqueous and organic phases, the concentrations of acetic acid, hydrogen peroxide, peracetic acid as well as double bonds in the reactant oil and epoxidized oil were determined by titrimetric analysis. The kinetics of ring opening reactions was studied separately and some of the ring opening products were identified by NMR analysis.

The results showed that an increased temperature, as well as higher concentrations of acetic acid and hydrogen peroxide accelerated both the epoxidation and the ring opening processes. The epoxidation of oleic acid occurs spontaneously in the absence of the catalyst, but the reaction yield can be considerably improved by exposing the system to microwave irradiation and incorporating a solid catalyst. Several heterogeneous catalysts were screened to find the highest performance. However, the microwave effect was not visible in the presence of heterogeneous catalysts and microwave irradiation showed to be detrimental for the yields of tall oil epoxidation.

Detailed mathematical modelling of the multiphase system was carried out, starting from first principles. Detailed kinetic models based on reaction mechanisms were derived and the model parameters were estimated by non-linear regression analysis. The models for epoxidation with conventional heating and microwave irradiation in the presence and absence of a solid catalyst had a good correspondence between the experimental and calculated concentrations of the reaction components. The rate constants and activation energies for the perhydrolysis, epoxidation and ring opening reactions were obtained as a result of the parameter estimation.

Resumen

Epoxidación de aceites vegetales – intensificación de procesos para la conversión de biomasa

Adriana Samantha Freites Aguilera

Los aceites extraídos de plantas, algas, semillas y madera son un importante recurso natural que puede ser utilizado para la elaboración de una amplia gama de derivados químicos. Por ejemplo, los aceites vegetales obtenidos partir de la madera de pino son un subproducto particularmente abundante en los países nórdicos y representan un buen candidato para su valorización mediante el desarrollo de procesos eco-responsables. Los aceites vegetales y ácidos grasos epoxidados se pueden utilizar para desarrollar productos plásticos, así como intermediarios para la síntesis de biolubricantes, polioles, glicoles, compuestos olefínicos y estabilizadores para polímeros. En resumen, los aceites vegetales epoxidados son una excelente alternativa verde para el desarrollo de productos que convencionalmente se producen a partir de derivados fósiles no renovables.

Esta tesis se centra en el estudio de la epoxidación de aceites vegetales con el método de Prilezhaev como un proceso verde, ya que utiliza materia prima renovable, produciendo únicamente productos biodegradables a través de una ruta de síntesis no tóxica. Un aspecto importante de esta tesis fue la aplicación de intensificación de procesos en forma de microondas, catálisis heterogénea y una nueva tecnología de agitación (un reactor de lecho giratorio), dando lugar a un proceso más eficaz en términos de rendimientos de producto y eficiencia energética, en comparación con enfoques más convencionales.

La reacción se ejecutó con ácido peracético formado *in situ* a partir de ácido acético y peróxido de hidrógeno. La epoxidación de ácido oleico como compuesto modelo y de mezclas de aceites de pino se realizó en un reactor batch acoplado a un bucle de reciclo. El reactor consiste en un tanque agitado, conectado a un circuito compuesto por una cavidad de microondas y un intercambiador de calor. El efecto de las microondas se comparó con los resultados obtenidos con calentamiento convencional. El sistema está equipado con una tecnología de agitación llamada Spinchem^{TM}, que permite inmovilizar catalizadores de resina sólidos y minimizar las limitaciones de transferencia de masa del sistema sólido-líquido-líquido. Una extensa serie de experimentos cinéticos se llevó a cabo en presencia y ausencia de microondas y catalizadores heterogéneos. El efecto de la temperatura se estudió en el rango de los 40-70°C. A partir de las fases acuosa y orgánica previamente separadas, las concentraciones de ácido acético, peróxido de hidrógeno, ácido peracético, dobles enlaces en el aceite y aceite epoxidado se determinaron mediante titración. La cinética de las reacciones de apertura del anillo se estudió por separado y algunos de los productos de estas reacciones se identificaron mediante análisis de RMN.

Los resultados mostraron que tanto un aumento de la temperatura, así como mayores concentraciones de ácido acético y peróxido de hidrógeno aceleran la epoxidación y los procesos de apertura del anillo. La epoxidación del ácido oleico se produce espontáneamente en ausencia de catalizador, pero el rendimiento de la reacción puede mejorarse considerablemente exponiendo el sistema a radiación de microondas y/o incorporando un catalizador sólido. Varios catalizadores heterogéneos fueron estudiados para encontrar el más adecuado en base a los rendimientos obtenidos. En este caso, no se observó ninguna influencia de la radiación con microondas en la reacción en términos de conversión. Al contrario, la irradiación de microondas demostró ser perjudicial para los rendimientos en la epoxidación de aceite de pino a causa de un incremento en la velocidad de degradación de estos productos.

Se realizó un modelado matemático detallado del sistema multifásico, a partir de principios básicos. Se obtuvieron modelos cinéticos rigurosos basados en los mecanismos de reacción. Los parámetros del modelo se estimaron mediante un análisis de regresión no lineal. Los modelos para epoxidación con calentamiento convencional e irradiación de microondas en presencia y ausencia de catalizador sólido mostraron una buena correspondencia entre las concentraciones experimentales de los componentes de reacción y las calculadas. A partir de estos modelos se obtuvieron las constantes de velocidad de reacción y las energías de activación para las reacciones de perhidrólisis, epoxidación y apertura del anillo.

Referat

Epoxidering av vegetabiliska oljor – processintensifiering för omvandling av biomassa

Adriana Samantha Freites Aguilera

Oljor som extraheras från växter, alger, frön och trä är en enorm biomassaresurs som kan användas för att utarbeta ett brett sortiment av produkter. Tallolja som utvinns från skogsbiomassa är en utmärkt källa för vegetabiliska oljor, eftersom den är en icke-ätbar biprodukt av Kraftprocessen i cellulosakok och den är ett rikligt förekommande råmaterial särskilt i Norden. Epoxiderade vegetabiliska oljor och fettsyror används för att tillverka PVC-baserade plastvaror, såväl som mellanprodukter för syntes av biosmörjmedel, polyoler, glykoler, olefiniska föreningar och stabilisatorer för polymerer. Med andra ord utgör epoxiderade vegetabiliska oljor en utmärkt grön plattform för utveckling av produkter som konventionellt är tillverkade av fossila råvaror.

Detta arbete fokuserade på studier av Prilezhaevs epoxidering av växtoljor som en grön process, eftersom den utnyttjar förnyelsebara råvaror och producerar biologiskt nedbrytbara produkter genom en icke-toxisk syntesväg. En viktig aspekt av denna avhandling var tillämpning av processintensifiering i form av mikrovågsbestrålning, heterogen katalys och ny omblandningsteknologi (en roterande bäddreaktor) för en mer energieffektiv process med högre produktutbyten jämfört med konventionella metoder.

Reaktionen genomfördes med perättiksyra som bildades in situ från ättiksyra och väteperoxid. Epoxidering av oljesyra som modellförening och talloljeblandningar utfördes i en tankreaktor med återcirkulation. Kärnan av reaktorsystemet utgjordes av en omrörd tank som kopplades till ett återcirkulationssystem som bestod av en rörlinje, en mikrovågstunnel och en värmeväxlare. Mikrovågseffekten jämfördes med de resultat som erhölls med konventionell uppvärmning. Reaktorsystemet var utrustat med en speciell omblandningsteknologi (Spinchem^{TM}), som gjorde det möjligt att immobilisera fasta katalysatorpartiklar och minska massöverföringsbegränsningarna för olja-vatten-fastfassystemet. En omfattande serie av kinetiska experiment genomfördes i närvaro och frånvaro av mikrovågsbestrålning och heterogena katalysatorer. Typiska reaktionstemperaturer var 40-70 °C. Från de separerade vattenhaltiga och organiska faserna bestämdes koncentrationerna av ättiksyra, väteperoxid, perättiksyra, dubbelbindningar i reaktantoljan och epoxiderad olja genom titrimetrisk analys. Kinetiken för ringöppningsreaktionerna studerades separat och några av ringöppningsprodukterna identifierades med NMR-analys.

Resultaten visade att en ökad temperatur såväl som högre koncentrationer av ättiksyra och väteperoxid påskyndade både epoxidations- och ringöppningsprocesserna. Epoxideringen av oljesyra sker spontant i frånvaro av katalysator, men reaktionsutbytet kan avsevärt förbättras genom att utsätta systemet för mikrovågsbestrålning och/eller inkorporera en fast katalysator. Några heterogena katalysatorer kartlades för att uppnå den bästa möjliga prestanda. Mikrovågseffekten var dock inte synlig i närvaro av heterogena katalysatorer. Dessutom visade sig mikrovågsbestrålningen vara skadlig för produktutbyten vid epoxidering av tallolja.

Detaljerad matematisk modellering av flerfassystemet genomfördes utgående från grundläggande principer. Detaljerade kinetiska modeller baserade på reaktionsmekanismer härleddes och modellparametrarna estimerades med hjälp av icke-linjär regressionsanalys. Modellerna för epoxidering med konventionell uppvärmning och mikrovågsuppvärmning i närvaro och frånvaro av en fast katalysator visade en god överensstämmelse mellan experimentella och beräknade koncentrationer av

reaktionskomponenterna. Numeriska värden på hastighetskonstanterna och aktiveringsenergierna för perhydrolys, epoxidering och ringöppningsreaktioner erhölls som resultat av parameterestimeringen.

List of publications

I. **Freites Aguilera, A.**, Tolvanen, P., Sifontes Herrera, V., Tourvielle, J.-N., Leveneur, S., Salmi, T., Reaction intensification by microwave and ultrasound techniques in chemical multiphase systems, *Process synthesis and Process Intensification – Methodological Approaches* (Ben Guang-Rong, ed.), Chapter 3, (2017) 111-138 (De Gruyter, ISBN 978-3-11-046505-1)

II. **Freites Aguilera, A.**, Tolvanen, P., Eränen, K., Leveneur, S., Salmi, T., Epoxidation of oleic acid under conventional heating and microwave radiation, *Chemical Engineering and Processing* 102 (2016) 70-87.

III. **Freites Aguilera, A.**, Tolvanen, P., Heredia, S., González Munoz, M., Samson, T., Oger, A., Verove, A., Eränen, K., Leveneur, S., Mikkola, J.-P., Salmi, T., Epoxidation of fatty acids and vegetable oils assisted by microwaves catalyzed by a cation exchange resin, *Industrial and Engineering Chemistry Research* 57 (2018) 3876-3886.

IV. **Freites Aguilera, A.**, Tolvanen, P., Oger, A., Eränen, K., Leveneur, S., Mikkola, J.-P., Salmi, T., Screening of ion exchange resin catalysts for epoxidation of oleic acid under the influence of conventional and microwave heating, *Journal of Chemical Technology and Biotechnology* 94 (2019) 3020-3031.

V. **Freites Aguilera, A.**, Tolvanen, P., Eränen, K., Wärnå, J., Leveneur, S., Marchant, T., Salmi, T., Kinetic modelling of Prileschajew epoxidation of oleic acid under conventional heating and microwave irradiation, *Chemical Engineering Science* 199 (2019) 426-438.

VI. **Freites Aguilera, A.**, Tolvanen, P., Wärnå, J., Leveneur, S., Salmi, T., Kinetics and reactor modelling of fatty acid epoxidation in the presence of heterogeneous catalyst, *Chemical Engineering Journal* 375 (2019) 121936.

VII. **Freites Aguilera, A.**, Rahkila, J., Nurmi, M., Hemming, J., Tolvanen, P., Torres, G., Eränen, K. Leveneur, S., Salmi, T., Epoxidation of tall oil catalyzed by ion exchange resin under microwave and conventional heating. *Journal of Cleaner Production* (submitted).

VIII. Cai, X., Zheng, J.-L., **Freites Aguilera, A.**, Vernières-Hassimi, L., Tolvanen, P., Salmi, T., Leveneur, S., Influence of ring opening reactions on the kinetics of bio-based cottonseed oil epoxidation, *International Journal of Chemical Kinetics* 50(10) (2018) 726-741.

Adriana Freites' contribution to articles I-VIII

I	Wrote part of the book chapter and contributed to the editing.
II, VII	Conducted the experiments and wrote the article.
III-IV	Conducted part of the experiments and wrote the article.
V	Carried out part of the modelling work and wrote the article.
VI	Carried out the modelling work and wrote the article.
VIII	Contributed in the article editing.

Conference publications related to the topic

I. **Freites Aguilera, A.**, Heredia, S., Tolvanen, P., Leveneur, S., Zheng, J. L., Samson, T., Gonzales, M., Mikkola, J.P., Salmi, T. Epoxidation and carbonation of vegetable oils to valuable platform chemicals. International Symposium on Green Chemistry, La Rochelle, France, May 2017. *Oral Presentation.*

II. **Freites Aguilera, A.**,Tolvanen, P., Heredia, S., Gonzales, M., Samson, T., Leveneur, S., Mikkola, J.P., Salmi, T. Improved Synthesis of Epoxidized Vegetable Oils Using Microwave Technology And Spinchem Rotating Bed Reactor. Royal Australian Chemical Institute National Centenary Conference, Chemeca, Melbourne, Australia, July 2017. *Oral presentation.*

III. Salmi, T., **Freites Aguilera, A.**, Tolvanen, P., Mikkola, J-P, Leveneur, S. Experimental work and modelling of catalyzed liquid-liquid reactions under conventional heating and microwave irradiation. 10th international symposium on Catalysis in Multiphase Reactors, CAMURE 10, Qingdao, P.R. China, July 2017. *Keynote lecture given by the supervisor.*

IV. **Freites Aguilera, A.**,Tolvanen, P., Heredia, S., Gonzales, M., Samson, T., Leveneur, S., Mikkola, J.P., Salmi, T. Process intensification in epoxidation of vegetable oils in the presence of heterogeneous catalysis and microwave irradiation in a superior recycled reactor system. 10th World Congress of Chemical Engineering WCCE, Barcelona, Spain. October 2017. *Oral presentation*.

V. **Freites Aguilera, A.**, Tolvanen, P., Leveneur, S., Mikkola, J.P., Marchant, T., Salmi, T. Tandem Process Intensification utilizing microwave irradiation and heterogeneous catalysis in the epoxidation of vegetable oils. International Symposium on Chemical Reaction Engineering ISCRE, Florence, Italy. May 2018. *Poster presentation.*

VI. **Freites Aguilera, A.**, Tolvanen, P., Leveneur, S., Mikkola, J.P., Marchant, T., Salmi, T. Process intensification utilizing microwave irradiation in homo-geneous and heterogeneous catalysis in the epoxidation of vegetable oils. International Symposium on Relations between Homogeneous and Heterogeneous Catalysis, Sydney, Australia. July 2018. *Oral presentation.*

VII. **Freites Aguilera, A.**, Tolvanen, P., Oger, A., Leveneur, S., Mikkola, J.P., Salmi, T. Screening of heterogeneous catalysts for microwave assisted epoxidation of vegetable oils. International Congress of Chemical and Process Engineering CHISA Prague, Czech Republic. August 2018. *Oral presentation.*

VIII. **Freites Aguilera, A.**, Tolvanen, P., Leveneur, S., Mikkola, J.P., Marchant, T., Salmi, T. Epoxidation of vegetable oils under microwave irradiation, process intensification for biomass conversion. Chemeca, Queenstown, New Zealand, October 2018. *Oral presentation.*

IX. **Freites Aguilera, A.**, Tolvanen, P., Wärnå, J., Leveneur, S., Marchant, T., Salmi, T. Kinetic modeling of a liquid-liquid reaction: epoxidation of oleic acid under conventional heating and microwave irradiation. 4th North American Symposium on Chemical Reaction Engineering, NASCRE. Houston, U.S.A. March 2019. *Oral presentation.*

X. **Freites Aguilera, A.**, Tolvanen, P., Eränen, K., Wärnå, J., Mikkola, J-P., Leveneur, S., Marchant, T., Salmi, T. Avant-garde process intensification in the production of epoxidized fatty acids and fatty acid esters. International Symposium on Green Chemistry, La Rochelle, France. *Oral Presentation.*

XI. **Freites Aguilera, A.**, Tolvanen, P., Eränen, K., Wärnå, J., Leveneur, S., Salmi, T. Intensification of fatty acid epoxidation in a loop reactor in the presence of microwave radiation and heterogeneous catalysts. 12th European Congress of Chemical Engineering, ECCE. Florence, Italy. September 2019. *Oral presentation.*

XII. **Freites Aguilera, A.**, Tolvanen, P., Leveneur, S., Salmi, T. Epoxidation of tall oil fatty acids for sustainable intermediates and bio-lubricants. 5th International Congress on Catalysis for Biorefineries, CATBIOR. Turku, Finland. September 2019. *Oral presentation.*

XIII. **Freites Aguilera, A.**, Tolvanen, P., Leveneur, S., Salmi, T., Process intensification in epoxidation of vegetable oils in the presence of heterogeneous catalysis in a superior recycled reactor system. International Conference on Unconventional Catalysis, Reactors and Applications UCRA. Zaragoza, Spain. October 2019. *Oral presentation.*

XIV. Salmi, T., **Freites Aguilera, A.**, Russo, V., Wärnå, J., Tolvanen, P., Eränen, K., Leveneur, S., Advanced modelling of fatty acid epoxidation process à la Prileschajew, International Congress of Chemical and Process Engineering CHISA Prague, Czech Republic. August 2020 (submitted)

Prize

A Flash-Poster Presentation Prize was awarded to Adriana Freites Aguilera at the Annual Meeting of the Johan Gadolin Process Chemistry Centre in November 2018.

Table of contents

1. Introduction

1.1 Biomass valorization - epoxidized plant oils

The year 2019 has been a critical one for climate change awareness. Uncountable sources point out the urgency to reduce globally the greenhouse emissions in order to prevent the rapid increase in the overall temperature of our planet. The rise of the temperature and the acidification of the oceans represent a significant threat to the ecosystem, food and water supplies, human health and the world economy.

The exploitation and refining of fossil resources as the core for energy production and feedstock for chemicals is by far the biggest greenhouse gas contributor. In sight of the latest alarming environmental concerns, it is urgent and important to shift to an economy based on ecologically responsible, efficient and sustainable processes. However, the idea of a single simple source or solution, which could be expected to completely replace oil, gas and coal, can be considered utopian. However, the combination of different technologies and sources, such as hydraulic, wind, tidal and solar power and/or biomass conversion, can lead to a feasible solution.

Biomass is the biological material extracted from living organisms, mostly plants that originate from forests, fields and oceans. Biomass is a renewable and vast resource with high energy content and an enormous potential for its chemical upgrade into valuable products. Oils extracted from plants, seeds and wood are one of the many biomass resources and it can be used to elaborate a wide range of products, from food, soaps and domestic products to lubricants and biodiesel components. According to the Statista database [1], the global production of vegetable oils has been steadily increasing for the past decades and for 2018–2019, 203.83 million metric tons of vegetable oils were produced.

Nonetheless, the production of certain plant oils can be harmful for the environment, e.g. the case of palm oil for fuel production. Palm oil is produced more than any other type of plant oil and it accounts for 36% of the overall vegetable oil production [1]. Palm oil plantations are responsible for the deforestation of large forests and the displacement of human and animal populations. For this reason, the production of certain oils must be restricted to the alimentary sector only.

On the other hand, tall oil is a non-edible by-product of the Kraft pulping process and it represents an inexpensive and domestically sourced alternative with a high potential as a renewable feedstock. The main components of tall oil are fatty acids, resin acids and neutral components. Depending on the source, tall oil comprises a mixture of fatty acids in triglyceride or free form, mainly oleic acid, linoleic acid, stearic acid as well as rosin acids. The valuable chemical components in tall oil can be refined to health-promoting components [2,3], green chemicals [4–10] and components in diesel fuels [11–14]. Particularly in the Nordic countries, tall oil fatty acids represent an abundant feedstock, because large areas of these countries have an enormous annual growing stock volume (e.g. 3.4×10^5 tons/year, Finland, 2016) [15].

A valuable platform molecule can be obtained when bio-sourced oils are subjected to epoxidation. Epoxidized plant oils can be used in the development of non-isocyanate polyurethanes, paints coatings, adhesives, surfactants, polyols, glycols, olefinic compounds and stabilizers for polymers as well as plasticizers for developing PVC-derived plastic ware [16–18]. They are also known to be excellent biodegradable lubricants [19,20]. These mentioned products are traditionally derived from non-renewable petroleum-based feedstocks.

1.2 Epoxidation methods - a brief review

The epoxidation reaction consists of the replacement of a double bond between two carbons by an oxygen atom, to form an oxirane ring, also called epoxide/epoxy group. The available known methods for epoxidation involve epoxidation with organic and inorganic peroxides, epoxidation with halohydrines, epoxidation with molecular oxygen and epoxidation with percarboxylic acids [21]. This brief review will emphasize on the epoxidation of plant oils which is the main topic of this thesis.

The most common inorganic peroxide used for the epoxidation of vegetable oils and fatty acids is hydrogen peroxide (i.e. H_2O_2). Hydrogen peroxide is fairly inexpensive and it has a high oxidative potential. Hydrogen peroxide is considered non-toxic because it decomposes into water and oxygen. However, hydrogen peroxide is a polar molecule and hence it is not miscible with non-polar oily components. This hinders the epoxidation process since mass transfer limitations might appear and solvents are usually required. Typical catalysts used for this method are metallic components, enzymes and alumina [22]. Moreover these catalysts can trigger hydrogen peroxide decomposition [23–25] or in the case of the enzymes, they can deactivate at high temperatures or high concentrations of H_2O_2[26]. For organic peroxides, moreover, transition state metal catalysts are commonly used [27,28].

Aqueous chlorine is the preferred reactant for the epoxidation with halohydrines and solvents are typically required for non-polar olefins. This process is highly toxic for the environment and it is best to be avoided [17,29].

In contrast to the methods mentioned previously, yields of epoxidation with molecular oxygen are rather low. This reaction can be carried out in the presence or absence of a catalyst. Transition metals like molybdenum, tungsten, chromium, titanium and vanadium are highly selective but have modest activity, whereas cobalt, nickel, copper, manganese, rhodium, iridium, platinum and ruthenium are more active but show less selectivity [17]. Moreover, epoxidation with molecular oxygen catalyzed by silver is the cheapest and greenest route available so far. This method leads to high yield products in case of ethylene and butadiene. However, in case of epoxidation of oils, the process is less selective to epoxide, since the oil is prone to degrade into volatile compounds with a low molecular weight such as aldehydes, ketones, and short chain dicarboxylic acids [21]. Therefore, it is not an efficient method for the epoxidation of plant oils.

Epoxidation of double bonds in vegetable oils can be carried out with percarboxylic acids. The percarboxylic acid used for the epoxidation reactions can be prepared in advance or it can be formed *in situ*. The preformed percarboxylic acid is usually prepared as a buffered equilibrium solution with its respective carboxylic acid, hydrogen peroxide and, sometimes, sulfuric acid. Subsequently the sulfuric acid is removed and the solution is added to the substrate for epoxidation [17,30]. On the other hand, in the *in situ* method, the percarboxylic acid is formed and consumed during the epoxidation reaction. This concept is considered the simplest and most common method for epoxidation of long chain olefins and vegetable oils and it is used in industrial scale [18]. The process occurs in two phases and it follows the Prilezhaev mechanism [31]. This reaction can be carried in the absence of a catalyst or in the presence of inorganic acids, acidic ion exchange resins, enzymes, metal complexes or metal oxides as catalysts. To summarize, a brief scheme on the epoxidation methods is displayed Figure 1.1.

Considering the factors discussed above, the epoxidation with percarboxylic acids has been the chosen method for the present studies in epoxidation of fatty acids and plant oils. This process was selected because of the availability of these reactants, low price, high reactivity with vegetable oils, and environmentally friendly production process [21,32]. The process follows the Prilezhaev mechanism [31] which is described with more detail in the following section.

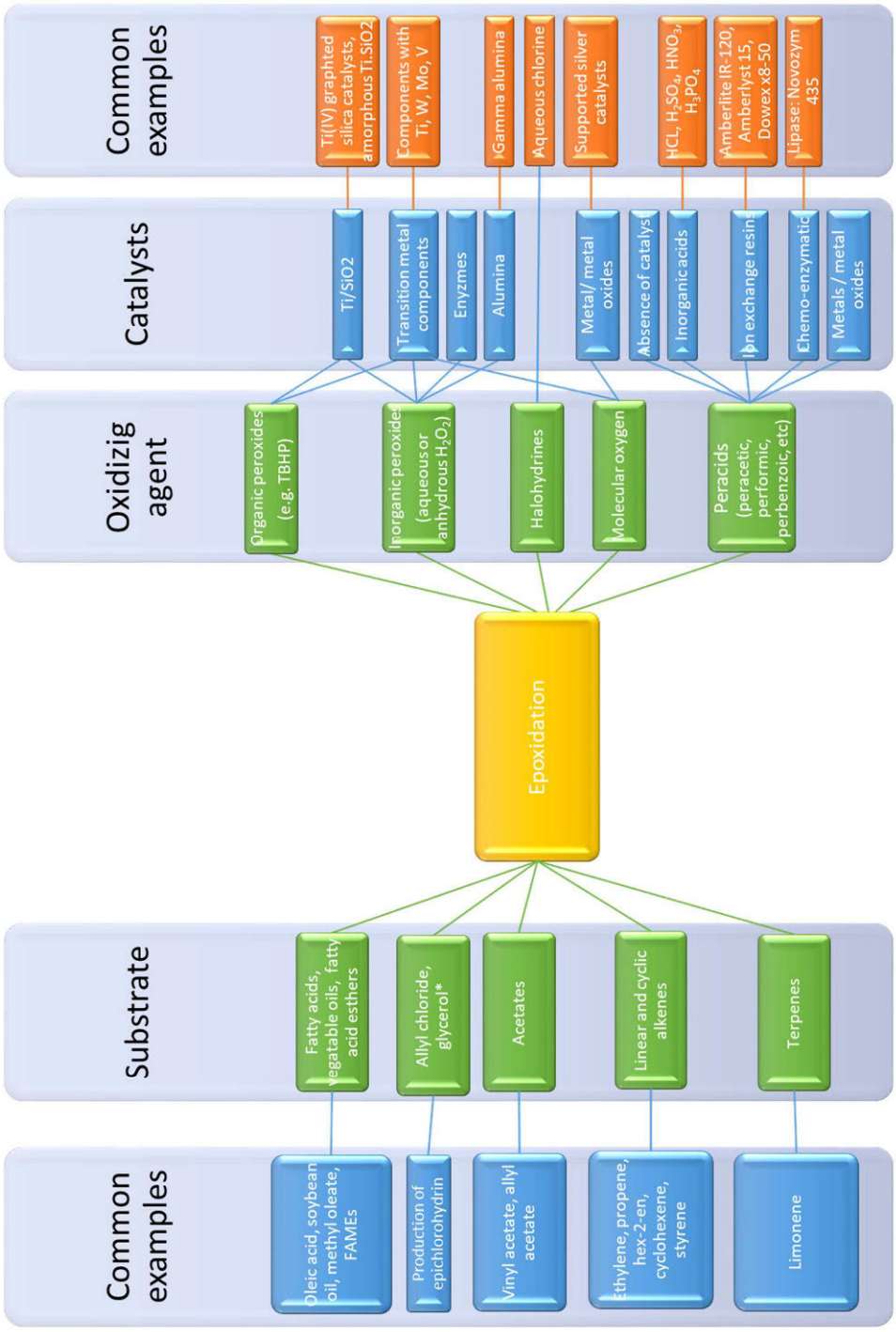

Figure 1.1. Summary on epoxidation methods.

1.3 Prilezhaev reaction

As mentioned previously, the Prilezhaev mechanism comprises two liquid phases which interact through an interphase provided with the help of an emulsion. The aqueous phase comprises the hydrophylic elements, i.e. water, hydrogen peroxide, the carboxylic acid and the percarboxylic acid formed *in situ*. The hydrophobic oily phase contains the oil substrate and the epoxidized oil. Furthermore, it is important to mention that, according to our observations, some of these components coexist in both phases, specifically the carboxylic acid and percarboxylic acid.

The reaction system is displayed in Figure 1.2 for oleic acid as the model compound for plant oils and acetic acid as the oxygen carrier. The characteristic feature is the *in situ* generation of the percarboxylic acid from the carboxylic acid and hydrogen peroxide. The percarboxylic acid carries out the epoxidation in the oil phase and returns back to the aqueous phase as a carboxylic acid. In the aqueous phase, the carboxylic acid is perhydrolyzed by hydrogen peroxide and the reaction cycle is completed. The reaction steps are as follows (CA = carboxylic acid, PCA = percarboxylic acid, VO = vegetable oil, aq = aqueous phase, oil = oil phase):

$$CA_{(aq)} + H_2O_2 \rightleftharpoons PCA_{(aq)} + H_2O \quad \text{(I)}$$

$$PCA_{(aq)} \leftrightarrow PCA_{(oil)} \quad \text{(II)}$$

$$VO_{(oil)} + PCA_{(oil)} \rightarrow Epoxide_{(oil)} + CA_{(oil)} \quad \text{(III)}$$

$$CA_{(oil)} \leftrightarrow CA_{(aq)} \quad \text{(IV)}$$

The selectivity of this reaction is an important issue because the epoxidized product is very sensitive to ring opening. The highly strained oxirane group is easily protonated under acidic conditions and a carbocation is formed. This species can further react with the nucleophilic species present in the oil phase or at the aqueous–oil interphase, such as hydrogen peroxide, carboxylic and percarboxylic acids and water to form undesired by-products. Plausible ring opening reactions are illustrated in Figure 1.3. In summary, the most important ones are the following (ROP = ring opening product):

$$Epoxide_{(oil)} + H_2O_2 \rightarrow ROP1 \quad \text{(V)}$$

$$Epoxide_{(oil)} + CA_{(oil)} \rightarrow ROP2 \quad \text{(VI)}$$

$$Epoxide_{(oil)} + PCA_{(oil)} \rightarrow ROP3 \quad \text{(VII)}$$

$$Epoxide_{(oil)} + H_2O_2 \rightarrow ROP4 \quad \text{(VIII)}$$

The perhydrolysis step (I) is relatively slow and but takes place spontaneously and it is considerably enhanced by acid catalysts. In general, the epoxidation of vegetable oils using the Prilezhaev method requires several hours to obtain high conversions [33]. To enhance the perhydrolysis rate, various catalysts can be used, such as enzymes, metals, metal oxides, inorganic acids and acidic ion exchange resins (AIER) [22,33]. A summary of several epoxidation homogeneous and heterogeneous catalysts is presented the following section.

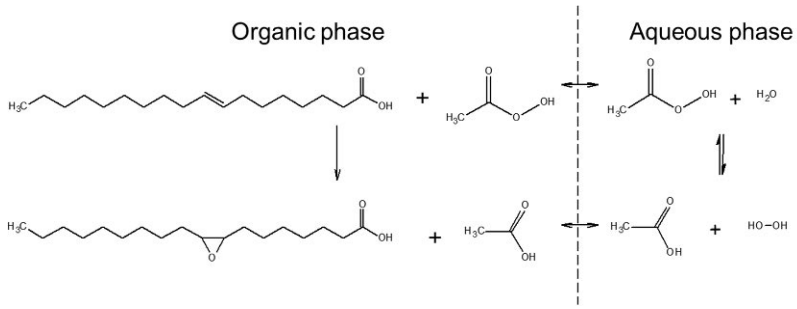

Figure 1.2. Epoxidation of oleic acid by the Prilezhaev method.

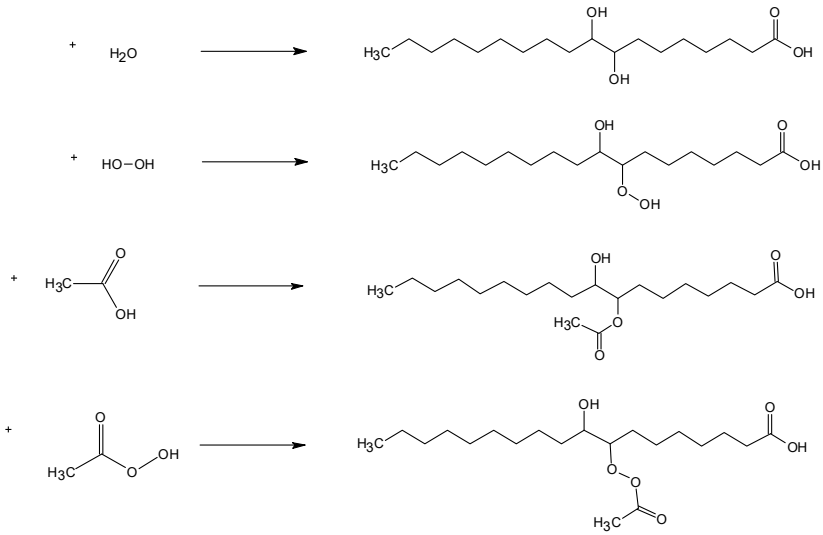

Figure 1.3. Possible ring opening mechanisms for epoxidized oleic acid (9,10-epoxysteraric acid)[34].

1.4 Catalysis in epoxidation

The classical catalyst applied for the Prilezhaev reaction is sulfuric acid. Overall, studies have shown that strong inorganic acids are good catalysts for the perhydrolysis reaction. Dinda *et al.* [21] have investigated the suitability of various inorganic acids as catalysts, *i.e.* HCl, H_2SO_4, HNO_3 and H_3PO_4, for the epoxidation of cottonseed oil with peracetic and performic acid generated *in situ* and concluded that sulfuric acid was the most effective catalyst. In fact, H_2SO_4 is the most common catalyst used in this synthesis. On the other hand, strong inorganic acids are highly corrosive and difficult to separate once the synthesis is completed. Furthermore, the presence of strong mineral acids in the epoxidation leads to ring opening reactions which suppresses the selectivity [35].

In general, heterogeneous catalysts are advantageous in terms of reusability and ease of separation when compared to its homogeneous counterparts. Among the solid catalysts for the epoxidation of vegetable oils, acidic ion exchange resins (AIER), lipase-based enzymes and metallic and metal-based catalysts are available. Previous reviews on the subject point out that metal-based catalysts are usually applied

for epoxidation with H_2O_2 and produce lower conversions and yields compared to AIERs and enzymes [Article IV]. Leveneur [36] studied the use of several highly complex zeolite catalysts for enhancing the perhydrolysis of peracetic and perpropionic acid with hydrogen peroxide and concluded that aluminosilicate materials were less beneficial than ion exchange resins in this reaction because aluminosilicates promoted the undesired decomposition of H_2O_2. Moreover, some enzymatic catalysts tend to become deactivated during the course of the reaction or are susceptible to degradation at high temperatures or high concentrations of hydrogen peroxide [26].

Epoxidation with AIER has been conducted for a wide variety of plant oils and operating conditions, and it is the most reported method. Its use affords easy catalyst separation and minimizes undesired ring opening reactions [34,37]. Ion exchange resins are the most active, selective and inexpensive catalysts available for this process. An acidic ion exchange resin is an acid in solid form which is insoluble in water. These resins have a network structure typically conformed by styrene-divinylbenzene, functionalized with acidic sulfonic groups. The ionic nature of the structure gives the resin the capacity to hydrate and retain water or polar/hydrophilic components into its network. This process is called water swelling and it provides the aqueous environment (gel water) where the exchange reactions take place [38]. A variety of ion exchange resins are commercially available with different matrix compositions, pore sizes, crosslinking percentages and particle sizes.

1.5 Process intensification aspects [I]

The concept of process intensification was first defined by Ramshaw in 1995 [39] and since then is has rapidly developed to a new branch in the study and development of chemical processes. This approach came as a response for the necessity of developing cleaner, safer, smaller and more energy-efficient processes. As a result, novel technologies have been developed, resulting in equipment which is, in the best cases, orders of magnitude smaller than the conventional chemical reactors and separation units. The application of process intensification covers a wide area of technologies, from the development of new process units, such as microreactors, structured reactors and more efficient mixing and separation units, to the use of alternative technologies such as microwave heating, ultrasound and high gravity.

A noteworthy feature of the Prilezhaev reaction system is the co-existence of two liquid phases, the aqueous phase, where the perhydrolysis takes place, and the organic phase where the epoxidation occurs. Taking this into consideration, the use of microwave irradiation as a process intensification method could in principle be advantageous. Selective heating is a phenomenon particularly induced by microwave irradiation in which the temperature of the polar substances present in the mixture increases whereas non-polar substances are transparent to the microwaves. In case of the Prilezhaev epoxidation, the aqueous phase would act as the absorbent and the oil as the transparent one. This is highly desirable because the slow step of the process occurs in the aqueous phase while the desirable epoxy groups formed in the organic phase are highly sensitive to ring opening with the increase of temperature. Additionally, the use of a heterogeneous catalysts in the perhydrolysis step of the process is a more efficient and greener alternative compared to mineral acids as homogeneous catalysts or to the reaction carried in the absence of catalyst. Shorter times are needed, higher yields are obtained and the separation of the catalyst is much simpler [Article III].

Complementarily, the rotating packed bed reactor used in the present work is also an innovative process intensification technology that is very suitable for the Prilezhaev reaction system. Stirring of the aqueous and oil phases plays a key role in the process, because it enables the generation of an emulsion in which

the reaction takes place. The aim of the novel mixing technology is to provide with a well stirred emulsion, immobilize the catalyst and minimize the external mass transfer limitations by forced, centrifugal flow through the catalyst bed. The use of solid catalysts can intensify the epoxidation reaction as well, however it can entail some limitations in the process such as mass transfer limitations or filtering issues. These problems are directly addressed by the used of the Spinchem device.

1.6 Goals of the research

This work focuses on the study the Prilezhaev epoxidation of plant oils as a green process, since it uses renewable raw materials and produces biodegradable products through a non-toxic synthesis route [40].

Experimental and modelling work was conducted in order to determine the kinetics of the epoxidation and the optimal operating parameters. Oleic acid was used as a model compound for plant oils since it is a rather simple fatty acid with only one unsaturation and an 18 carbon chain. Besides, oleic acid is highly present in most vegetable oils and its simplicity facilitates the stoichiometric considerations

Three main simultaneous reactions conform the Prilezhaev epoxidation system as illustrated in Figure 1.2: perhydrolysis, epoxidation and ring opening. The reaction network was studied as a whole and separately for each individual reaction, combining an extensive experimental study with the development of mechanistically sound mathematical models. A study on perhydrolysis and decomposition of percarboxylic acids by Leveneur *et al.* [36] and a recent work by Cai *et al.* [Article VIII] on the ring opening of epoxidized cottonseed oil, have been used as support for this research.

This research work emphasizes the use of process intensification methods for a cleaner and more energy efficient process with higher yields of the desired product, when compared to the conventional approach. The study includes the application of the following process intensification concepts:

- Microwave irradiation
- Heterogeneous catalysis
- Rotating bed reactor

The described studies with oleic acid as the model compound served as a guide to the research of more complicated mixtures, such as cottonseed oil and tall oil. Two types of tall oil mixtures were investigated in the present work, a mixture of tall oil fatty acids (TOFA) and a distilled version of tall oil (DTO). Both products are manufactured in Finland. The goal of the last part of the work was to compare the behavior of the model compound, oleic acid to the behaviors of DTO and TOFA and to get a deeper insight in the reaction mechanisms of epoxidation and ring opening of tall oil.

In general, the epoxidation of plant oils such as tall oil as a building block for chemicals is a step towards the diversification of an economy based on renewables and environmentally friendly components.

2. Experimental section

2.1 Reactor setup

The reaction setup was constructed and operated as a batch system. The system comprised an unbaffled glass reactor (Lenz®) connected to a loop system with a microwave cavity (MW) and a heat exchanger. The reaction mixture was pumped through the loop and recycled back to the reactor vessel. The reactor vessel was surrounded by a jacket filled with a mixture of ethylene glycol for cooling or heating to control and maintain the reactor temperature constant. Considering the exothermic nature of the reaction and the very efficient heating capacity of the microwaves [41], this loop system was designed to be able to control the temperature in a very safe way and avoid thermal runaway. Experiments under conventional heating where assisted by the heat exchanger and the microwave-heated experiments with a microwave generator (Sairem®), at 250W.

Stirring played a key role in the experiments, given that it enabled the generation of an emulsion in which the reaction took place. The SpinChem® RBR was placed inside the reactor, as represented in Figure 2.1. This device consists of a hollow rotating bed device which contains the immobilized catalyst inside and works as the stirring element itself. In this mixing system, the reaction solution was suctioned from the bottom of the bed, percolated through the solid catalyst and was returned to the storage vessel. The design of SpinChem® RBR maximizes both axial mixing and convective heat transport [42]. When the reaction was conducted in the absence of a solid catalyst, the SpinChem® RBR was used as an empty chamber. For experiments carried out without the SpinChem® RBR, a six-blade radial stirrer connected to a turbine engine was implemented.

The schematic configuration of the reactor system is displayed in Figure 2.1. A peristaltic pump (Heidolph®) was used to circulate the mixture through the system and to avoid a contact with metal materials that can trigger the catalytic decomposition of hydrogen peroxide and peracetic acid [36]. In addition, a reflux condenser was incorporated to prevent evaporation of volatile compounds, *i.e.*, the carboxylic acids. Thermocouples were located inside the reactor, before the preheater, after the preheater, before the microwave and after the microwave zone. The temperatures were displayed and recoded by the software Picolog®.

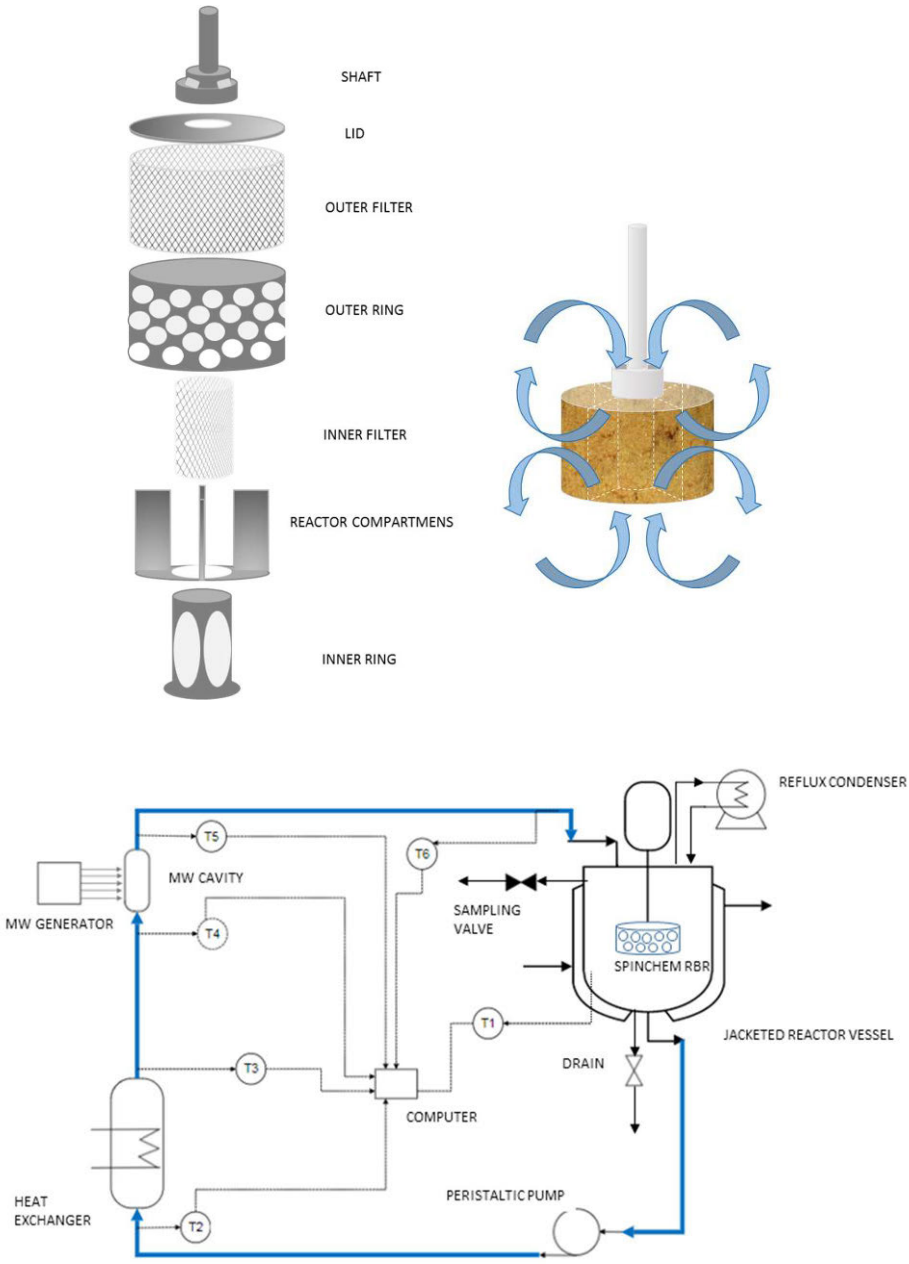

Figure 2.1. Scheme of the stirring effect and the flow paths by SpinChem and exploded-view of the seven pieces which are retained in the SpinChem® system (upper) and schematic view of the reactor setup (lower).

2.2 Epoxidation of oleic acid, cottonseed oil and tall oil

The oil and carboxylic acid were added first into the reactor vessel under vigorous stirring to create the emulsion. When used, the solid catalyst was placed into the chamber of the stirring device (SpinChem®) and washed with water to remove the free sulfonic acid groups. To prevent a high temperature peak, hydrogen peroxide (HP) at room temperature was added into the mixture dropwise over a period of 30-40 seconds. The HP addition time was negligible compared to the total reaction time, which was typically several hours. The moment when the first droplet of HP reached the mixture was considered as time zero. After completing the addition of all reagents, the peristaltic pump was switched on for the mixture to circulate through the loop system comprised by the heat exchanger, the microwave cavity and the reactor vessel. The temperature profile throughout the loop system was maintained the same for both cases: conventional and microwave heating. Samples were periodically withdrawn by a plastic syringe.

Experiments were performed under different pumping and stirring speeds. The experimental temperatures were 40-70ºC and the catalyst amount (Amberlite IR-120) was varied between 0 and 18% (dry w.r.t oil mass). Different initial ratios of double bonds, hydrogen peroxide, carboxylic acid and water were used in the experiments. The repeatability of the kinetic experiments was confirmed by duplication of some experiments. The average experimental error was 4–5% in the experiments based on the experimental repetitions.

2.3 Catalyst screening

Seven heterogeneous catalysts (Table 2.1) were screened under similar reaction conditions, using 50ºC as the reaction temperature. This specific temperature was chosen based on previous experience on the reaction kinetics [Article III]. The epoxidation rate is very low at 40ºC; high temperatures, on the other hand, promote ring opening reactions. The repeatability of the kinetic experiments was confirmed by duplication of some experiments.

Table 2.1 Properties of the cation exchange resins used.

Catalyst	Polymer type	Polymer nature	Active group	Cross-linking (%)	Moisture content (% mass)	Capacity by dry weight (meq/g)	Native particle size range (mm)	Pores (nm)
Amberlite IR-120	Gel	Styrene-divinylbenzene	Sulfonic acid	8	52	4.4	0.30 - 1.20	-
Amberlyst 15	Macroreticular	Styrene-divinylbenzene	Sulfonic acid	20-25	5	4.7	0.45 - 0.60	40 - 80
Dowex 50Wx2-100	Gel	Styrene-divinylbenzene	Sulfonic acid	2	79	4.8	0.15 - 0.30	-
Dowex 50Wx8-100	Gel	Styrene-divinylbenzene	Sulfonic acid	8	51	4.8	0.15 - 0.30	-
Dowex 50Wx8-50	Gel	Styrene-divinylbenzene	Sulfonic acid	8	52	4.8	0.30 - 0.84	-
Smopex-101	Fibre	Styrene sulfonic acid grafted polyolefin fiber	Sulfonic acid	2	44	2.6	-	-
Nafion™ NR40	Beads	Tetrafluoroethylene and perfluoro-3,6-dioxa-4-methyl-7-octenesulfonyl fluoride	Perfluorosulfonic acid	-	<2	1.0	3-4	-

2.4 Microwave and conventional heating

A heat exchanger was incorporated to the loop to be used as the energy source in experiments with conventional heating (CH); both equipment (microwave cavity and heat exchanger) remained fixed to the system even when they were not used, in order to maintain the experimental setup unchanged (Figure 2.1). While microwave (MW) irradiation was applied, the heat exchanger remained off and vice versa. In this system, the MW frequency was fixed to 2.45 GHz to avoid interfering with radar and telecommunication activities; most domestic and commercial microwave instruments operate at this frequency [43]. The reaction medium flowed through a transparent quartz tube, which allows microwaves to heat the reaction medium without any interference.

When applying CH, the heat exchanger was switched on at least 10 min before the experiment to achieve the anticipated reactor temperature. In the case of using MW heating, the radiation and security measures were activated after the addition of hydrogen peroxide. The temperatures in the loop system (T1 to T6 in Figure 2.1) were maintained at the same levels for both conventional and MW heating. Parallel experiments with MW heating and CH were performed in order to compare both types of heating.

2.5 Ring opening of epoxides

Epoxidized cottonseed oil (ECSO) was prepared as described by Zheng et al [44].180 g of cottonseed oil (CSO), 180 g of hydrogen peroxide solution (H_2O_2; 33 wt%) and 50 g of distilled water were introduced into the glass reactor at 60ºC. Formic acid was introduced via a dosing pump at a volumetric flow-rate of 2.9 mL/min for 25 min. Formic acid was chosen because it undergoes a more rapid perhydrolysis than acetic acid. After one hour, the agitation system was stopped and the reaction mixture stratified into two phases and the aqueous phase was removed. The organic phase left in the reactor was washed with 300 mL of sodium carbonate (Na_2CO_3; 10wt%) and then washed three times with distillated water to remove the residual sodium salt. The product was evaporated using an IKA RV10 control vacuum rotary evaporator (VWR, Darmstadt, Germany) at 60ºC and dried over magnesium sulfate. The resulting ECSO was kept at 3ºC under an argon atmosphere. The molar fraction of the ECSO was 91.8%.

In order to study the ring opening reactions 150 mL of ECSO was added into the reactor with a specific amount of water at the desired temperature. Then, a calculated amount of acetic acid, sulfuric acid or hydrogen peroxide was preheated and added into the reactor, depending on the type of ring opening reaction to be investigated. Several sets of experiments were conducted to study ring opening reaction by water, hydrogen peroxide, peracetic acid and acetic acid. To validate the model of ring opening by acetic acid at different epoxide concentrations, several experiments were performed by mixing a pure solution of ECSO with a fresh solution of CSO in different ratios.

2.6 Analysis methods and procedures

The mixture contained in the samples separated spontaneously into two phases in few seconds after being withdrawn. Each phase was placed in separate vials and they were centrifuged to ensure a more thorough separation. The organic phase was washed with distilled water to remove the remaining acetic acid and to prevent any further reactions. To remove aqueous residuals from the organic phase, a small amount of molecular sieve beads (Sigma 5A, 8-12 mesh) was added. The organic phase was stored in a

freezer and analyzed within the next days to determine the conversion to oxirane and the iodine value, whereas the aqueous-phase samples were analyzed immediately after being withdrawn from the reactor to determine the concentrations of hydrogen peroxide, acetic acid and peracetic acid.

2.6.1 Aqueous phase analysis

The Greenspan and MacKellar method [45] was applied for the analysis of hydrogen peroxide and the percarboxylic acid. Hydrogen peroxide was titrated with an ammonium cerium sulfate solution; after the end point, the percarboxylic acid reacts with hydrogen iodide (formed with an excess of potassium iodide) to produce acetic acid and molecular iodine. The resulting iodine is titrated with a sodium sulfate solution. The reaction stoichiometry is displayed in Figure 2.2:

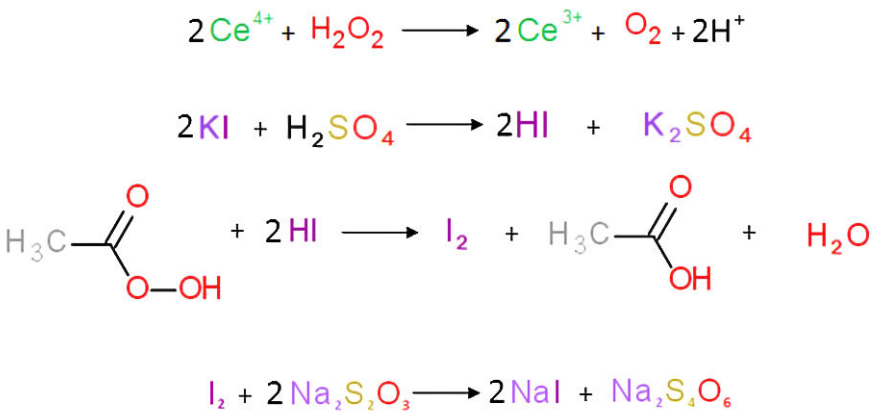

Figure 2.2 Greenspan and Mackellar analysis for hydrogen peroxide and percarboxylic acid.

In the method performed, 0.1g of sample were added to 50mL of a 10% acetic acid solution and ice was added to decrease the temperature to 10°C or below. Three drops of ferroin indicator were added and the solution was titrated with ammonium cerium sulfate from orange color to light blue. Then, 10mL of 10% potassium iodide was added to the mixture and the solution was titrated with 0.1M sodium thiosulfate from brown to orange using starch as an color indicator.

Additionally, colorimetric test stripes were used for a quick determination of the percarboxylic acid concentration to detect any sudden accumulation of the acid in the system, which could signify any risk of explosion.

For the determination of the carboxylic acid content, an automatic titrator with a 0.2M sodium hydroxide solution was used. This analysis was carried on through a potentiometric titration in which the following acid-base reaction took place according to Figure 2.3.

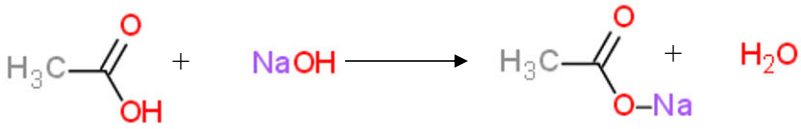

Figure 2.3 Stoichiometry of acetic acid analysis.

For this method, approximately 0.2g of a sample were added to 50mL of distilled water and titrated with a 0.2M solution of sodium hydroxide.

2.6.2 Organic phase analysis

Samples were heated in an oven at 70°C until they melted and had a high enough fluidity to be handled with a pipette. For the sake of comparison, organic phase type of analysis was carried out on samples that were withdrawn immediately and the results showed to be comparable (with an error of 4%) with the samples which had been stored in a freezer for 72 hours and melted in the oven at 70ºC.

The iodine value is a concept commonly used to describe the degree of unsaturation in fatty acids and it is a measurement of the progress of the reaction. The iodine value is expressed as grams of iodine consumed by 100 grams of oil. The oil reacts with an excess of iodine present in iodine monobromide (IBr). The remaining iodine is obtained with a potassium iodine solution added after the reaction was ended; the liberated iodine is titrated with a sodium thiosulfate solution. The amount of carbon-carbon double bonds can be calculated by the subtraction of the total iodine added and the iodine titrated by the sodium thiosulfate solution as illustrated in Figure 2.4.

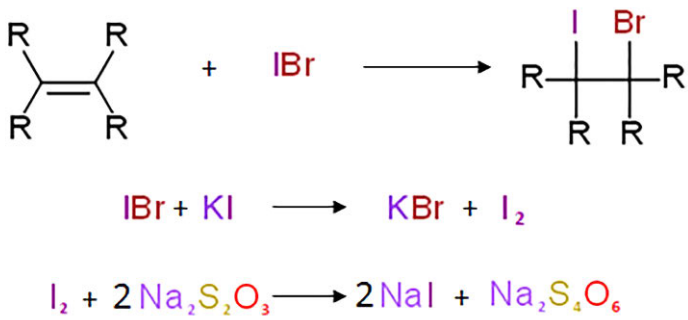

Figure 2.4 Stoichiometry of iodine value analysis.

In the method employed for the determination of the iodine value [46], 0.1g of oil phase was diluted in approximately 20mL of chloroform. An aliquot of 25mL of Hanus reagent (IBr solution) was added and the mixture was left covered in darkness. After one hour, 20mL of a 10% potassium iodide solution was added to the flask to stop the reaction and 100mL of distilled water was used to rinse the walls of the flask. The solution was titrated with 0.1M sodium thiosulfate solution using starch as indicator. The same procedure was applied to a blank solution.

The oxirane number describes the amount of epoxy groups present in the oil phase. For the determination of the content of oxirane oxygen, Jay's method [47] was applied. In this method, a direct titration of the epoxy groups was made with hydrogen bromide generated *in situ* by the addition of perchloric acid to a tetraethylammonium bromide (TEAB) following the stoichiometry shown in Figure 2.5.

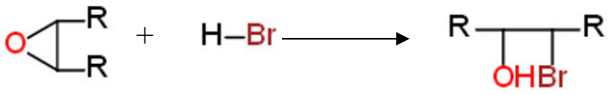

Figure 2.5 Stoichiometry of oxirane number.

0.1g of oil sample was dissolved in 10 mL of chloroform, followed by addition of 10mL of 20 wt% of TEAB in acetic acid. The mixture was titrated by 0.1M of perchloric acid in acetic acid solution using a potentiometric titrator.

The acid values of oleic acid and tall oil were measured by titration with a 0.2M sodium hydroxide solution; the samples were dissolved in 2-propanol

The conversion of the double bonds was calculated from

$$\%\boldsymbol{C} = \frac{(\boldsymbol{IV_0} - \boldsymbol{IV_f})}{\boldsymbol{IV_0}} \cdot \mathbf{100} \tag{1}$$

where IV_0 is the initial iodine value of the oil sample and IV_f is the iodine value of the final oil sample. For illustration purposes, the conversion of double bonds is shown as 100% - %C in the graphs in order to represent the reduction of the concentration of double bonds.

From the oxirane content values, the relative fractional conversion to oxirane (RCO), also called the yield of oxirane, was estimated from the expression

$$\%\boldsymbol{RCO} = \frac{\boldsymbol{OO_{expt}}}{\boldsymbol{OO_{th}}} \cdot \mathbf{100} \tag{2}$$

where OO_{expt} is the experimentally determined content of oxirane oxygen, and OO_{th} is the theoretical maximum oxirane oxygen content in 100 g of oil, which was determined using the following expression,

$$OO_{\text{th}} = \left\{ \frac{IV_0/2MM_i}{100 + \left(IV_0/2MM_i\right) \cdot MM_O} \right\} \cdot MM_O \cdot 100 \quad (3)$$

where MM_i is the atomic mass of iodine (126.9 g/mol) and MM_O is the atomic mass of oxygen (16.0 g/mol).

2.6.3 Gas chromatography (GC)

The composition of oleic acid, tall oil fatty acids (TOFA) and distilled tall oil (DTO) was measured by GC analysis. Samples were analyzed by gas chromatography (GC-FID) on a PerkinElmer Clarus 500 GC using hydrogen as carrier gas (14 psi), after silylation with a mixture of pyridin-BSTFA-TMCS (1:4:1). The capillary column used was a HP-1 (Agilent J&W), 25 m (L) x 0.200 mm (ID), and 0.11 µm film thickness, and oven temperature was programmed at 6°C/min from 120°C (1 min hold) to 320°C (15 min hold).

2.6.4 Nuclear magnetic resonance spectroscopy (NMR)

NMR spectra were recorded on a Bruker (Bruker BioSpin, GmbH, Rheinstetten, Germany) AVANCE III spectrometer operating at 500.10 MHz (^{1}H) and 125.75 MHz (^{13}C) equipped with a BB/1H SmartProbe. Characterization of the reaction mixtures was carried out by recording a set of 1D and 2D spectra: ^{1}H, ^{13}C, DQF-COSY (Double-Quantum Filtered COrrelation SpectroscopY), HSQC (Heteronuclear Single-Quantum Correlation, multiplicity edited CH/CH_3 positive, CH_2 negative) HMBC (Heteronuclear Multiple-Bond Correlation) and TOCSY (TOtal Correlation SpectroscopY). All samples were dissolved in MeOD-d_4 and the spectra were recorded at 25°C.

2.6.5 Physical properties

The densities of the oil mixtures were measured with an Anton Paar density meter mPDS 2000V3 at 25, 50, 60 and 70°C. The shear viscosities of the samples were measured with an Anton Paar Physica MCR300 modular compact rheometer at 25, 50, 60 and 70°C, from 0 to 1000s^{-1} shear rates.

3. Epoxidation of oleic acid in the absence of heterogeneous catalyst (Articles I, II, V)

The epoxidation of oleic acid as a model compound was conducted in the absence of a solid catalyst and the influence of several experimental parameters was studied.

3.1 Temperature effect

The following experiments were performed under similar conditions at 40ºC, 50ºC and 60ºC to reveal the temperature dependence of the epoxidation process. The molar ratio of double bonds-acetic acid-hydrogen peroxide (DB:AA:HP) was kept as 1:5.6:2.4 based on previous studies [32].

The results revealed that the conversion of oleic acid takes place clearly faster with increasing temperature and that the initial rate is close to zero order as the number of double bonds decreased linearly with time.

These results are in accordance with previous studies, which in fact state that the rate of epoxidation of fatty acids increases with temperature [37,48–50]. The conversion of double bonds and the relative conversion to oxirane are displayed in Figure 3.1. The first samples of each experiment were withdrawn after four minutes of having added the acetic acid, in order to wait for the acid to be well-mixed in the system, i.e., the reactor and the loop. In accordance to literature, the iodine value measured for oleic acid is 90. The iodine value for three temperatures under conventional heating showed that the initial points of each experiment were relatively close to this value: 88 for 40ºC, 82 for 50ºC and 81 for 60ºC, which indicates that the conversion of double bonds at four minutes after adding the acetic acid is already noticeable and the increase of temperature immediately affects the reaction rate. The three experiments were executed over different total reaction times with the intention of reaching similar double bond conversions.

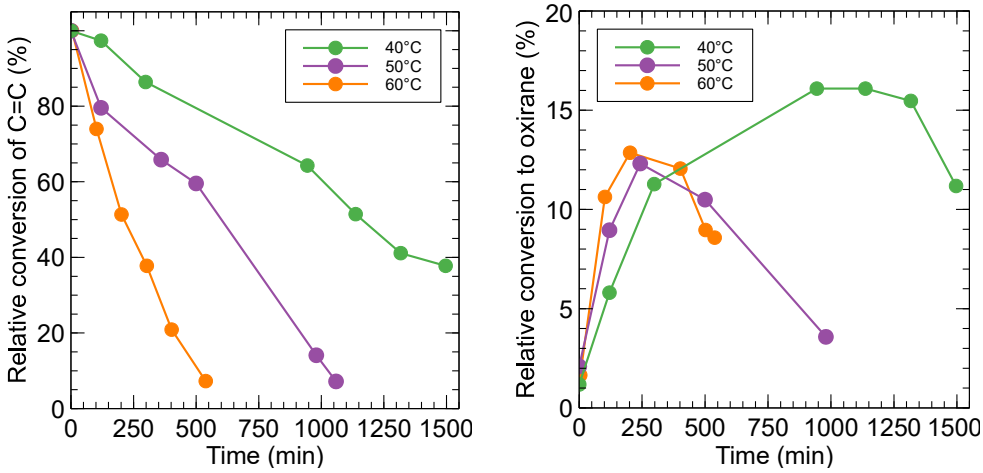

Figure 3.1 Relative conversion of double bonds (left) and relative conversion to oxirane (right) at different temperatures.

In terms of the selectivity, Figure 3.1 shows that for these experiments, the conversion to oxirane increased to a maximum point after which it started to decrease rapidly. This can be attributed to ring

opening reactions which consume the product. For the organic phase, the pH of the samples was determined to be around 3.5, which indicates that the conditions for the oxirane group protonation are favorable and ring opening can easily take place [18,48,51,52] . The formation of epoxyoleic acid was faster at higher temperatures, but also ring opening accelerates as the temperature is increased. For the reaction at 40ºC, higher oxirane contents are reached and ring opening starts much later. Comparing the conversion and the oxirane content in Figure 3.1, it can be concluded that the double bonds are still consumed at the same rate while the ring opening reactions start, which indicates that ring opening proceeds faster than epoxidation under these conditions, especially for experiments at 50 and 60ºC. Turco et al. [49] have also observed that higher conversions were achieved at higher temperatures, but the decline of the epoxyoleic acid selectivity was more prominent.

Regarding the aqueous phase, the concentrations of hydrogen peroxide and acetic acid with time are displayed in Figure 3.2. A linear decrease was observed for the hydrogen peroxide concentration and its consumption was accelerated with increasing temperature. The concentration of peracetic acid (PAA) generated in situ, remained almost constant during the experiments. In general, the concentration of peracetic acid in the aqueous phase remained under 2 wt-%, which is considered to be a safe concentration level [36,53]. Acetic acid (AA) is consumed to form peracetic acid which takes part in the epoxidation step, where acetic acid is regenerated. Figure 3.2 reveals that the acetic acid concentration was virtually constant at 40ºC. However, at higher temperatures some acetic acid was consumed. This concentration decrease can be attributed to the ring opening reactions carried out by acetic acid, since the acetic acid consumption is higher at higher temperatures as well as the ring opening.

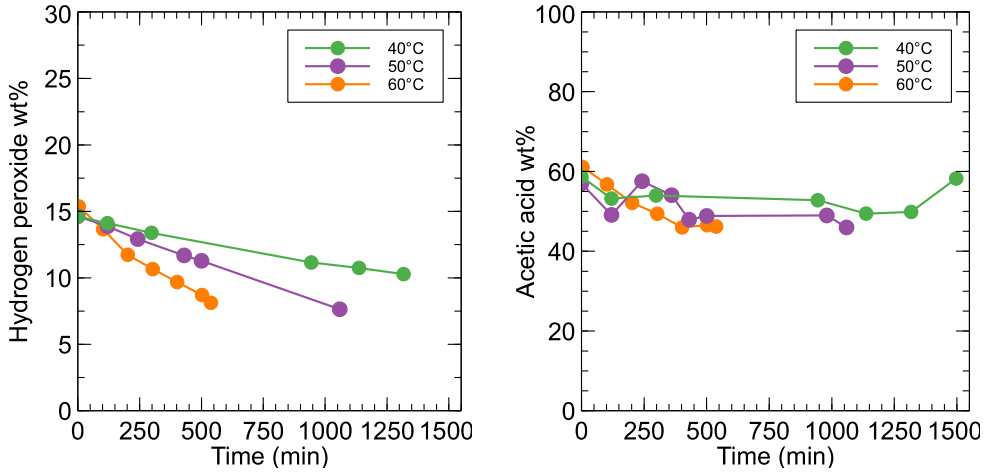

Figure 3.2 Concentration of hydrogen peroxide (left) and acetic acid (right) in the aqueous phase for different temperatures.

3.2 Acetic acid amount

Due to the strong presence of the ring opening reactions in the first set of experiments, it was decided to study the acetic acid-double bond ratio (AA:DB) in order to minimize these side reactions. The reaction temperature was 60ºC and the hydrogen peroxide-double bond ratio (HP:DB) was kept to 2.4:1, as in the previous set of experiments. The results are displayed in Figure 3.3 andFigure 3.4.

For the experiment with the highest acetic acid amount (AA:DB 5.6:1) the decrease of the double bond concentration was more rapid than for the other experiments with less acetic acid. Likewise, Figure 3.3 shows that relevant ring opening was only found for the experiment with the highest amount of acetic acid. Figure 3.4 displays that the acetic acid concentration was constant for lower ratios of acetic acid-double bonds (2.4:1 and 1.2:1), but decreased linearly with a higher concentration of acetic acid.

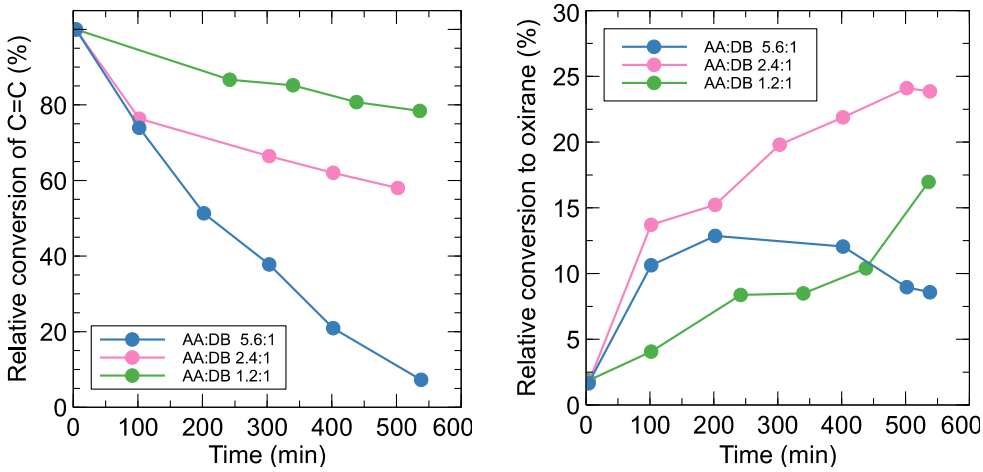

Figure 3.3 Relative conversion of double bonds (left) and relative conversion to oxirane (right) for different acetic acid-double bond ratios.

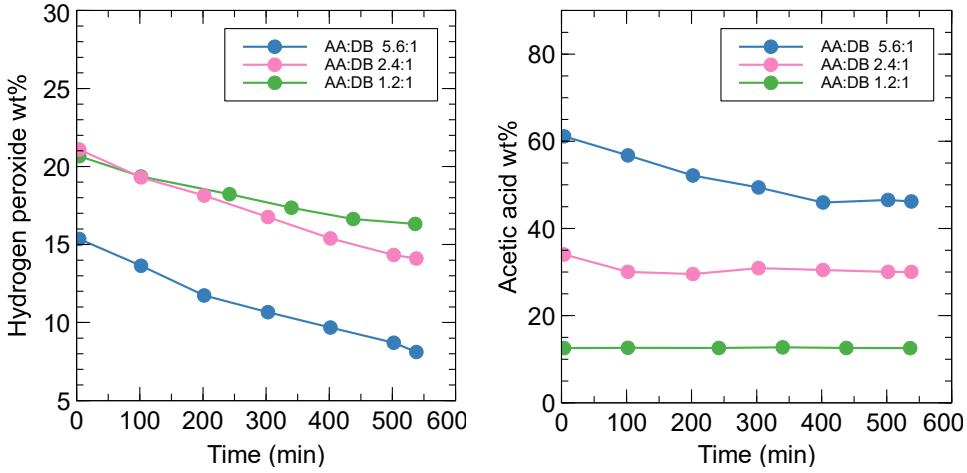

Figure 3.4 Concentration of hydrogen peroxide (left) and acetic acid (right) in the aqueous phase for different acetic acid-double bond ratios.

The hydrogen peroxide consumption for the three experiments was almost linear and almost with the same apparent rate. For the case of lowest acetic acid amount (AA:DB 1.2:1) the concentration decrease was slightly slower because the oleic acid consumption rate was also lower than the other two reactions. For this set of experiments, the peracetic acid amount was practically constant, which is in accordance to the epoxidation in situ scheme (Figure 1.2) —peracetic acid is generated in the aqueous phase, distributed between the aqueous and the oil phases and consumed during the epoxidation. There was no

accumulation of the acid because double bonds were still available, therefore the generated peracetic acid was subsequently consumed in the epoxidation process. It should be noticed that in the case of saturation of all double bonds, the peracetic acid concentration would increase until it reaches the equilibrium concentration, given that the perhydrolysis reaction is reversible [36].

It can be concluded that acetic acid boosts both oleic acid conversion and ring opening, which has been confirmed by Turco et al. [49] and Campanella et al. [50,54]. In this case, the best ratio that allows highest oleic acid conversion and minor ring opening was 2.4:1, which was kept for the forthcoming experiments.

3.3 Hydrogen peroxide

After having adjusted the acetic acid-to-oleic acid molar ratio for a better selectivity of epoxyoleic acid, the relative conversion to oxirane for the best experiment was only 24%. The influence of the hydrogen peroxide-to-oleic acid molar ratio was then studied, aiming to obtain a higher oxirane yield. The results are depicted in Figure 3.5 and Figure 3.6.

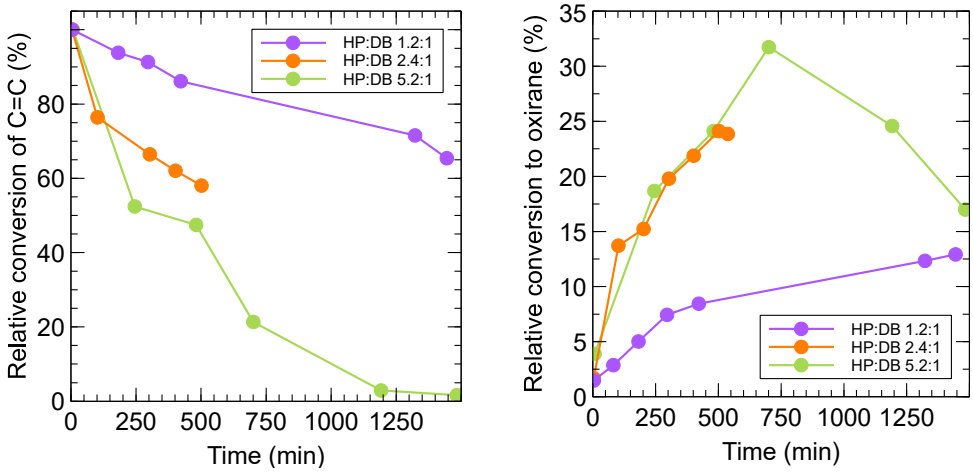

Figure 3.5 Relative conversion of double bonds (left) and relative conversion to oxirane (right) for different hydrogen peroxide-double bond ratios.

The double bond consumption seems to be highly affected by the amount of hydrogen peroxide. For the 1.2:1 ratio of HP:DB, the double bond conversion was low: it only reached 35% in 24 h. For the HP:DB ratio of 5.2:1, the double bonds were almost completely consumed as the conversion was 98%. The reaction yield increases with increasing hydrogen peroxide concentration, reaching 32% of relative conversion to oxirane for the highest amount of hydrogen peroxide. Nonetheless the ring cleavage had a profound influence on the reaction system. This behavior is in accordance with the observations of Campanella et al. [50,54] who used a high excess of hydrogen peroxide to boost the epoxidation process. However, they used benzene as a solvent to suppress the ring opening reactions. In our case, no solvent was added and the ring opening had a strong impact. As the conversion approached 100%, peracetic acid started to accumulate very rapidly and the reaction was stopped before the peracetic acid concentration reached a dangerous level. As for the acetic acid, all three experiments showed a minor decrease of its concentration. For the experiments with a low hydrogen peroxide-to-oleic acid ratio (1.2:1 and 2.4:1), no major sign of ring opening was detected. For the experiment with the 5.2:1

hydrogen peroxide-to-oleic acid ratio, a minimum decrease of the acetic acid concentration was observed, probably because the highly concentrated hydrogen peroxide was the protagonist of the ring cleavage reactions.

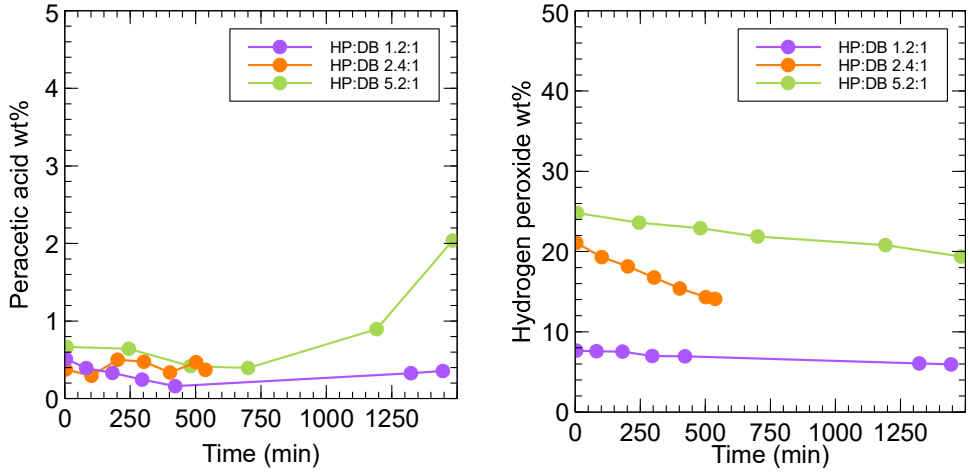

Figure 3.6 Concentration of peracetic acid (left) and hydrogen peroxide (right) in the aqueous phase for different peroxide-double bond ratios.

3.4 Stirring speed

The stirring speed played a key role in the creation of an emulsion that facilitates a good contact between the aqueous and organic phases. Experiments were conducted under similar conditions and different stirring speeds. Three different stirring rates were tested, 300, 450 and 900rpm.

For all the experiments conducted at 300 rpm, the stirring speed was not high enough to create a complete emulsion, and consequently a part of the oleic acid added to the reactor system remained accumulated on the upper part of the reactor. Therefore, 300rpm was discarded as a suitable stirring speed for the system.

Subsequently, different experiments were performed with 450rpm and 900rpm at 40°C and 60°C. The results displayed in Figure 3.7 indicate that the temperature was the main influencing factor for this set of experiments, while the stirring speed did not have any major impact. At 40°C and 60°C, the double bond conversion and conversion to oxirane followed similar behaviors for both stirring rates.

For experiments at 450 rpm and 900 rpm, the conversion of double bonds was quite similar (69% and 71% at 40°C and at 54% and 52% at 60°C respectively). Some differences were noticed in the relative conversion of oxirane for 450 and 900rpm at 40°C, the kinetic curves follow slightly different trends during the reaction time. However more data would have been required to discard some deviations in the analysis. In general terms, the results indicate that within the range of 450-900rpm it can be assumed that liquid-liquid mass transfer limitations can be neglected, since the results at both stirring rates were comparable within experimental error. This result is in accordance to those of Leveneur et al. [32] who concluded that in the range between 400rpm and 650rpm, the agitation velocity did not have an effect in the reaction kinetics. Even if it is a different system, the average droplet size, also called Sauter

number, will only depend on the continuous phase density, the impeller diameter and interfacial surface tension. Moreover, for this system it can be concluded that the interfacial mass transfer area was already close to optimal for the stirring speed 450–900 rpm range. To remain in the conservative side, experiments conducted further on were done under 1200rpm.

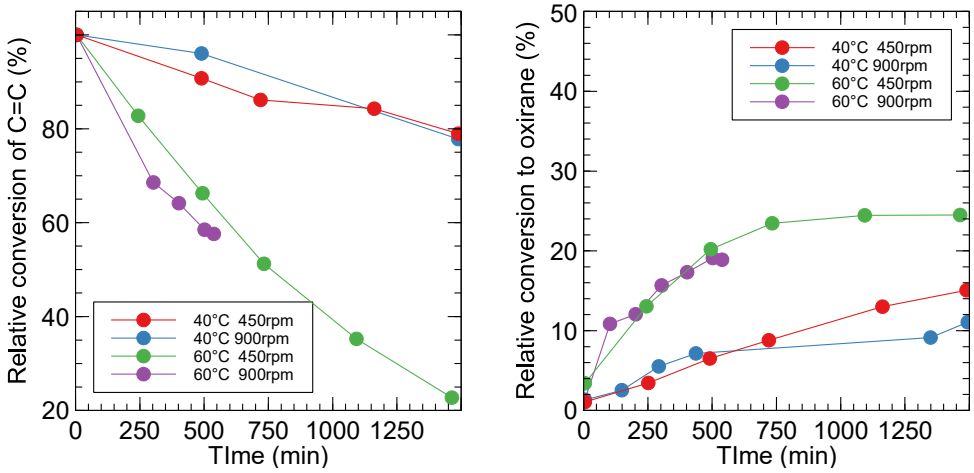

Figure 3.7 Relative conversion of double bonds (left) and relative conversion to oxirane (right) for different temperatures and stirring speeds.

3.5 Microwave heating

Experiments conducted with conventional heating were repeated under microwave (MW) irradiation for comparison, at 40, 50 and 60°C. The experiments are compared in Figure 3.8, Figure 3.9 andFigure 3.10. For the experiments with microwave heating and a reactor temperature of 60°C, the temperature in the probe was maintained at 60°C in order to have an isothermal system. The results show that the double bond conversion was considerably accelerated under microwave radiation while the conversion to oxirane was on the same level as in the corresponding experiment carried out under conventional heating. The hydrogen peroxide and peracetic acid concentrations followed the same tendency for both reactions. However, the acetic acid showed a slightly higher decrease of its concentration for microwave heating. Hence it can be inferred that microwave irradiation boosts the ring opening reactions because the conversion rate of oleic acid was faster but the yield of epoxyoleic acid was practically the same.

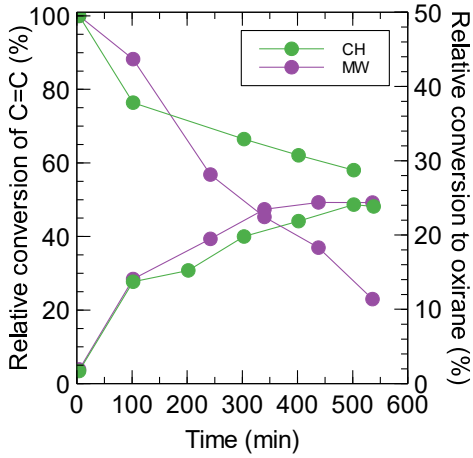

Figure 3.8 Relative conversion of double bonds (left axis) and relative conversion to oxirane (right axis) for microwave and conventional heating at 60°C.

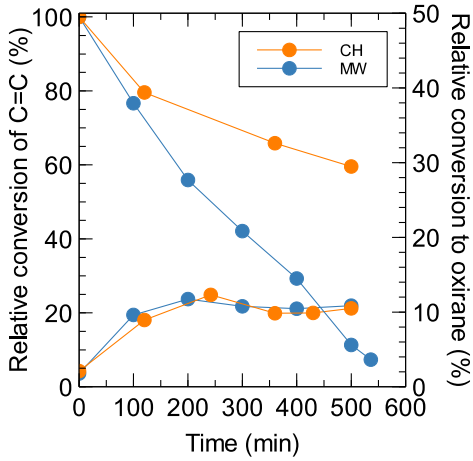

Figure 3.9 Relative conversion of double bonds (left axis) and relative conversion to oxirane (rightaxis) for microwave and conventional heating at 50°C.

The same experimental procedure was repeated at 50°C and conventional heating and microwave irradiation were compared. However the temperature of the probe in the microwave cavity was 60°C. The results are shown in Figure 3.9. Similarly to the previous set conducted at 60°C, the double bond conversion was enhanced by microwaves.

The lowest temperature used in these experiments was 40°C, therefore, it was decided to prolong the experiments from 9 hours to 24 hours. In order to avoid the presence of bubbles in the loop that could interfere with microwave irradiation, extra water (70mL to complete 420mL) was added to the reaction mixture. Then the temperature in the cavity for the microwave experiment was 70°C, therefore cooling

by the reactor jacket was needed to keep the reactor temperature at 40°C. The analysis results of the organic phase showed a major enhancement in both conversion and yield as illustrated by Figure 3.10.

For conventional heating, the oleic acid conversion was 22% and the conversion to oxirane was 12% in the end of the experiment, but for microwaves the conversion of oleic acid was 45% and the conversion to oxirane was 23%. The hydrogen peroxide consumption was more accelerated in the presence of microwave irradiation, given that the epoxidation rate was higher. The peracetic acid concentration remained at same level for both experiments and did not present any signs of accumulation because double bonds were still available for the epoxidation at the end of the experiment, so peracetic acid was consumed in the epoxidation step.

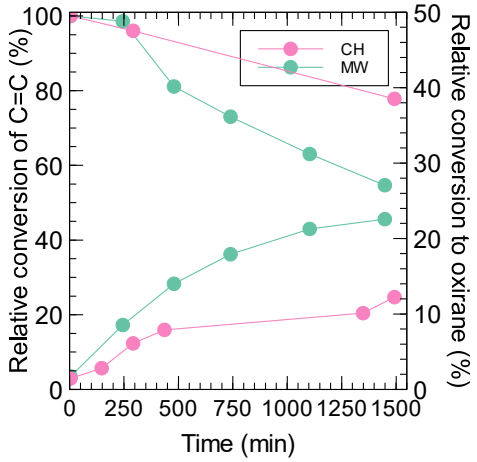

Figure 3.10 Relative conversion of double bonds (left axis) and relative conversion to oxirane (right axis) for microwave and conventional heating at 40°C.

Acetic acid also remained at the same levels for both experiments and did not present a significant decrease because, as shown in Figure 3.10, the epoxidized product did not show any significant decrease. Even though microwave irradiation produced a remarkable enhancement in the experiment conducted at 40°C, it might not be correct to rush into the assumption that a non-thermal effect was responsible for such an enhancement. First and foremost, there was a 30°C difference between the reactor and the microwave cavity which was regulated by applying cooling in the reactor jacket. Hosseini et al. [55] described in their work that applying cooling to the reaction allows higher levels of microwave power to be directed to the reaction mixture, thus enhancing microwave effects while removing heat simultaneously. They sustained that any rate enhancement was a product of increased temperatures and no signs of a specific thermal effect were found. They concluded that the results with microwaves could be reproduced by conventional heating.

A particular microwave thermal effect, namely selective heating might have contributed to the rate enhancement. Leveneur et al. [32] claim that higher rates are observed when the continuous phase is the aqueous phase. Because water is a microwave absorbent while oil is transparent to microwaves, a higher temperature gradient between the phases is achieved in comparison to conventional heating. If the temperature in the aqueous phase is higher, the perhydrolysis proceeds faster. Because the experiment at 40°C was the only experiment within the sets, where extra water was added, the aqueous-to-organic phase ratio was the highest and, consequently, the high temperature gradient between phases might have

produced a rate enhancement. In conclusion, the significant difference of the yields obtained with conventional heating and microwaves was owed to the incensement of the aqueous-oil phase ratio and the high temperature in the cavity followed by cooling in the reactor. The improvement of the conversion in the presence of microwaves in all three sets of experiments was possibly caused by the selective heating effect. Moreover, in the following experiments, the temperature profiles in the loop system for conventional and microwave experiments was kept the same in order to make a more straightforward comparison. Still, the results shown in Figure 3.11 revealed a higher oxirane yield but a lower conversion of double bonds in the presence of microwaves, which is an indication of suppressed ring opening reactions. These results support the hypothesis of the selective heating effect of microwave heating.

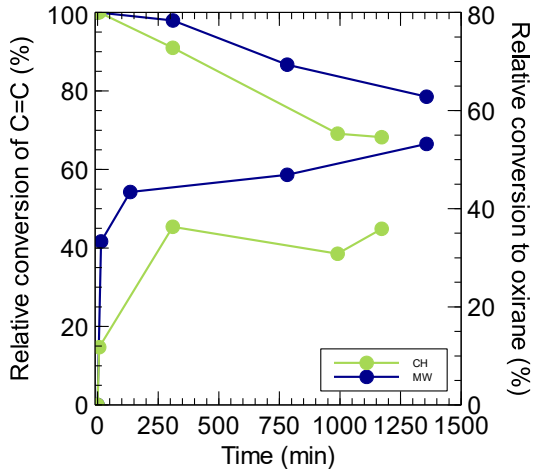

Figure 3.11 Relative conversion of double bonds (left axis) and relative conversion to oxirane (right axis) for microwave and conventional heating at 50°C under equal temperature profiles.

It is worth mentioning that according to our experimental observations, the microwave absorbance depends not only in the water-to-oil ratio of the mixture, but also in the pumping speed of the system, given that the mixture can be exposed for longer at lower pumping speeds and therefore receive a longer time to the radiation exposure. Moreover, the pumping speed was kept at 112mL/min in order to keep the residence time of the loop much shorter than the one in the reactor vessel. This simplified the mathematical modelling of the system. According to Lee and Marchant [56], the absorbance of a substance depends on the concentration and the nature (polar or non-polar) of the substance, the electric field amplitude (in this case it was maintained constant) and also the temperature. This indicates that, in accordance to some authors [57,58] and given the exothermal nature of the system, special precautions must be considered to prevent a thermal runaway.

Even though this work cannot be regarded as a proof of the controversial existence of non-thermal effect of microwaves, it is clear that there are facts which justify the use of microwave irradiation in chemical processes. Selective heating for example, is one of the greatest advantages that microwaves can bring; in this work, higher yields were achieved under microwave irradiation because a temperature gradient between the phases can be produced. Additionally, microwave irradiation offers rapid, efficient and safe heating. Conventional heating requires longer times and higher energy requirements. As an example, Pati et al. [59] reported that for the synthesis of biodiesel from Camelina sativa oil, the reaction rate constant was improved by two orders of magnitude in the microwave-assisted transesterification reaction as compared with those obtained with conventional heating.

3.6 Kinetic modelling

3.6.1 Reaction mechanism, kinetics and reactor modelling principles

The chemical reactions considered for the kinetic model are summarized in equations I-IV and in Figure 1.2. The decomposition of hydrogen peroxide is neglected in this study, because the conditions are considered mild [58,60,61]. Furthermore, according to Zhen et al. ring opening reactions caused by hydrogen peroxide and water at this temperature range are negligible [44].

For the conventionally heated experiments, the system was considered to be an isothermal batch. On the other hand, the mathematical model developed for the MW-heated experiments consisted of the system comprising two continuous stirred tank reactors (CSTR) in series, one being the reaction vessel while the other one being the MW cavity. This approach was applied because the temperatures were different in both locations. The loop in the system was considered to be very short so the reactions only took place in the reactor vessel or in the MW cavity. Both CSTRs were assumed to be perfectly back-mixed. The reactor vessel (Tank 1) was described as a perfectly mixed tank reactor because of vigorous stirring, and the use of stirred tank model for the MW cavity was justified by the low conversion per cycle. The mean residence time in Tank 1 was 3.02 minutes, whereas it was 6.6 seconds in Tank 2. Figure 3.12 illustrates the schemes considered for the kinetic modelling.

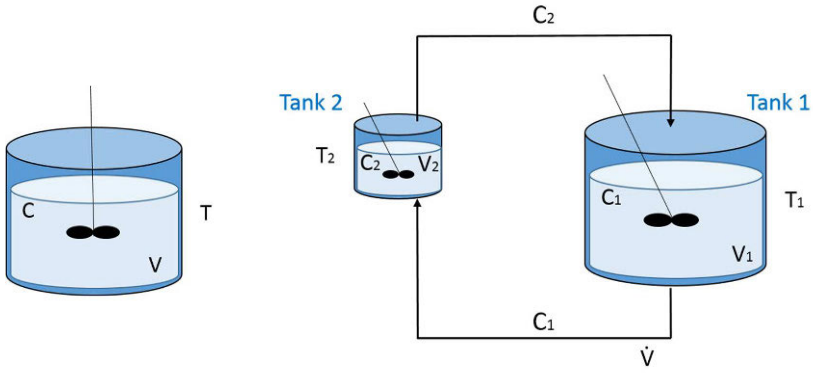

Figure 3.12 Epoxidation reactor modelling principles for conventional heating (left) and microwave irradiation (right).

3.6.2 Kinetic equations

The rate equations applied to the various processes in the system are summarized below. The expressions are based on previous studies on perhydrolysis, decomposition of peracids as well as epoxidation and ring opening of analogous systems [36,44,62,63].

Perhydrolysis of acetic acid

Perhydrolysis, which proceeds in the aqueous phase, is a reversible, acid catalyzed process. Under the experimental conditions, the dominating catalytic process is enhanced by acetic acid itself. It is a weak acid, which means that the concentration of protons is proportional to the square root of the acetic acid concentration. Consequently, the rate equation for the perhydrolysis becomes

$$R_{perh} = k_{per} \cdot \left(C_{AA_{aq}} \cdot C_{HP_{aq}} - \frac{1}{A_{eq} \cdot e^{\frac{-\Delta H}{R.T}}} \cdot C_{PAA_{aq}} \cdot C_{W_{aq}} \right) \cdot \sqrt{\frac{K'_{AA} \cdot C_{AA_{aq}}}{C_{W_{aq}}}} = R_1 \quad (1)$$

where parameters k_{perh} and $\sqrt{K'_{AA}}$ are merged to a single parameter $k'_{perh} = k_{perh}\sqrt{K'_{AA}}$.

Decomposition of PAA

Decomposition of peracetic acid in the aqueous phase is shown to be a first order process,

$$R_{decom} = k_{decom} \cdot C_{PAA_{aq}} = R_2 \quad (2)$$

Epoxidation of oleic acid

Epoxidation of double bonds in the oil phase is a second order reaction,

$$R_{epox} = k_{epox} \cdot C_{OA_{oil}} \cdot C_{PAA_{oil}} = R_3 \quad (3)$$

Ring opening of epoxide

The epoxide ring opening in the oil phase can principally take place via several parallel pathways. Water, hydrogen peroxide, carboxylic and percarboxylic acids can act as reagents and the process is acid-catalysed. In the actual reaction environment, acetic acid is the dominating catalyst for ring opening. Thus, the rate equation becomes

$$R_{RO} = k_{RO} \cdot C_{E1_{oil}} \cdot \sqrt{\frac{K'_{AA} \cdot C_{AA_{oil}}}{C_{W_{aq}}}} = R_4 \quad (4)$$

where parameters k_{RO} and $\sqrt{K'_{AA}}$ are merged to a single parameter in regression analysis $k'_{RO} = k_{RO}\sqrt{K'_{AA}}$.

3.6.3 Mass balances for components in the aqueous and oil phases

Previous studies in the epoxidation of oleic acid by performic acid have concluded that interfacial mass transfer is clearly faster than the rates of chemical reactions [64,65]. By analogy with the epoxidation by peracetic acid in agreement with other authors [34,66,67], rapid mass transfer for the epoxidation of the oleic acid by peracetic acid will be assumed here. Therefore, the balance equations for the aqueous and oil phases can be added and the equilibrium condition can be applied to relate the concentrations in both phases.

Using a similar methodology to that applied by Zhen et al. [44], the solubility of hydrogen peroxide and water in the organic phase were approximated to be negligible and the solubility of acetic acid and peracetic acid in the organic phase were approximately equal. Additionally, by presuming the other organic species are not soluble in the aqueous phase, it is possible to simplify the mass balances to a system of ordinary differential equations (ODEs). The model is summarized below and the symbols are defined in the Notation section.

Conventional heating, Batch system

Aqueous phase (aq)

$$\frac{dC_{AA_{aq}}}{dt} = \left(\alpha + \frac{1-\alpha}{K_{AA}}\right)^{-1} . \left(-\alpha R_{perh} + (1-\alpha) R_{Epox}\right) \quad (5)$$

$$\frac{dC_{HP_{aq}}}{dt} = -R_{perh} \quad (6)$$

$$\frac{dC_{PAA_{aq}}}{dt} = \left(\alpha + \frac{1-\alpha}{K_{PAA}}\right)^{-1} . \left(\alpha\left(R_{per} - R_{decom}\right) - (1-\alpha) R_{epox}\right) \quad (7)$$

$$\frac{dC_{W_{aq}}}{dt} = R_{perh} \quad (8)$$

Oil phase (oil)

$$\frac{dC_{OA_{oil}}}{dt} = -R_{epox} \quad (9)$$

$$\frac{dC_{EOA_{oil}}}{dt} = R_{Epox} - R_{RO} \quad (10)$$

Microwave heating, CSTRs in cycle

Tank 1

Aqueous phase (aq)

$$\frac{dC_{AA1_{aq}}}{dt} = \frac{C_{AA\ aq} - C_{AA1_{aq}}}{\tau_1} + \left(\alpha + \frac{1-\alpha}{K_{AA}}\right)^{-1} . \left(-\alpha R_{perh} + (1-\alpha) R_{Epox}\right) \quad (11)$$

$$\frac{dC_{HP\ aq}}{dt} = \frac{C_{HP\ aq} - C_{HP1_{aq}}}{\tau_1} - R_{perh} \quad (12)$$

$$\frac{dC_{PAA1_{aq}}}{dt} = \frac{C_{PAA2_{aq}} - C_{PAA1_{aq}}}{\tau_1} + \left(\alpha + \frac{1-\alpha}{K_{PAA}}\right)^{-1} . \left(\alpha\left(R_{per} - R_{decom}\right) - (1-\alpha)R_{epox}\right) \quad (13)$$

$$\frac{dC_{W1_{aq}}}{dt} = \frac{C_{W2_{aq}} - C_{W1_{aq}}}{\tau_1} + R_{perh} \quad (14)$$

Oil phase (oil)

$$\frac{dC_{OA1_{oil}}}{dt} = \frac{C_{OA2_{oil}} - C_{OA\ oil}}{\tau_1} - R_{epox} \quad (15)$$

$$\frac{dC_{EOA1_{oil}}}{dt} = \frac{C_{EOA2_{oil}} - C_{EOA1_{oil}}}{\tau_1} + R_{Epox} - R_{RO} \quad (16)$$

In the above equations, all the reaction rates (R) are calculated with the concentrations in Tank 1 ($R(C_1)$).

Tank 2

For Tank 2, the mass balance equations are written in an analogous way. All the reaction rates are calculated with the concentrations in Tank 2 ($R(C_2)$).

Aqueous phase (aq)

$$\frac{dC_{AA\ aq}}{dt} = \frac{C_{AA1_{aq}} - C_{AA2_{aq}}}{\tau_2} + \left(\alpha + \frac{1-\alpha}{K_{AA}}\right)^{-1} . \left(-\alpha R_{perh} + (1-\alpha)R_{Epox}\right) \quad (17)$$

$$\frac{dC_{HP2_{aq}}}{dt} = \frac{C_{HP1_{aq}} - C_{HP\ aq}}{\tau_2} - R_{perh} \quad (18)$$

$$\frac{dC_{PAA2_{aq}}}{dt} = \frac{C_{PAA1_{aq}} - C_{PAA2_{aq}}}{\tau_2} + \left(\alpha + \frac{1-\alpha}{K_{PAA}}\right)^{-1} . \left(\alpha\left(R_{per} - R_{decom}\right) - (1-\alpha)R_{epox}\right) \quad (19)$$

$$\frac{dC_{W2_{aq}}}{dt} = \frac{C_{W1_{aq}} - C_{W2_{aq}}}{\tau_2} + R_{perh} \quad (20)$$

Oil phase (oil)

$$\frac{dC_{OA\ oil}}{dt} = \frac{C_{OA\ oil} - C_{OA2_{oil}}}{\tau_2} - R_{epox} \quad (21)$$

$$\frac{dC_{EOA2_{oil}}}{dt} = \frac{C_{EOA1_{oil}} - C_{EOA2_{oil}}}{\tau_2} + R_{Epox} - R_{RO} \quad (22)$$

The initial conditions of the balance equations (5)-(22) are simple: the concentration of the components in the corresponding phases are known in the beginning of the experiments, at t=0.

3.6.4 Energy balances

For conventional heating, the conditions were presumed to be isothermal and no energy balance was developed. In the case of microwave heating, the change in the temperature at the microwave cavity is determined by the temperature in the reactor and an additional component that in proportional to the total input microwave power ($|u|^2$) and the aqueous-to-oil volume ratio (α).

$$\frac{dT_{MW}}{dt} = T_{reactor} - T_{MW} + D \tag{23}$$

$$D \sim |u|^2 . \alpha \tag{24}$$

where D represents the temperature difference between the temperatures in the reactor and the MW cavity.

3.6.5 Parameter estimation procedure

The program package used for the kinetic modelling was ModEst (Model Estimation), which is written in Fortran 90 Compaq Visual FORTRAN 6.0. The ordinary differential equations (ODEs) describing this system can be stiff due to the presence of rapid and slow reactions. All the ODEs were solved during the parameter estimation using the ODESSA solver which uses the backward difference method and is implemented in the software ModEst. The accuracy of the parameters was checked by standard mathematical analysis and a Markov Chain Monte Carlo (MCMC) method.

The temperature dependences of the rate constants were described by the Arrhenius equation:

$$k = k_0 . e^{\frac{-E_a}{RT}} \tag{25}$$

The objective function (ω) was minimized by using a combined Simplex and Levenberg-Marquardt algorithm. The objective function for the concentration differences was defined as

$$\omega = \sum (C_i - \hat{C}_i)^2 \tag{26}$$

where C_i is the experimental concentration and $\hat{C}$ is the estimated concentration obtained from the kinetic model, eqs. (5)-(22).

3.6.6 Parameter estimation results

The highly coupled relationship of the steps involved in the epoxidation of oleic acid by peracetic acid formed *in situ* makes the parameter estimation challenging. Given the complexity of the system, the model seems to reflect efficiently the physical reality of the reaction system. The coefficient of determination for both models in CH and MW configurations exceeded 97% (See Table 3.1 and Table 3.4) showing a good agreement between the experimental and calculated values. The estimation of the kinetic constant and activation energy for the peracetic acid decomposition became cumbersome since extremely high estimated errors where obtained and the parameters tended to converge to very low values for the kinetic constant and high activation energies. This implied that the influence of peracetic acid decomposition on this system was too low to be numerically determined from the available data. This observation is in agreement with Leveneur [36], who explains that peracetic acid is more stable

compared with performic acid, whose decomposition is commonly considered in the modelling of epoxidation systems. Because the decomposition of peracetic acid was very slow, it was neglected in this modelling effort.

Conventional heating

The experiments conducted under conventional heating were modelled as a pseudo-homogeneous, isothermal batch system (Figure 3.12). Statistical results are displayed in Table 3.1 and Table 3.2 which show the estimated parameters with their standard deviations. According to Chou et al. [68] and experimental studies by our group (Article III), the perhydrolysis reaction seems to be the slow step of the reaction system. In this case, perhydrolysis is the slowest reaction, followed by the epoxidation and the ring opening. Also the activation energy for the perhydrolysis is higher than for the other reactions. Ring opening shows to be the most prominent reaction above all, which is in accordance to the experimental data. In Figure 3.14, the consumption of the double bonds (in red) proceeds faster than the creation of epoxidized oleic acid (in black).

The distribution coefficient of acetic acid was estimated to be 2.75 ± 1.13, which indicates that acetic acid is present in larger proportion in the aqueous phase. This is in accordance with the physical character of the system. For the case of peracetic acid, the correlation $K_{PAA} = 0.33K_{AA}$ was used for the estimation of this value, which results in 0.908 ± 0.373, indicating that peracetic acid exists in a higher proportion in the organic phase.

Table 3.1 Statistical results for conventional heating.

Total SS (corrected for means)	0.2005E+04
Residual SS	0.4247E+02
Std. Error of estimate	0.3571E+00
Explained (%):	97.88

Table 3.2 Estimated kinetic constants, activation energies and acetic acid distribution coefficient for epoxidation under conventional heating.

	Estimated Parameters	Estimated Std Error	Est. Relative Std Error (%)	Parameter Std. Error
k_{perh}	0.132E-03	0.835E-05	6.3	15.8
k_{epox}	0.345E-02	0.524E-03	15.2	6.6
k_{RO}	0.700E-02	0.153E-02	21.9	4.6
$E_{a_{perh}}$	0.823E+05	0.624E+04	7.6	13.2
$E_{a_{epox}}$	0.519E+05	0.127E+05	24.5	4.1
$E_{a_{RO}}$	0.371E+05	0.208E+05	56.1	1.8
K_{AA}	0.275E+01	0.113E+01	41.1	2.4

The units: k_{perh}, k_{epox}, k_{RO} = ( ) L/mol/min; activation energies (E_a) = () J/mol, K_{AA}, A_{eq}= (). A_{eq} is the pre-exponential factor of the perhydrolysis equilibrium constant, eq. (1).

Table 3.3 displays the correlation matrix for the estimated parameters. Overall, the correlation between the parameters is rather insignificant.

Table 3.3. Correlation matrix of the parameters for conventional heating

	k_{perh}	k_{epox}	k_{RO}	$E_{a_{perh}}$	$E_{a_{epox}}$	$E_{a_{RO}}$	K_{AA}
k_{perh}	1.000						
k_{epox}	-0.234	1.000					
k_{RO}	0.053	0.087	1.000				
$E_{a_{perh}}$	-0.434	0.065	-0.038	1.000			
$E_{a_{epox}}$	0.141	-0.390	-0.071	-0.454	1.000		
$E_{a_{RO}}$	-0.039	-0.061	-0.704	0.059	0.110	1.000	
K_{AA}	-0.207	-0.547	0.020	0.106	0.014	-0.005	1.000

Figure 3.13 represents the parameter set plot for the sensitivity analysis, which demonstrates a rather well-defined minima for most of the parameters. In Figure 3.14, it can be observed that the model describes the experimental data fairly well.

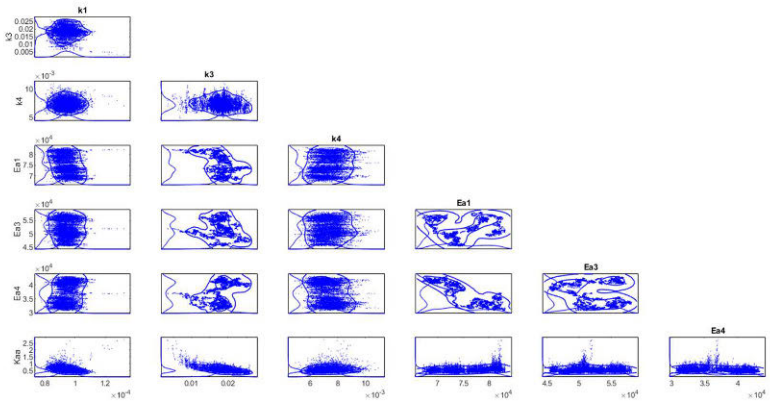

Figure 3.13. MCMC sensitivity plot. Predictive distribution for the estimated parameters for conventional heating.

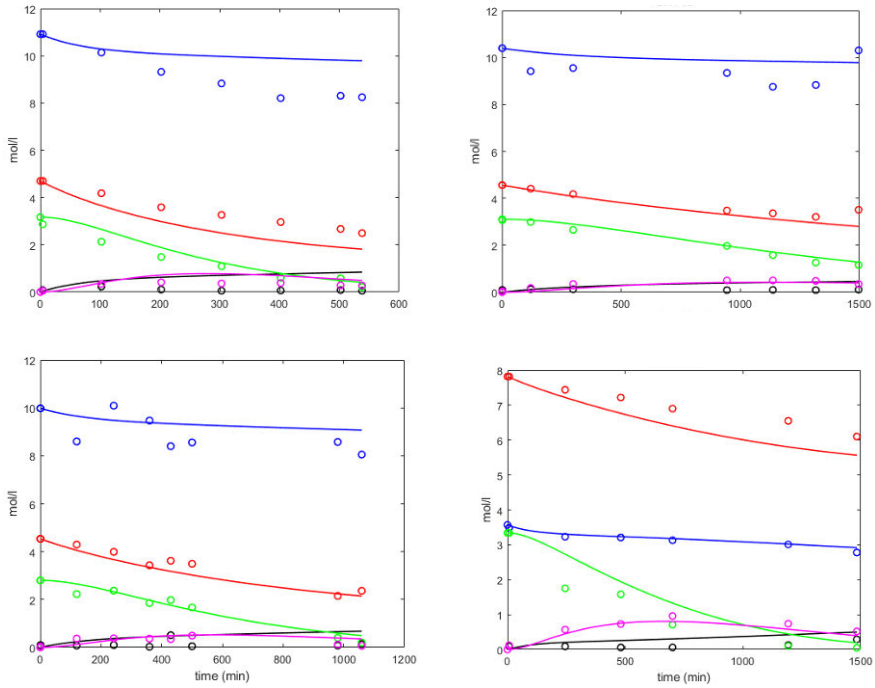

Figure 3.14. Fitting of the model to the experimental data for conventional heating. In black: **epoxyleic acid**, pink: peracetic acid, red: oleic acid, green: hydrogen peroxide and blue: acetic acid (V).

Microwave heating

Experiments under microwave heating were modelled as a pseudo-homogeneous system composed of two CSTRs in recirculation (Figure 3.12). Overall statistical results are displayed in Table 3.4 and Table 3.5 which show the estimated parameters and their standard deviations. The estimated parameters show a similar tendency to the model for conventional heating: perhydrolysis is the slowest reaction, followed by epoxidation and ring opening. Moreover, the estimation of the activation energies for perhydrolysis and ring opening presented high standard errors. This might be due to the complexity of the system and the relatively narrow temperature interval of the experiments. It must be taken into consideration that the current model is a simplified view of the system, whereas the reality is much more complex. The distribution coefficient of acetic acid was estimated to be 0.393 ± 0.073 and for peracetic acid 0.130 ± 0.024. This indicates that for microwave heating, acetic acid and peracetic acid are in larger proportion in the organic phase.

Table 3.4**.** Statistical results for microwave heating.

Total SS (corrected for means)	0.2426E+04
Residual SS	0.5624E+02
Std. Error of estimate	0.3295E+00
Explained (%):	97.68

Table 3.5. Estimated kinetic constants, activation energies and acetic acid distribution coefficient for epoxidation under microwave heating.

	Parameters	Std Error	Std Error (%)	Std. Error
k_{perh}	0.615E-03	0.374E-04	6.1	16.4
k_{epox}	0.331E-02	0.517E-03	15.6	6.4
k_{RO}	0.807E-01	0.576E-01	71.4	1.4
$E_{a_{perh}}$	0.600E+05	0.119E+04	19.8	5.1
$E_{a_{epox}}$	0.362E+05	0.167E+05	46.3	2.2
$E_{a_{RO}}$	0.708E+05	0.152E+06	214.6	0.5
K_{AA}	0.439E+00	0.870E-01	19.8	5.0

The units: k_{perh}, k_{epox}, k_{RO} = ( ) L/mol/min; activation energies (E_a) = () J/mol, K_{AA}, A_{eq}= (). A_{eq} is the pre-exponential factor of the perhydrolysis equilibrium constant, eq. (1).

Table 3.6 displays the correlation matrix for the estimated parameters for which the correlation between the parameters seems to be negligible.

Table 3.6. Correlation matrix of the parameters for microwave heating

	k_{perh}	k_{epox}	k_{RO}	$E_{a_{perh}}$	$E_{a_{epox}}$	$E_{a_{RO}}$	K_{AA}
k_{perh}	1.000						
k_{epox}	0.316	1.000					
k_{RO}	0.004	0.024	1.000				
$E_{a_{perh}}$	0.257	0.226	-0.008	1.000			
$E_{a_{epox}}$	-0.193	-0.270	-0.008	-0.437	1.000		
$E_{a_{RO}}$	-0.008	-0.028	0.120	-0.015	0.090	1.000	
K_{AA}	0.121	-0.748	0.012	-0.078	-0.059	-0.005	1.000

Figure 3.15 represents the parameter set plot for sensitivity analysis. Well-defined minima are found between most of the parameters. In Figure 3.16, the fit of the model to the experimental data shows that the kinetic models can well predict the trends of the concentrations with time.

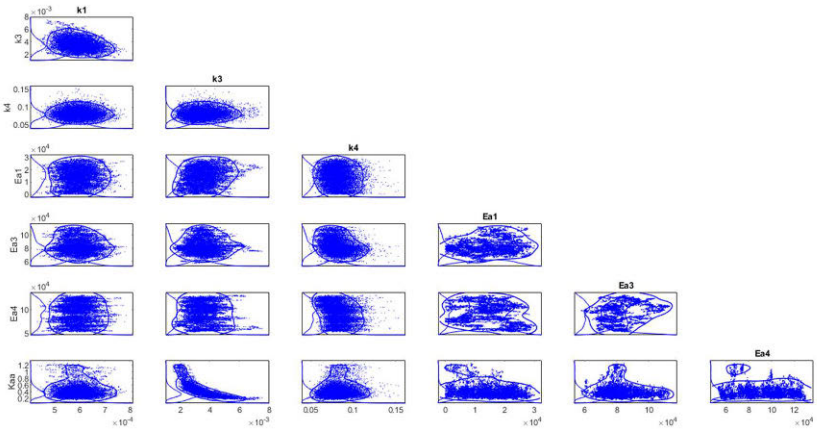

Figure 3.15. MCMC sensitivity plots. Predictive distribution for the estimated parameters for microwave heating.

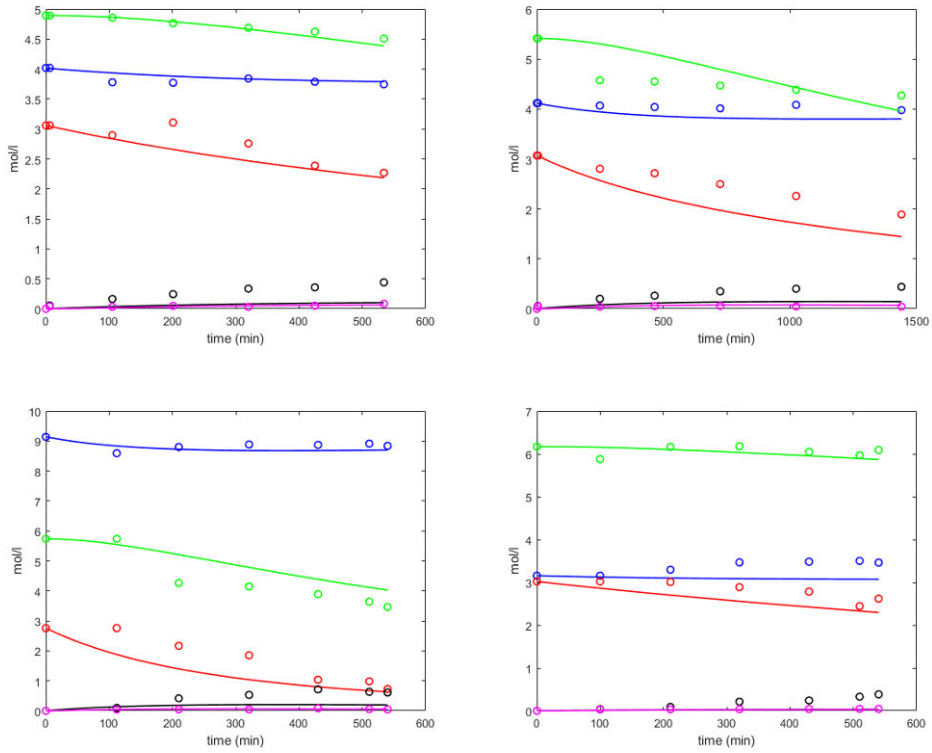

Figure 3.16. Fitting of the model to the experimental data for microwave heating. In black: **epoxyoleic acid**, pink: peracetic acid, red: oleic acid, green: hydrogen peroxide and blue: acetic acid (V).

According to M. Lee and Marchant [56], the thermal absorptivity of a mixture to microwaves is dependent on three parameters: temperature, reactant concentration and electric field amplitude, which is associated directly to the input power. In this study, the temperature increase between the reactor and the microwave cavity (D) was measured and a correlation was found with the product between the input power (lul^2) and the aqueous-to-oil phase ratio (α) (Eq. 24). Figure 3.17 indicates that a rather linear trend between these two parameters is obtained.

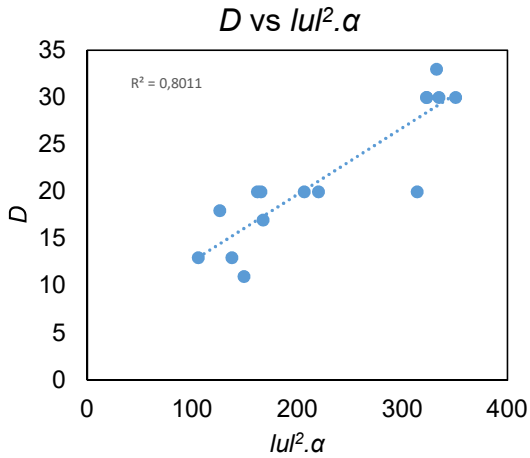

Figure 3.17. Correlation between temperature difference between MW cavity and reactor with input power and aqueous-to-oil phase ratio.

4. Epoxidation of oleic acid in the presence of heterogeneous catalyst (Articles III, IV, VI)

4.1 Screening of solid catalysts

In the previous chapter, epoxidation of oleic acid with peracetic acid was performed in the absence of added catalysts. Optimal reactant molar ratios were obtained and the influence of temperature, stirring speed, and microwave heating was studied. However, to reduce the reaction times (from 24 h to 6 h) and to improve the yield of epoxide, several acidic ion-exchange resins were screened to enhance the formation rate of percarboxylic acid. The results are reported in the present chapter.

A variety of ion exchange resins are commercially available with different matrix compositions, pore sizes, degrees of cross-linking and particle sizes. This part of the study focuses on the catalyst screening with seven types of acidic ion exchange resins (AIER) for the epoxidation of oleic acid: Amberlite IR-120, Amberlyst 15, Smopex®, Dowex 50x8-100, Dowex 50x8-50, Dowex 50x2-100 and Nafion™.

The catalysts described in Table 4.1 were screened under similar reaction conditions, using 50°C as the reaction temperature. This specific temperature was chosen based on the experiments from Chapter 3: the epoxidation rate is very low at 40°C but high temperatures, on the other hand, promoted ring opening reactions. The relative consumption of the double bonds of oleic acid and the conversion to epoxyoleic acid with time are presented in Figure 4.1. Overall, two reaction paths for epoxidation can be distinguished: a non-catalytic and a catalytic one. In the absence of a solid catalyst, the reaction still takes place slowly because the perhydrolysis of acetic acid proceeds spontaneously. The use of any solid catalyst is highly advantageous as compared with the results obtained in the absence of a solid catalyst.

In terms of the conversion of double bonds, the catalysts Dowex 50x8-50, Dowex 50x8-100 and Amberlite IR-120 exhibited the best performance and similar activity, because all three catalysts have equal capacities, degrees of crosslinking and moisture contents.

The results displayed in Figure 4.1 are in agreement with those of Turco et al.[49] and Rios et al.[69], who found that the conversion of double bonds and the selectivity towards epoxide increased as the degree of crosslinking incremented from 2% (Dowex 50Wx2-100) to 8% (Dowex 50x8-50, Dowex 50x8-100 and Amberlite IR-120). However, when there is a further increase in the degree of crosslinking up to 20% (Amberlyst 15), the selectivity decreased. The degree of crosslinking has a strong effect on the resin structures, because it controls the porosity of the resin [70,71]. Higher crosslinking implies a smaller pore size, thus a higher surface area and an increased probability of hydrogen peroxide and acetic acid having contact with the acid sites. However, the structure of Amberlyst 15 has a macroreticular nature which might enable an easy protonation of the oxirane ring and ring opening [49]. These so-called macroporous structures have wide internal surface areas and larger molecules can penetrate the interior of the resin structure [38]. Taking into consideration that the average lengths of oleic acid and epoxyoleic acids at their most stable shapes are 1.8 – 2.1 nm, a pore size of 40 – 80 nm is large enough to allow the epoxyoleic acid to enter into the macropores.

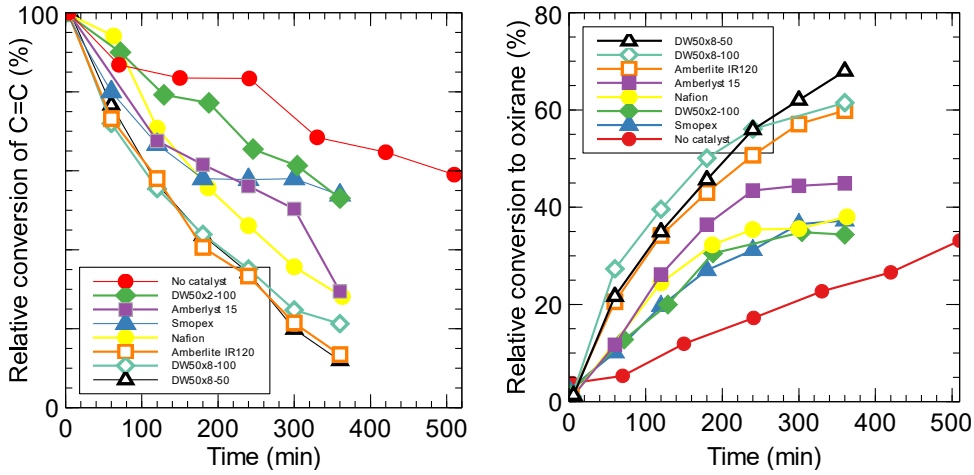

Figure 4.1 Relative conversion of double bonds (left) and relative conversion to oxirane (right) for eight different catalysts at 50 °C for the epoxidation of oleic acid by peracetic acid.

Table 4.1 Properties of the cation exchange resins used.

Catalyst	Polymer type	Polymer nature	Active group	Cross-linking (%)	Moisture content (% mass)	Capacity by dry weight (meq/g)	Native particle size range (mm)	Pores (nm)
Amberlite IR-120	Gel	Styrene-divinylbenzene	Sulfonic acid	8	52	4,4	0,30 - 1,20	-
Amberlyst 15	Macroreticular	Styrene-divinylbenzene	Sulfonic acid	20-25	5	4,7	0,45 - 0,60	40 - 80
Dowex 50Wx2-100	Gel	Styrene-divinylbenzene	Sulfonic acid	2	79	4,8	0,15 - 0,30	-
Dowex 50Wx8-100	Gel	Styrene-divinylbenzene	Sulfonic acid	8	51	4,8	0,15 - 0,30	-
Dowex 50Wx8-50	Gel	Styrene-divinylbenzene	Sulfonic acid	8	52	4,8	0,30 - 0,84	-
Smopex-101	Fibre	Styrene sulfonic acid grafted polyolefin fiber	Sulfonic acid	2	44	2,6	-	-
Nafion™ NR40	Beads	Tetrafluoroethylene and perfluoro-3,6-dioxa-4-methyl-7-octenesulfonyl fluoride	Perfluorosulfonic acid	-	<2	1,0	3-4	-

Swelling is another key factor to be considered when using ion exchange resins. In general, the swelling capacity is strongly dependent on the degree of crosslinking and the nature of the surrounding medium. With a higher degree of crosslinking, the moisture content is reduced and swelling behavior of the ion exchange resin is hampered. As a result, only macroporous ion exchange resins are suitable for reactions in nonpolar media [38]. Moreover, catalysts with high degrees of crosslinking and or low moisture contents, such as Amberlyst 15 and Nafion, allow contact of the catalyst surface with nonpolar media and the opening of the oxirane ring is promoted.

The large particle size and lower capacity of Nafion show to be unfavourable for the epoxidation process. Similar results were obtained by Rios et al.[69] when applying a composite material made of Nafion –

low conversions were obtained because of a lower concentration of active sites compared to Amberlyst 15.

In the case of Smopex-101, the external mass transfer limitations were highly influential because of the compaction of the fibres inside of the rotating bed reactor (RBR) chamber. This might be the reason why the double bond conversion reaches a plateau around 200 min of the reaction. Experiments with Smopex fibres floating freely in the reaction medium were conducted and they revealed better yields of epoxide. This indicated that the use of the Spinchem basket was not suitable for this catalyst. However, the degree of ring opening was quite high since the active sites were completely exposed and able to easily protonate the oxirane ring.

The screening study revealed that Dowex 50Wx8-50 was the most active and suitable catalyst for the epoxidation of oleic acid, followed by Dowex 50Wx8-100 and Amberlite IR-120. Dowex 50Wx8-50 was selected for evaluating the effect of the temperature on the reaction in order to optimize the operating conditions. Moreover, additional studies on the epoxidation under heterogeneous catalysis were conducted with Amberlite IR-120.

4.1.1 Dowex x8-50 - Temperature effect

Kinetic experiments were conducted at 40, 50 and 60°C to reveal the effect of this parameter on the activity of the selected catalyst. Figure 4.2 reveals that the conversion of double bonds increases with temperature and it confirms that the selectivity to oxirane seems to decay with temperature after reaching a maximum for 60°C. This is due to the oxirane ring cleavage reactions which are intensified by the increase of temperature [18,21,72–78]. Higher oxirane contents were found at 60°C but a minimum degree of ring opening throughout the reaction was observed at 40°C. Since the highest possible operating temperature of Dowex-x8-50 exceeds 100°C, the stability of the catalyst does not play any role in the observed results. Nonetheless, according to Campanella and Baltanás [52], ring cleavage is triggered by the protonation of the oxirane ring in acidic media, and this process is highly promoted by the reaction temperature. Moreover, Campanella and Baltanás also suggested that the ring opening reactions proceed on the surface of the catalyst (Amberlite IR120) and confirmed that the external surface protons of the resin are the main factor responsible for the degradation of the ring as the degradation rate was directly proportional to the available external area of the catalyst. Because Dowex-x8-50 has a relatively low degree of crosslinking and high moisture content, the nonpolar agents in the mixture are not able to access the bulk of the catalyst; however, the active sites in the outermost external surface of the catalyst are exposed and available to participate in the ring opening reactions.

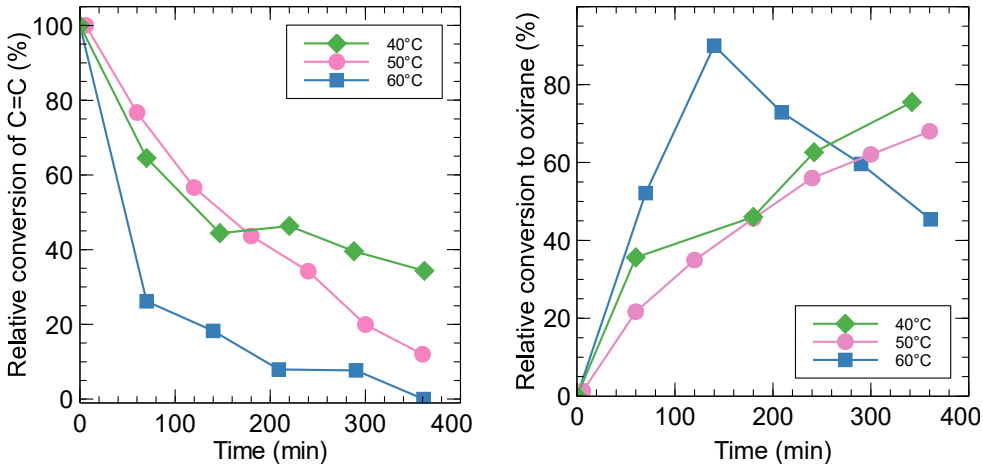

Figure 4.2 Relative conversion of double bonds (left) and relative conversion to oxirane (right) at different temperatures.

4.2 Amberlite IR-120

4.2.1 Spinchem Rotating Bed Reactor (RBR) - Catalyst loading

In the absence and presence of catalyst, the kinetics of epoxidation system, including conversion of double bonds and formation of oxirane groups, has been found to be quite similar by using a conventional stirrer and a SpinChem RBR system [Article III]. Moreover, the series of experiments performed for testing different catalyst loadings were conducted while implementing the RBR.

The effect of applying a solid-acid catalyst (Amberlite IR-120) on the epoxidation of oleic acid (OA) was investigated by using four different catalyst amounts: 0, 6, 12, and 18wt% (w.r.t. oils mass) loading on a dry basis at 50°C. Figure 4.3 shows the conversion of double bonds and relative conversion to oxirane versus time at different catalyst loadings. The results revealed that the conversion of OA and the oxirane formation become faster with an increasing amount of catalyst. Epoxidation seemed to proceed more rapidly than ring opening, given that, for all of the experiments, the tendency to increase the epoxy content was maintained.

In these experiments, the concentration of hydrogen peroxide (HP) decreased linearly during the reaction time. The content of HP diminished faster as the catalyst amount was

increased. The concentration of acetic acid (AA) seems to remain constant, confirming the fact that it is regenerated in the organic phase upon epoxidation and transferred back to the aqueous phase (Figure 1.2) and, additionally, it confirms that it was not consumed in ring opening reactions.

As expected, an increase in the catalyst amount resulted in an increase in the rate of the in situ peracetic acid formation. In the experiments conducted with 0% and 6% Amberlite, the PAA content remained rather constant under 1wt% during the course of the reaction, indicating that it is generated in the perhydrolysis step and consumed by the epoxidation step. However, for the experiment with 18wt% Amberlite, it was observed that, as complete conversion of OA into epoxidized OA was approached, the peracetic acid content started to increase and accumulate in the aqueous phase. This is due to the fact

that the consumption of PAA for the epoxidation is decreasing with less available double bonds in the oil. Similarly, accumulation of PAA was also detected in the experiment with a catalyst load of 12wt%.

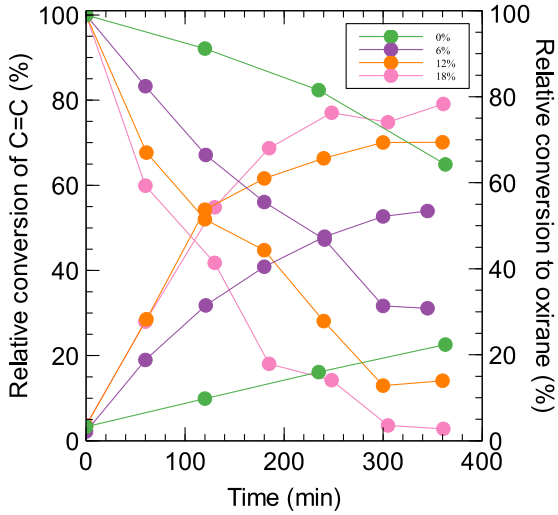

Figure 4.3 Relative conversion of double bonds (left axis) and relative conversion to oxirane (right axis) at different catalyst loadings.

Figure 4.4 shows that the conversion of the double bonds increases with an approximate linear tendency with the catalyst amount within the catalyst mass range of 0−21 g. A linear dependency might indicate the absence of external mass transfer limitations. Moreover, the small deviation from a linear behavior can be attributed to the fact that, with the increase of the catalyst mass, the catalyst placed inside the SpinChem chamber is more compacted and the mass transfer might be slightly influenced

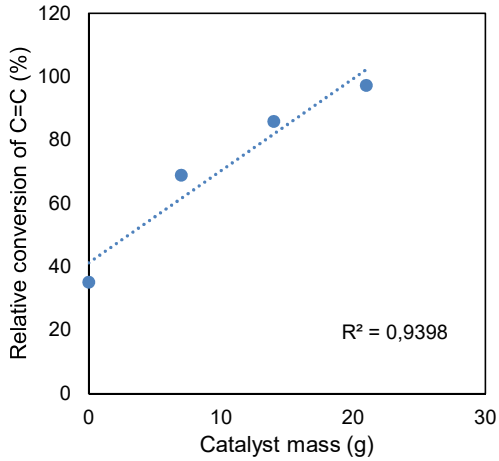

Figure 4.4 Conversion of double bonds in 6 h at 50 °C, as a function of the catalyst mass.

In the previous chapter, it was reported that stirring rates exceeding 450 rpm would suppress the mass transfer limitations. This observation, in addition to the approximate linear behavior of the double bond conversion with the catalyst amount, suggests that, when the Spinchem RBR is operated at a minimum stirring speed of 1200 rpm, the reaction occurs in the kinetic regime. This means that the reaction rate is governed by the rate limiting steps of the chemical reaction, rather than by the mass transfer.

In addition, the use of the Spinchem RBR streamlines the experimental procedure, because no filtrations are needed at the end of the reaction to separate the solid catalyst from the liquid medium. In addition, the use of RBR might extend the lifespan of the catalyst, because no mechanical wear of the particles occurs, whereas, upon classical stirring operation, the particles are pushed against the reactor walls because of the centrifugal forces of the stirring.

4.2.2 Acetic acid and propionic acid

Epoxidation of vegetable oils and free fatty acids is usually conducted with performic or peracetic acid. Performic acid (HCOOOH) is chemically less stable than peracetic acid (CH_3COOOH), because undergoes very exothermic secondary reactions, leading to gaseous products. By increasing the carbon chain of the percarboxylic acid, the risk of thermal runaway is diminished. Thus, acetic acid was considered to be a safer oxygen carrier for this study. Moreover it has been recently demonstrated that the use of perpropionic acid (CH_3CH_2COOOH) for the epoxidation of vegetable oils and free fatty acids is thermally safer than the use of peracetic acid or performic acid [58]. Therefore, the effect of propionic acid on the epoxidation of oleic acid was investigated and compared to acetic acid. Three different catalyst amounts were tested: 0%, 3%, and 12% (weight percent w.r.t. oil mass). The conversion of double bonds over time for epoxidation with several catalyst loadings is presented in Figure 4.5.

In all of the cases, epoxidation in the presence of acetic acid (AA) resulted in a more rapid conversion, compared to propionic acid (PA). This evidences how AA works as a more efficient oxygen carrier than PA. According to Leveneur et al. [79], the apparent rate constant of the perhydrolysis reaction catalyzed by Amberlite IR-120 is higher with AA compared to PA. Furthermore, a review article points out that perpropionic acid is less reactive than peracetic acid [80]. In a third study by Leveneur et al.[32], it was corroborated that in the epoxidation of oleic acid under microwave and conventional heating, higher yields were achieved with AA, compared to PA. This indicates that acetic acid provides a suitable balance between safety and efficiency among the three carboxylic acids: formic, acetic and propionic acid.

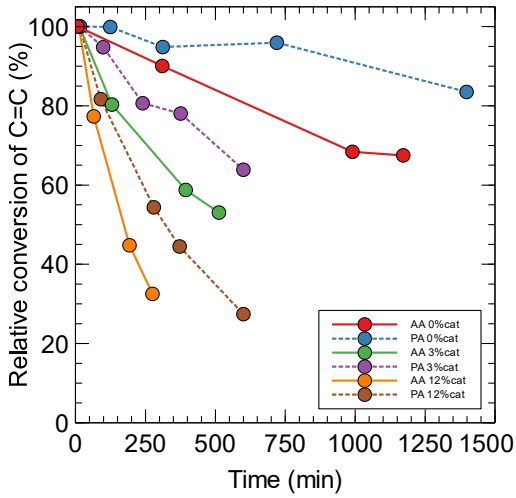

Figure 4.5 Conversion of double bonds for AA and PA with different catalyst loadings at 40 °C.

4.3 Microwave heating

In the previous chapter, it was reported that microwave irradiation (MW) affects positively the epoxidation of oleic acid in the absence of a heterogeneous catalyst, producing significantly higher yields than those obtained in the presence of conventional heating at 40°C. The observation was attributed to a combination of the selective heating effect of the microwaves and the higher temperature profile for the experiments with MW heating, which was possible due to the fact that the reactor was cooled externally. Subsequently, the reaction was carried out with exactly identical temperature profiles throughout the reactor system for MW and CH and higher epoxide yields were achieved under MW irradiation. This was attributed to the selective heating effect of microwaves: the aqueous phase acted as a microwave absorbent while the oil phase is transparent to microwaves [32]. Consequently, higher temperatures were reached in the aqueous phase compared to CH where the phases have the same temperature throughout the system. The slow step of the process is the perhydrolysis step, which takes place in the aqueous phase. Therefore selective heating of the aqueous phase is expected to have a positive effect.

To study this phenomenon under heterogeneous catalysis, epoxidation of oleic acid under MW irradiation was conducted in the presence of six different catalysts, with CH and MW in parallel. Figure 4.6 displays a comparison between the CH and the MW experiments for each catalyst studied. The relative conversion of double bonds and the relative conversion to oxirane for the epoxidation of oleic acid with peracetic acid are depicted versus the reaction time. The results reveal almost identical evolutions of the double bond conversion and oxirane formation with time for MW and CH for each catalyst, which implies that MW heating did not essentially affect the conversion of the double bonds and the formation of the desired products any differently from CH. However, Figure 4.6 reflects that the conversions for Amberlite IR-120, Amberlyst 15 and Nafion and RCO for Dowex50x8-50 and Smopex are higher with CH compared to MW. This might be explained by the fact that the mixture is exposed for longer to higher temperatures inside the heat exchanger compared to the MW cavity, which is only

3 cm long. MW heating is much more rapid so it requires less exposure to reach a high temperature, compared to convective heating. Even though temperature profiles in the loop were similar and the highest temperatures reached for both MW and CH were identical, the exposure time of the reactants to that temperature was longer for CH. The longer exposure time to higher temperatures enabled a higher conversion of double bonds and epoxide formation. Taking into consideration the pattern followed by five out of six catalysts tested and the similarities in the properties of Dowex 50x8-100, Dowex 50x8-50 and Amberlite IR-120, the slightly higher conversion observed for Dowex 50x8-100 in the presence of MW irradiation compared to CH can be considered odd.

On the other hand, it is important to point out that rapid heating is responsible for a more energy-efficient process. This opens up the possibility of designing a new reactor setup that could exploit the advantages of microwave irradiation by allowing the mixture to remain at a higher temperature for a longer time within the safety constraints.

When comparing the results with the non-catalytic experiments reported in the previous chapter, a profound enhancing effect of MW exposure was visible by increasing the reaction rate; i.e. a higher product yield was obtained within a shorter reaction time. This enhancement is clearly absent during the epoxidation of oleic acid in the presence of the solid resin catalysts.

Several authors have reported that the formation of peracetic acid is the slow step of the epoxidation of double bonds [68]. As discussed previously, the enhancing effect of the MW heating was attributed to the so-called selective heating, which produces an increase in the temperature of the aqueous phase, thus boosting the production of peracetic acid. Cation exchange resins have a similar effect upon epoxidation because they have the ability to accelerate the rate of perhydrolysis [60,81]. It can be concluded that the enhancing effect of the MW heating observed previously for non-catalytic epoxidation of oleic acid is very much masked by the effect of the heterogeneous catalyst. The total perhydrolysis rate (r_{TOT}) consists of two contributions: $r_{\mathrm{TOT}} = r_{\mathrm{HOMOG}} + r_{\mathrm{HETEROG}}$. The homogeneous rate ($r_{\mathrm{HOMOG}}$) is enhanced by microwavess, but because $r_{\mathrm{HETEROG}} \gg r_{\mathrm{HOMOG}}$, the microwave effect becomes ‘shadowed’ by the heterogeneously catalysed part of the rate (r_{HETEROG}).

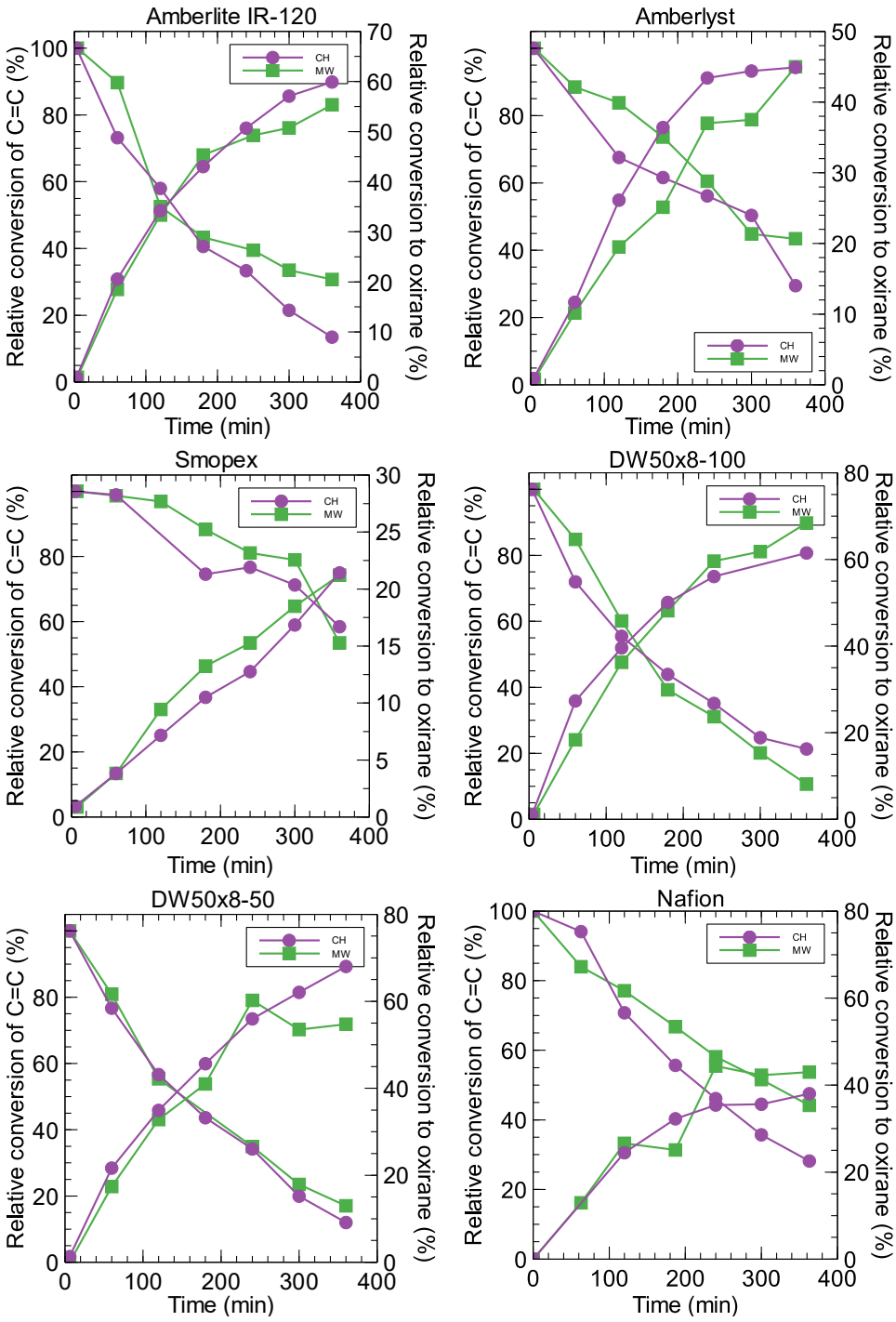

Figure 4.6 Conversion of double bonds for AA and PA with different catalyst loadings at 40 °C.

4.3.1 Water-to-oil ratio

Previously in this work, increasing the aqueous-to-oil phase ratio seemed to have an effect of improving the epoxidation of OA. In this section, the influence of the aqueous-to-oil phase volume ratio was studied for both microwave and conventional heating. Amberlite IR-120 was used as the catalyst. Figure 4.7 depicts the experiments with the maximum water loading as "+++" (addition of 200 mL of water), experiments with medium water loading as "++" (addition of 120 mL of water) and the experiments with no additional water as "+", which contain only the water present in the 30% H_2O_2 solution.

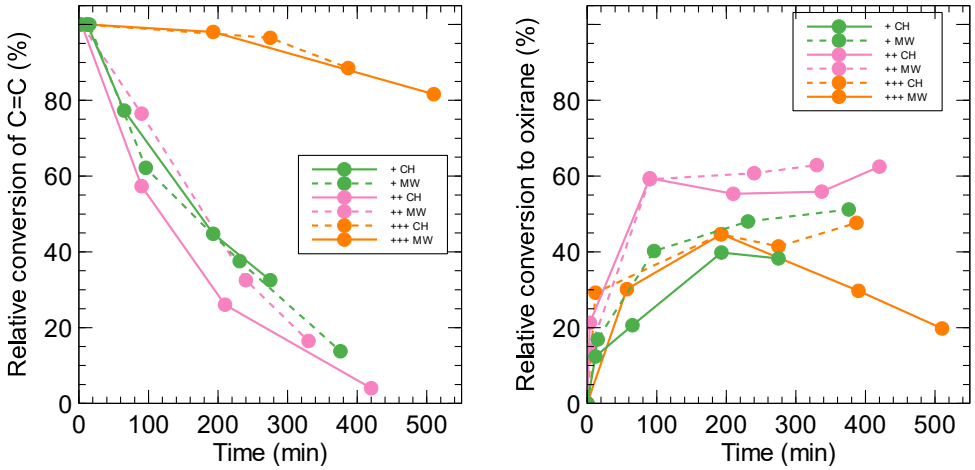

Figure 4.7 Conversion of double bonds with time (left) and relative conversion to oxirane with time (right) for MW and CH for three different volumes of additional water at 40 °C.

The conversion of double bonds decreased more rapidly for the medium water loading with CH (++); only in this case the conversion of double bonds was almost complete. The reaction of the double bonds was slowest at the maximum dilution.

Figure 4.7 shows that the ring opening reactions are more pronounced for the experiment at the maximum water loading and under microwave irradiation. Indeed, after 200 min of reaction, the RCO reached the value of 45%; after 500 min, the selectivity decreased to 20%. This could be due to the fact that, at high water content, the MW absorption of the aqueous phase is higher than that for lower water contents; a higher temperature is achieved, which can promote the ring opening reactions.

In both MW and CH experiments, the best yields were obtained in the case of the medium water content. MW irradiation seemed to promote epoxidation and prevent ring opening in all the experiments, except when the aqueous phase was much larger than the organic one (+++).

In accordance with the work of Leveneur et al. [32], higher yields were achieved when using MW irradiation and higher aqueous-to-oil phase volume ratios. However, this tendency reverts when there is too much water in excess, i.e., experiments with the highest amount of water (+++). This can be attributed to the fact that, when diminishing the concentration of the components in the aqueous phase, namely, the peracid, the concentration in the organic phase also decreases, according to the partition coefficient [64].

4.4 Kinetic modelling

In the presence of a heterogeneous catalyst, a three-phase reaction system is formed. A schematic overview of the epoxidation process is provided in Figure 1.2 and the overall reaction stoichiometry is summarized in equations I-VIII.

The perhydrolysis step is mainly catalysed by the solid catalyst, but also the carboxylic acid itself is able to catalyse the process, as discussed the previous section. Consequently, the total rate of perhydrolysis in the presence of a heterogeneous catalyst is

$$R_1 = R_{1ncat} + R_{1ca} \cdot \rho_B \tag{27}$$

where $\rho_B = m_{cat}/V_L$, i.e. mass of catalyst-to-liquid volume ratio, the subscripts *cat* and *ncat* refer to the heterogeneously catalysed epoxidation and the epoxidation proceeding spontaneously in the absence of an added catalyst.

The surface reaction mechanism in the presence of the cation-exchange resin catalyst is described by the scheme below. The main hypothesis for the heterogeneously catalysed mechanism is that it is completely analogous with the homogeneous one, but the dissolved homogeneous acid is replaced by the sulfonic acid groups on the cation exchange resin in the reaction mechanism.

The carboxylic acid adsorbs on the acid site on the solid catalyst ($* = -\mathrm{SO_3}H$) and H_2O_2 from the bulk of the aqueous phase makes a nucleophilic attack, whereas H_2O_2 adsorbed on the catalyst surface has the role of a spectator. The process can be summarized as

$$RCOOH + * \rightleftharpoons RCOOH^*$$
$$RCOOH^* + H_2O_2 \rightleftharpoons RCOOOH + * + W$$

The proton transfer step is rapid, whereas the nucleophilic attack is presumed to be the rate limiting step. The steps following the nucleophilic attack are generally considered to be rapid and they can thus be merged. The total site balance for the catalyst surface can be written as

$$C_{AA}* + C_{PAA}* + C_{HP}* + C_W* + C* = C_0 \tag{28}$$

where the asterisk (*) refers to a surface site and C_0 is the total concentration of sites available on the surface.

The Langmuir adsorption equilibria of each species give the relation

$$C_i* = K_i\, C_i\, C* \tag{29}$$

where K_i denotes the adsorption equilibrium constant. The relation (29) is inserted in the balance equation (28) from which the concentration of vacant sites is solved,

$$C* = \frac{C_0}{1 + \Sigma K_i C_i} \tag{30}$$

and the concentrations of the adsorbed species are given by

$$C_i* = \frac{K_i C_i C_0}{1+\Sigma K_i C_i} \tag{31}$$

After inserting this relation to the rate equation is obtained,

$$R_{1cat} = k_1 C_{AA} * C_{HP} - k_{-1} C_{PAA} * C_W \tag{32}$$

The expressions for the surface concentrations of acetic acetic (AA) and peracetic acid (PAA) are inserted in the rate expression (32) according to equation (31), which gives the rate of heterogeneously catalysed perhydrolysis,

$$R_{1cat} = \frac{k_{cat}\left(C_{AA}C_{HP} - \frac{C_{PAA}C_W}{K}\right)}{1+\Sigma K_i C_i} \tag{33}$$

The rate equation for the perhydrolysis in the absence of an added catalyst is given by Leveneur et al. [82] (*ncat* in eq. 34). The overall rate of the perhydrolysis step becomes

$$R_1 = R_{perh} = \left(\frac{k_{cat}\rho_B}{1+\Sigma K_i C_{i_{aq}}} + k_{ncat}\sqrt{\frac{K'_{AA}.C_{AA_{aq}}}{C_{W_{aq}}}}\right)\left(C_{AA_{aq}}C_{HP_{aq}} - \frac{C_{PAA_{aq}}C_{W_{aq}}}{K}\right) \tag{34}$$

The epoxidation step is considered to be elementary and the rate equation is obtained in a straightforward way,

$$R_2 = k_{epox}.C_{OA_{oil}}.C_{PAA_{oil}} \tag{35}$$

The ring opening reactions are acid catalysed, i.e. a proton transfer takes places to the epoxide ring. The steps are summarized below,

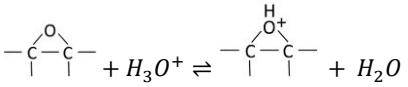

(A)

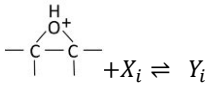

(B1)

$$Y_i + H_2O \rightleftharpoons ROP_i + H_3O^+ \tag{B2}$$

where X_i is the ring opening agent (W, HP, AA, PAA) and Y_i is the corresponding reaction intermediate. The ring opening with these agents always leads to a formation of a hydroxyl group, whereas the neighbouring group in the product molecule is OH, OOH, $OCOCH_3$ or $OOCOCH_3$, depending on the ring opening agent [Article VIII].

The protonation step is rapid, while the ring opening step is slower. The steps are denoted by

$$EOA + H^+ \rightleftharpoons EOA^+ + W \quad \text{(I)}$$
$$EOA^+ + X_i + W \rightleftharpoons ROP_i + H^+ \quad \text{(II)}$$

The quasi-equilibrium hypothesis for the rapid steps gives

$$K_{\mathrm{I}} = \frac{C_{EOA+}C_{Woil}}{C_{EOA}C_{H+}} \quad (36)$$

from which the concentration $C_{\mathrm{E+}}$ is solved and inserted in the rate equation which becomes

$$R_{\mathrm{ROi}} = k_{ROPi}C_{H+}C_{EOA}C_{Xi} \quad (37)$$

In this case, the protons (H^+) originate mainly from acetic acid, which is a much stronger acid than peracetic acid. For weak acids the proton concentration is proportional to the square root of the acid concentration. Thus rate equation (37) can in the actual case be written as

$$R_{ROP} = (k_{ROP,AA}\ C_{AA_{oil}} + k_{ROP,PAA}\ C_{PAA_{oil}} + k_{ROP,W}C_{W_{oil}} + k_{ROP,HP}C_{HP_{oil}}).C_{EOA_{oil}}.\sqrt{\frac{K'_{AA}.C_{AA_{oil}}}{C_{W_{oil}}}}$$

4.4.1 Reactor model

4.4.1.1 Mass balances for multiphase stirred tank reactors

The structure of the loop reactor system is displayed schematically in Figure 2.1. Since the temperatures in the stirred vessel and in the loop were different, the system was described as two stirred tanks (T1 and T2), as assumed for the microwave heating modelling described in detail in Chapter 3. The assumption of stirred tank was fully motivated for the reactor vessel, which was exposed to very vigorous stirring (1200 rpm). For the loop, the hypothesis of stirred tank can be motivated by the short residence time inside the loop, i.e. low reactant conversion for one cycle. At low reactant conversions, different reactor models give very similar conversions and selectivities. Three phases co-exist in the stirred reactor vessel (oil, liquid, solid catalyst), while the loop is a two-phase system, because the catalyst was fixed in the mixing device in the stirred tank. The modelling principle is illustrated in Figure 3.12 (right).

The mass balance equation for the aqueous-phase (*aq*) components in T1 can be written as

$$C_{i2_{aq}}\dot{V_{aq}} + \sum v_{ij}R_{jaq}V_{aq} = N_{i1}A_1 + \frac{dn_{i1_{aq}}}{dt} + C_{i1_{aq}}\dot{V_{aq}} \quad (38)$$

where N and A denote the interfacial flux and interfacial (oil-aqueous phase) area, n is the amount of substance, $\dot{V}$ is the volumetric flow rate and V is the volume. All the symbols are explained in Notation.

For the components in the oil (*oil*) phase, an analogous mass balance equation can be written,

$$C_{i2_{oil}}\dot{V_{oil}} + N_{i1}A_1 + \sum v_{ij}R_{joil}V_{oil} = \frac{dn_{i2_{oil}}}{dt} + C_{i1_{oil}}\dot{V_{oil}} \quad (39)$$

In the most general case, both mass balance equations are needed, and a suitable correlation for the mass transfer coefficients in the interfacial fluxes (N_i) is incorporated. Previous experience however indicates that the interfacial mass transfer is rapid compared to the perhydrolysis kinetics [64]. Therefore, it is justified to add balance equations (19) and (20) and to apply the hypothesis of phase equilibria for the oil and aqueous phases. The result of the addition becomes

$$\left(C_{i2_{aq}} - C_{i1_{aq}}\right)\dot{V_{aq}} + \left(C_{i2_{oil}} - C_{i1_{oil}}\right)\dot{V_{oil}} + \sum v_{ij}R_{jaq}V_{aq} + \sum v_{ij}R_{joil}V_{oil} = \frac{dn_{i1_{aq}}}{dt} + \frac{dn_{i2_{oil}}}{dt} \tag{40}$$

The amounts of substance are expressed with concentrations

$$n_{i1_{aq}} = C_{i1_{aq}}V_{aq} = C_{i1_{aq}}\alpha V_1 \tag{41}$$

$$n_{i2_{oil}} = C_{i2_{oil}}V_{oil} = C_{i1_{oil}}(1-\alpha)V_1 \tag{42}$$

where $\alpha = V_{aq}/V_1$ and the hypothesis of phase equilibrium is assumed

$$\frac{C_{i1_{oil}}}{C_{i1_{aq}}} = {K_i}^{-1} \tag{43}$$

Differentiation of equation (24) gives

$$\frac{dC_{i_{oil}}}{dt} = {K_i}^{-1}\frac{dC_{i_{aq}}}{dt} \tag{44}$$

The ratios of the volumetric flow rates of the aqueous and oil phases are expressed by the factor β,

$$\dot{V_{aq}} = \beta\dot{V} \tag{45}$$

$$\dot{V_{oil}} = (1-\beta)\dot{V} \tag{46}$$

The balance equation becomes

$$\left(C_{i2_{aq}} - C_{i1_{aq}}\right)\beta\dot{V} + \left(C_{i2_{oil}} - C_{i1_{oil}}\right)(1-\beta)\dot{V} + \sum v_{ij}R_{jaq}\alpha V_1 + \sum v_{ij}R_{joil}(1-\alpha)V_1 = \left(\alpha + \frac{1-\alpha}{K_i}\right)V_1\frac{dC_{i1_{aq}}}{dt} \tag{47}$$

The residence time is defined by

$$\frac{V_1}{\dot{V}} = \tau_1 \tag{48}$$

after which we obtain

$$\frac{\beta\left(C_{i2_{aq}} - C_{i1_{aq}}\right)}{\tau_1} + \frac{(1-\beta)\left(C_{i2_{oil}} - C_{i1_{oil}}\right)}{\tau_1} + \alpha\sum v_{ij}R_{jaq} + (1-\alpha)\sum v_{ij}R_{joil} = \left(\alpha + \frac{1-\alpha}{K_i}\right)\frac{dC_{i1_{aq}}}{dt} \tag{49}$$

The partition coefficient for the phase equilibrium is assumed to be temperature independent within the narrow temperature interval applied in the experiments,

$$\frac{C_{i1_{oil}}}{C_{i1_{aq}}} = \frac{C_{i2_{oil}}}{C_{i2_{aq}}} = K_i^{-1} \tag{50}$$

After a final arrangement, the mass balances of the components in the aqueous and oil phases become

$$\frac{dC_{i1_{aq}}}{dt} = \left(\alpha + \frac{1-\alpha}{K_i}\right)^{-1} \left(\frac{(\beta + \frac{1-\beta}{K_i})\left(C_{i2_{aq}} - C_{i1_{aq}}\right)}{\tau_1} + \alpha \sum v_{ij} R_{jaq} + (1-\alpha) \sum v_{ij} R_{joil} \right) \tag{51}$$

$$\frac{dC_{i1_{oil}}}{dt} = (\alpha K_i + 1 - \alpha)^{-1} \left(\frac{(\beta + \frac{1-\beta}{K_i})\left(C_{i2_{aq}} - C_{i1_{aq}}\right)}{\tau_1} + \alpha \sum v_{ij} R_{jaq} + (1-\alpha) \sum v_{ij} R_{joil} \right) \tag{52}$$

By assuming that the ratio between the volumetric flow rates is equal to the ratio between the corresponding volumes of the oil and aqueous phases, $\beta = \alpha$,

$$\frac{\dot{V_{aq}}}{\dot{V}} = \frac{V_{aq}}{V_1} \rightarrow \beta = \alpha \tag{53}$$

After some simplifying assumptions (Article VI), the operative forms of the mass balances for the first tank (T1) are written as

$$\frac{dC_{i1_{aq}}}{dt} = \frac{C_{i2_{aq}} - C_{i1_{aq}}}{\tau_1} + \left(\alpha + \frac{1-\alpha}{K_i}\right)^{-1} \left(\alpha \sum v_{ij} R_{jaq} + (1-\alpha) \sum v_{ij} R_{joil}\right) \tag{54}$$

$$\frac{dC_{i1_{oil}}}{dt} = \frac{C_{i2_{oil}} - C_{i1_{oil}}}{\tau_1} + (\alpha K_i + 1 - \alpha)^{-1} \left(\alpha \sum v_{ij} R_{jaq} + (1-\alpha) \sum v_{ij} R_{joil}\right) \tag{55}$$

For the second tank (T2), a new derivation of the mass balances is not needed, but we can write analogously to the first tank (T1),

$$\frac{dC_{i2_{aq}}}{dt} = \frac{C_{i1_{aq}} - C_{i2_{aq}}}{\tau_2} + \left(\alpha + \frac{1-\alpha}{K_i}\right)^{-1} \left(\alpha \sum v_{ij} R'_{jaq} + (1-\alpha) \sum v_{ij} R'_{joil}\right) \tag{56}$$

$$\frac{dC_{i2_{oil}}}{dt} = \frac{C_{i1_{oil}} - C_{i2_{oil}}}{\tau_2} + (\alpha K_i + 1 - \alpha)^{-1} \left(\alpha \sum v_{ij} R'_{jaq} + (1-\alpha) \sum v_{ij} R'_{joil}\right) \tag{57}$$

4.4.1.2 *Application of the general mass balances to perhydrolysis, epoxidation and ring opening*

For the actual cases, all the components do not appear in both liquid phases (oil and water), but hydrogen peroxide and water are present in the aqueous phase only, while the fatty acid, the epoxide and the ring opening products are predominantly in the oil phase. For acetic acid and peracetic acid, a phase equilibrium is presumed. Based on this this reasoning, the equilibrium ratios become

$$K_{HP} \rightarrow \infty$$
$$K_W \rightarrow \infty$$
$$K_{OA} = 0$$
$$K_{EOA} = 0$$
$$K_{ROP} = 0$$
$$K_{AA} \neq 0$$
$$K_{PAA} \neq 0$$

The reaction stoichiometry, equations (I)-(VIII), gives the relation between the generation rates of the components and the reaction rates.

After inserting the rate expressions in the balance equations for the first tank (T1), we obtain

$$\frac{dC_{AA1_{aq}}}{dt} = \frac{C_{AA2_{aq}} - C_{AA1_{aq}}}{\tau_1} + \left(\alpha + \frac{1-\alpha}{K_{AA}}\right)^{-1} . \left(-\alpha R_{perh} + (1-\alpha)(R_{Epox} - R_{ROP,AA})\right) \quad (58)$$

$$\frac{dC_{HP1_{aq}}}{dt} = \frac{C_{HP\ aq} - C_{HP\ aq}}{\tau_1} - R_{perh} \quad (59)$$

$$\frac{dC_{PAA1_{aq}}}{dt} = \frac{C_{PAA2_{aq}} - C_{PAA1_{aq}}}{\tau_1} + \left(\alpha + \frac{1-\alpha}{K_{PAA}}\right)^{-1} . \left(\alpha\left(R_{perh} - R_{decom}\right) - (1-\alpha)\ (R_{epox}\ - R_{ROP,PAA})\right) \quad (60)$$

$$\frac{dC_{W1_{aq}}}{dt} = \frac{C_{W2_{aq}} - C_{W1_{aq}}}{\tau_1} + R_{perh} \quad (61)$$

$$\frac{dC_{OA1_{oil}}}{dt} = \frac{C_{OA\ oil} - C_{OA\ oil}}{\tau_1} - R_{epox} \quad (62)$$

$$\frac{dC_{EOA1_{oil}}}{dt} = \frac{C_{EOA2_{oil}} - C_{EO\ \ oil}}{\tau_1} + R_{Epox} - \Sigma R_{ROP,j} \quad (63)$$

For the second tank (T2), the balance equations become analogously

$$\frac{dC_{AA2_{aq}}}{dt} = \frac{C_{AA\ aq} - C_{AA\ aq}}{\tau_2} + \left(\alpha + \frac{1-\alpha}{K_{AA}}\right)^{-1} . \left(-\alpha R_{perh} + (1-\alpha) R_{Epox}\right) \quad (64)$$

$$\frac{dC_{HP\ aq}}{dt} = \frac{C_{HP1_{aq}} - C_{HP2_{aq}}}{\tau_2} - R_{perh} \quad (65)$$

$$\frac{dC_{PAA2_{aq}}}{dt} = \frac{C_{PAA1_{aq}} - C_{PAA2_{aq}}}{\tau_2} + \left(\alpha + \frac{1-\alpha}{K_{PAA}}\right)^{-1} . \left(\alpha\left(R_{per} - R_{decom}\right) - (1-\alpha) R_{epox}\right) \quad (66)$$

$$\frac{dC_{W2_{aq}}}{dt} = \frac{C_{W1_{aq}} - C_{W2_{aq}}}{\tau_2} + R_{perh} \quad (67)$$

$$\frac{dC_{OA2_{oil}}}{dt} = \frac{C_{OA\ oil} - C_{OA\ oil}}{\tau_2} - R_{epox} \quad (68)$$

$$\frac{dC_{EOA2_{oil}}}{dt} = \frac{C_{EOA1_{oil}} - C_{EOA2_{oil}}}{\tau_2} + R_{Epox} - R_{RO} \quad (69)$$

The temperature dependences of the rate constants were described by the modified Arrhenius equation,

$$k = k_0 . e^{\frac{-E_a}{R\theta}} \quad (70)$$

where $\frac{1}{\theta} = \frac{1}{T} - \frac{1}{T_0}$ and T_0 denotes the reference temperature (typically close to the average temperature of the experiments). The transformation of the Arrhenius equation was done to suppress the mutual correlation of the pre-exponential factor and the activation energy. Furthermore, the parameter k_0 gives the numerical value of the rate constant at the reference temperature.

The complete model consists of twelve ordinary differential equations (ODEs), an initial value problem (IVP) (six equations for each tank). The ordinary differential equations describing this system can be stiff due to the presence of rapid and slow reactions, therefore the ODEs were solved numerically by the backward difference method implemented in the code ODESSA [83], which was operated under a parameter estimation routine in the software ModEst (Fortran 90 Compaq Visual FORTRAN 6.0). The objective function, (ω) was minimized by using a combined Simplex and Levenberg-Marquardt [84] algorithm implemented in ModEst,

$$\omega = \sum(C_i - \hat{C}_i)^2 \tag{71}$$

where C_i is the experimental concentration and $\hat{C}$ is the estimated concentration obtained from the model equations (58)-(69). The accuracy of the parameters was checked by standard mathematical analysis and a Markov Chain Monte Carlo (MCMC) method [85].

4.4.2 Parameter estimation results and discussion

The overall statistical analysis of parameter estimation is provided in Table 4.2. The numerical values of the parameters obtained from the nonlinear regression analysis are collected in Table 4.3, while Table 3.5 (in previous section) displays the values of the parameters obtained with one of the models from our previous work carried out in the absence of heterogeneous catalysts. The rate constant for the homogeneous part of the perhydrolysis shows to be of the same order of magnitude compared with the ones estimated with one of the models developed in our previous study (Chapter 3). The rate constants for epoxidation and ring opening are within one order of magnitude in comparison to the model from the previous chapter. Furthermore, the tendency observed in our previous studies is maintained: the perhydrolysis is the slowest reaction, followed by the epoxidation and the ring opening. Regarding the contributions of the homogeneous and heterogeneous parts of the perhydrolysis, the estimated values of the rate constants are in agreement with the physical sense of the system given that $\rho_B \gg 1$ and $\sqrt{\frac{K'_{AA} \cdot C_{AA_{aq}}}{C_{W_{aq}}}} \ll 1$ (Eq. 34) which make the contribution of the homogeneous part much smaller than the solid-catalyzed part. Preliminary parameter estimation efforts indicated that the contribution of the adsorption terms in the rate equation (33) was minor; therefore the simplification $1 + \Sigma K_i C_{i_{aq}} \simeq 1$ was applied.

The estimation of the activation energies for perhydrolysis and epoxidation was cumbersome and very reliable results could not be obtained. This is due to two main factors, the small range of temperatures of the experiments and the rapid tendency of the experimental data for acetic acid and peracetic acid to reach equilibrium and remain constant throughout the reaction (Figure 4.8). Given that acetic acid and peracetic acid play key roles in both the perhydrolysis and epoxidation and there is a limited temperature range in the experimental set, the activation energies for these two reactions converged towards zero.

In comparison to the previous model, the activation energy for the ring opening is in the same order of magnitude but it presents a high margin of error. On the other hand, it is to be expected that the activation energy of the solid-catalyzed perhydrolysis present lower values compared with the homogeneous perhydrolysis, especially when taking into consideration that the result obtained is the apparent activation energy and it comprises the enthalpies of adsorption into the catalyst surface, which are negative and make the apparent activation energy even smaller. However, the activation energies for the

solid-catalyzed perhydrolysis and the homogeneous perhydrolysis seem to be within the same order of magnitude because of the lack of accuracy in the determination of the activation energies of this system is due to the narrow temperature window in which the experiments were performed.

Taking into consideration that the activation energies have been successfully determined in our previous study (Chapter 3) and that there was a strong motivation to focus on the enhancing effect of the addition of the solid catalyst, the experimental program was focused on the variation of the catalyst amount. Moreover, it is important to emphasize that we were limited to conduct the kinetic experiments within a very narrow temperature window in the presence of the heterogeneous catalyst, because high concentrations of peracetic acid (>15%) exhibit some degree of explosiveness and instability [86] and a high risk of thermal runaway exists due to the exothermic nature of the reactions involved [64].

The partition coefficients for the phase equilibrium for acetic acid and peracetic acid were not determined very precisely because the concentrations of these components remain virtually constant throughout the reaction (Figure 4.8), as there is consumption and generation of both components at similar rates.

Table 4.2. Statistical results for oleic acid epoxidation.

Total SS (corrected for means)	2.733E+03
Residual SS	1.041E+02
Std. Error of estimate	0.4178E+00
Explained (%):	96.19

Table 4.3. Estimated kinetic constants, activation energies, distribution coefficients and pre-exponential factor of perhydrolysis equillibrium in oleic acid epoxidation

	Estimated Parameter	Estimated Std Error	Est. Relative Std Error (%)
k_{perh}	0.317E-03	0.375E-04	11.8
k_{epox}	0.348E-03	0.232E-04	6.7
k_{RO}	0.219E-01	0.116E-01	52.9
$k_{\ perhCat}$	0.341E-04	0.288E-05	8.4
$E_{a_{RO}}$	0.964E+05	0.234E+06	242.9
$E_{a_{perhCat}}$	0.595E+05	0.207E+05	34.8
K_{AA}	0.140E-01	0.176E-01	125.8
A_{eq}	0.281E+01	0.441E+00	15.7

The units: k_{perh}, k_{epox}, k_{RO} = () L/mol/min; $k_{perhCat}$= ()L^2/mol/g/min; activation energies (E_a) = () J/mol, K_{AA}, A_{eq}= (). A_{eq} is the pre-exponential factor of the perhydrolysis equilibrium constant, eq. (34).

Table 4.4 displays the correlation matrix for the estimated parameters. In general, the correlation between the parameters is rather low, which supports the model.

Table 4.4. Correlation matrix of the parameters

	k_{perh}	k_{epox}	k_{RO}	$k_{perhCat}$	$E_{a_{RO}}$	$E_{a_{perhCat}}$	K_{AA}	A_{eq}
k_{perh}	1.000							
k_{epox}	-0.224	1.000						
k_{RO}	-0.027	0.096	1.000					
$k_{perhCat}$	-0.073	-0.036	-0.001	1.000				
$E_{a_{RO}}$	-0.001	0.003	-0.190	-0.001	1.000			
$E_{a_{perhCat}}$	0.067	-0.033	-0.010	0.116	0.028	1.000		
K_{AA}	0.019	-0.006	0.034	0.015	0.006	-0.046	1.000	
A_{eq}	-0.036	-0.086	0.019	-0.550	0.008	-0.048	0.188	1.000

The fit of the model to the experimental data is compared in Figure 4.8, which indicates that the model fits with the experimental data well. The main features of the experimental data are well reproduced by the model: the decrease of the double bond and hydrogen peroxide concentrations, the formation of epoxide as well as the close to steady state behavior of acetic and peracetic acid. Figure 4.9 displays the parameter set plot for the sensitivity analysis, demonstrating rather well-defined minima for most of the parameters.

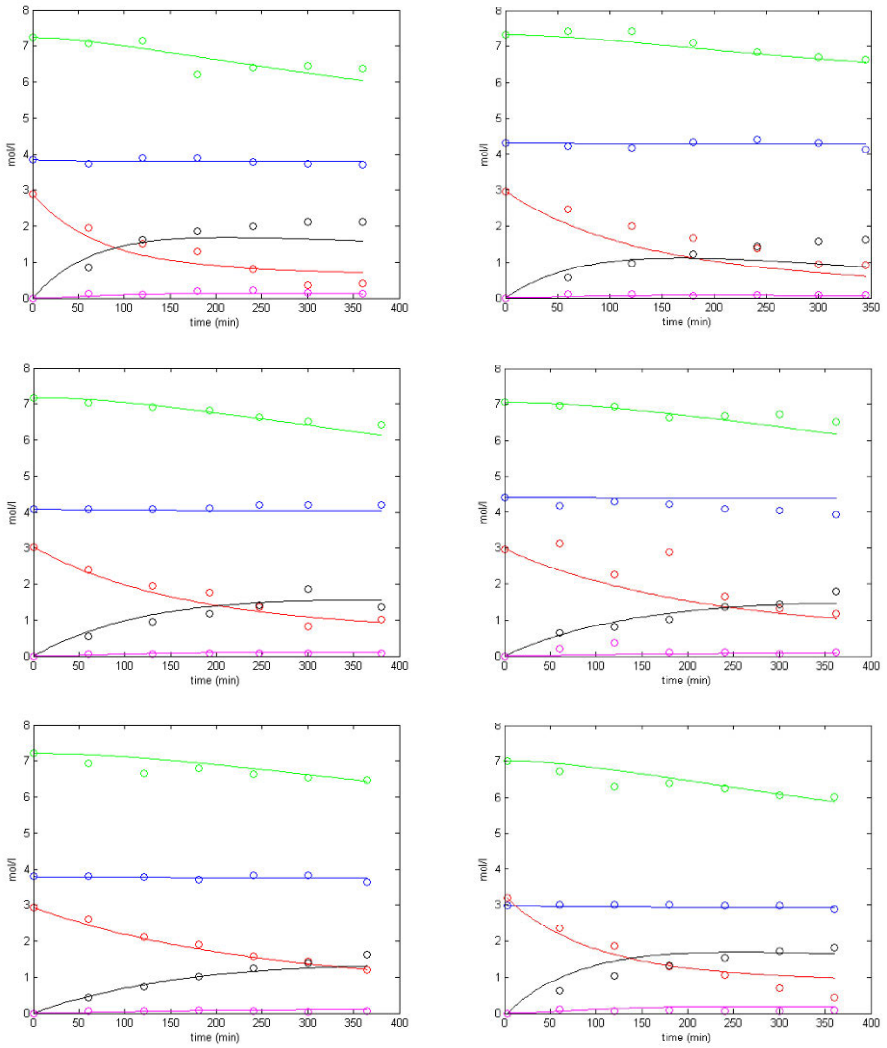

Figure 4.8. Fitting of the model to the experimental data for oleic acid epoxidation. In black: **epoxyoleic acid**, pink: peracetic acid, red: oleic acid, green: hydrogen peroxide and blue: acetic acid (VI).

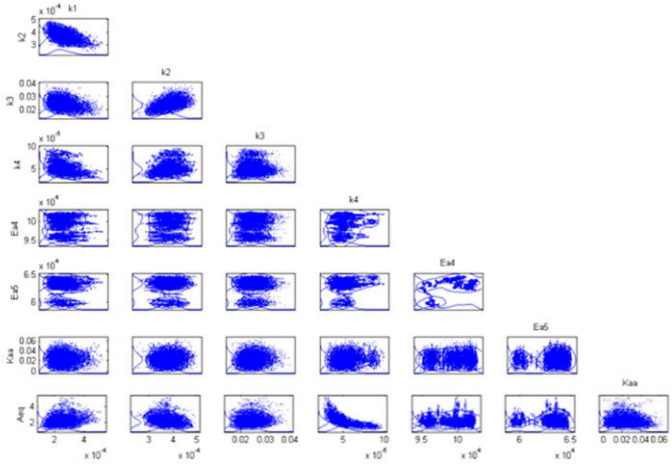

Figure 4.9. MCMC sensitivity plot. Predictive distribution for the estimated parameters.

Figure 4.10 displays the probability distribution of the estimated parameters. The distributions of the values of the rate constants and the acetic acid distribution constant confirm to be normal, whereas the distributions for the activation energies and the pre-exponential factor for perhydrolysis equilibrium A_{eq} seem to be multimodal. Moreover, it is important to consider the high complexity of the system can lead to different solutions in this kind of calculations.

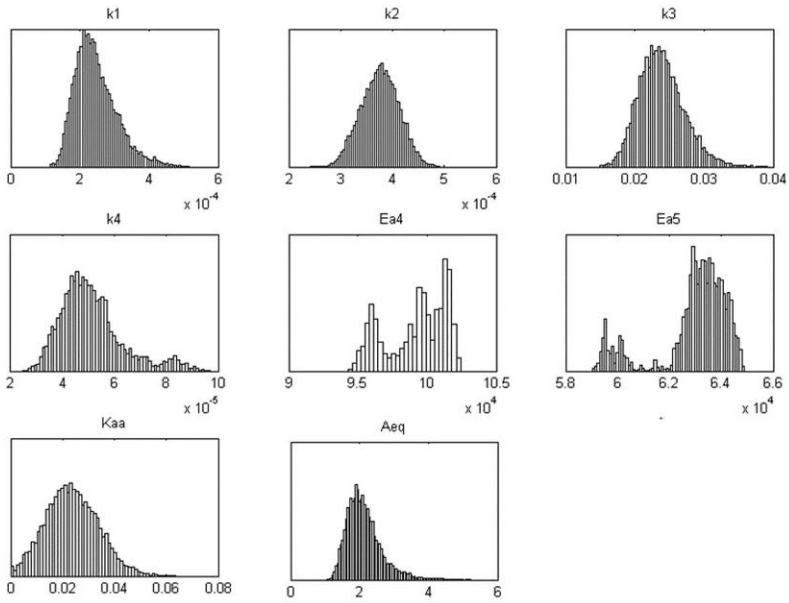

Figure 4.10. MCMC probability distributions of the model parameters.

Finally, a parity plot is displayed in Figure 4.11 where generally a good agreement with experimental and calculated values can be observed.

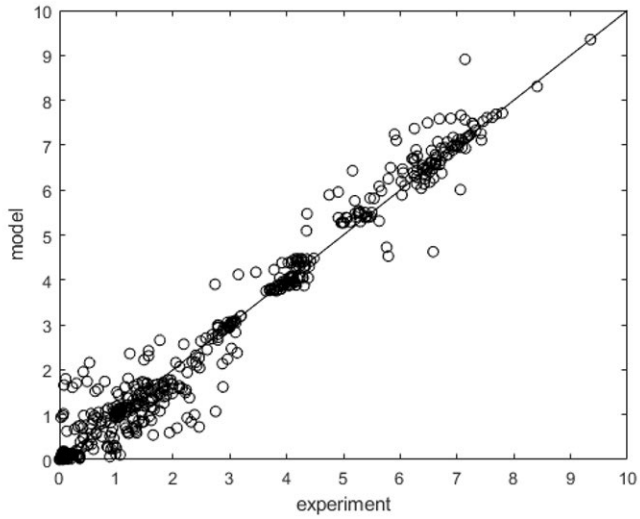

Figure 4.11. MCMC parity plot between experimental and calculated values (concentrations).

5. Tall oil epoxidation (Article VII)

5.1 From model compound to oil mixtures

The previous chapters have focused on the epoxidation of oleic acid as a model compound for plant-based oil mixtures. Thorough studies on epoxidation of oleic acid have drawn a clearer picture on optimal conditions for the epoxidation of oils for a simple fatty acid with only one unsaturation to be functionalized. Moreover, when shifting to tall oil mixtures conformed by oleic acid, linoleic acid, stearic acid and rosin acids, new aspects must be taken into account, such as steric hindrance, different viscosities and densities and the proximity between the double bonds within one fatty acid chain. Ideally, the reactivity of a mixture could be predicted by the composition of the mixture. Two tall oil mixtures were studied in this work: tall oil fatty acids (TOFA) and distilled tall oil (DTO). The tall oil fatty acid mixture contains 93.5% of free fatty acids and 1.55% of free resin acids, whereas the distilled tall oil consists of a more complex mixture of 86.1% of free fatty acids and 8.9% of free rosin acids (detailed composition analyzed by GC can be found in the supplementary information of Article VII). The rest of the composition was unsaponifiables.

Figure 5.1 displays the relative conversion to oxirane for the epoxidation of oleic acid, tall oil fatty acids and distilled tall oil in the presence and absence of Amberlite IR-120 at 50°C. The results show that despite the differences on the mixtures, the reaction kinetics is rather similar, which proves that oleic acid is indeed a very suitable model molecule for tall oil fatty acid mixtures. In this case, the presence of several double bonds in one fatty acid chain does not seem to promote the ring opening of the epoxide. According to La Scala and Wool [87], the reactivity of epoxidation of oleic and linoleic acids is equal in triglycerides and it increases with the number of double bonds for fatty acid methyl esters. Following this logic, the epoxidation rates should be higher for TOFA and DTO compared to oleic acid. This effect might however be counteracted by the increased viscosity of the mixture.

In case of distilled tall oil, the higher viscosity does seem to play a more prominent role in retarding the mass transfer and thus the overall reaction rate. Table 5.1 displays the densities and viscosities of oleic acid, tall oil fatty acids and distilled tall oil at room temperature and at the reaction temperature. Additionally, the presence of rosin acids (mostly abietic acid) in the DTO (8.9%) might have played a role in inhibiting the epoxidation and/or promoting the ring opening reactions. Rosin acids are fairly reactive species whose reactivity is principally based on the presence of an olefin system and a carboxylic group [88].

Table 5.2 shows that the acid values of TOFA and DTO are very similar and they are slightly lower compared to oleic acid. This indicates that the presence of rosin acids does not play a role in increasing the acidity of the mixture and therefore it can be presumed that the carboxylic groups of the rosin acids do not play a role in promoting the protonation of the oxirane oxygen. When the pK_a-values of the acids are compared at 50ºC, the oleic and linoleic acid have the values 8.3 and 7.8, respectively and abietic acid has the pK_a-value of 6.2 [89], i.e. they are very weak acids compared for example with acetic acid (pK_a=4.8). Acids with high pK_a-values are very prone to esterification. It is possible that these carboxylic groups participate in an esterification reaction with the protonated oxirane oxygen, since the NMR analysis for the epoxidation of oleic acid shows evidence of esterification reactions with the carboxylic groups in the acetic acid and the oleic acid. In the absence of the catalyst, however, the ring opening reactions do not seem to have an important role in the DTO epoxidation because the conversions were relatively low.

The olefin system in abietic acid can be epoxidized as well, and the ring is opened by water [90], leading to the formation of alcohols, whose presence has been confirmed by NMR analysis. Alcohols can participate in the alkoxylation of double bonds, inhibiting the epoxidation, or in the ring opening to form an ether, which was identified in the NMR spectrum. The latter reaction might occur with alcohols from the ring opening of the fatty acids as well, but it can be presumed that the alcohols from the abietic acid are more sterically available when comparing the average size of oleic acid (1.8-2.1nm) and abietic acid (0.78nm) [91].

As shown in Figure 5.2, the viscosity of the mixture increases significantly with the formation of epoxide groups and even more with the ring opening products [48]. Additionally, the acidic environment can trigger the dimerization of the rosin acids [92]. The combination of epoxide groups, ring opening products and rosin acid dimers contributes to a significant increase of the viscosity of the DTO mixture with time, which hampers the mass transfer gradually.

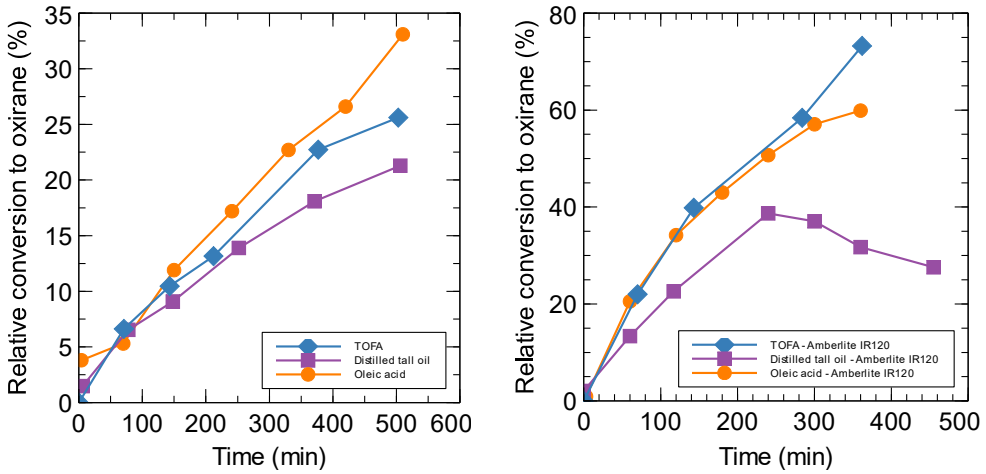

Figure 5.1. Relative conversion to oxirane for the epoxidation of oleic acid, TOFA and distilled tall oil in the absence (left) and presence (right) of Amberlite IR-120 at 50°C.

Table 5.1. Dynamic viscosities and densities of oleic acid and tall oil.

	25°C		50°C	
	Density (g/mL)	**Viscosity (cP)**	**Density (g/mL)**	**Viscosity (cP)**
Oleic acid	0.8948	26.7	0.8750	18.9
TOFA	0.9104	33.8	0.8910	20.3
Distilled tall oil	0.9155	51.2	0.9011	22.2

Table 5.2. Acid values of oleic acid and tall oil.

	Acid value (mg_{KOH}/g_{oil})
Oleic acid	202.56
TOFA	192.92
Distilled tall oil	195.00

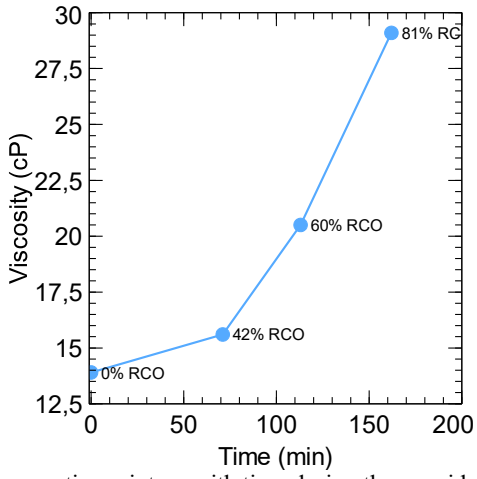

Figure 5.2. Viscosity of the reaction mixture with time during the epoxidation of oleic acid at 50ºC.

Figure 5.3 and Figure 5.4 display the different kinetics for epoxidation of TOFA and distilled tall oil in the presence and absence of Amberlite IR-120. In accordance with the results presented in previous chapters, both figures illustrate the existence of two parallel paths for epoxidation: a non-catalytic and a catalytic one. On the other hand, the epoxidation of distilled tall oil in the presence of the solid catalyst presents a high degree of ring opening after 250 minutes. This observation can be explained by the presumed influence of the rosin acids in promoting the ring opening reactions.

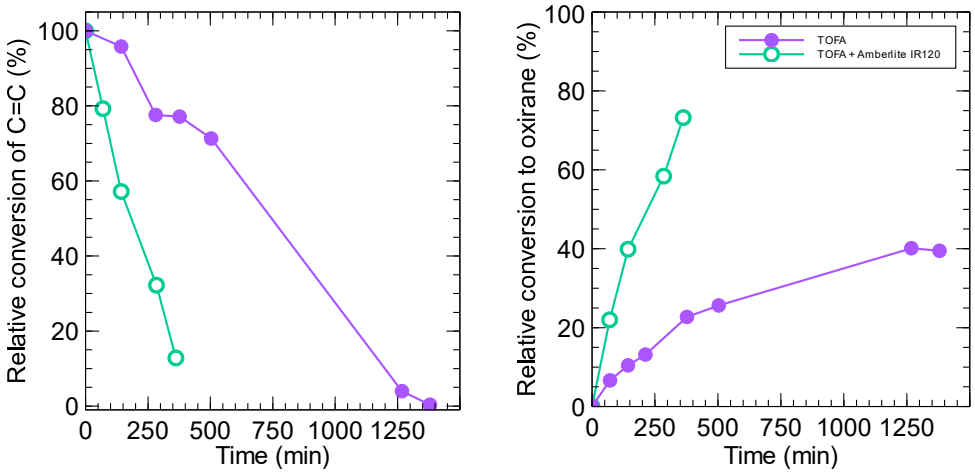

Figure 5.3. Relative conversion of double bonds (left) and relative conversion to oxirane (right) for the epoxidation of TOFA in the presence and absence of Amberlite IR-120 at 50°C.

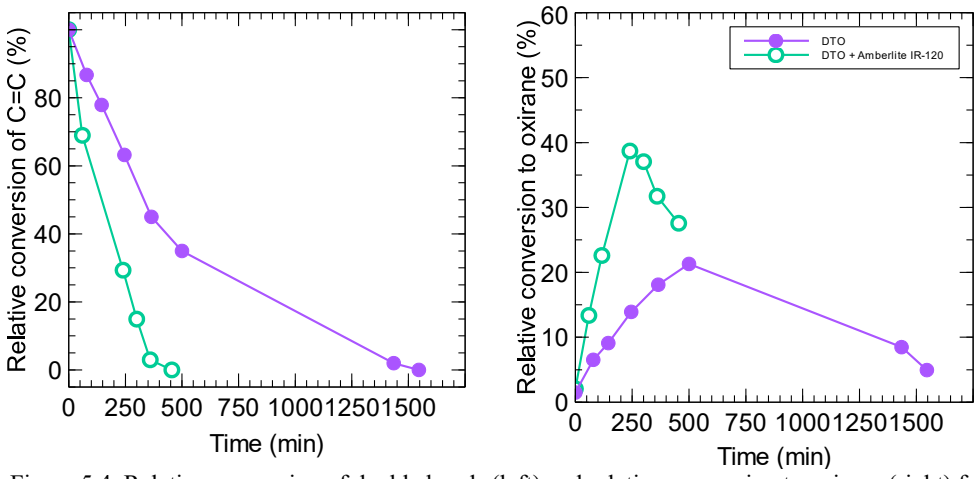

Figure 5.4. Relative conversion of double bonds (left) and relative conversion to oxirane (right) for the epoxidation of distilled tall oil in the presence and absence of Amberlite IR-120 at 50°C.

5.2 Epoxidation of tall oil fatty acids (TOFA)

In congruence to the studies carried out with oleic acid hitherto, the influence of the initial molar ratios, the catalyst loading and the temperature on the reaction kinetics were studied this time for the tall oil fatty acid mixture (TOFA).

5.2.1 Hydrogen peroxide and acetic acid

According to several studies [37,48,52,66,74,93–95], including our work (Articles II and III), an excess of hydrogen peroxide and/or acetic acid compared to the amount of double bonds favors the Prilezhaev epoxidation of fatty acids and vegetable oils. From the reactions displayed in Figure 1.2, one can observe that hydrogen peroxide and acetic acid react in an 1:1 ratio, therefore a ratio of 1:2:2 of DB:HP:AA was used. However, considering the high complexity of the system, the ratios of 1:1.5:3 and 1:3:1.5 were investigated as well.

Figure 5.5 displays the relative conversion of double bonds and the relative conversion to oxirane for the three molar ratios at 50°C with 7% (w.r.t oil mass) of Amberlite IR-120 on dry basis. The kinetic results confirmed what we have found previously for oleic acid, i.e. the epoxidation rates are higher for a larger excess of hydrogen peroxide. A similar trend was observed for the experiments conducted at 60°C, which are displayed in Figure 5.6. This can be explained by the fact that hydrogen peroxide is consumed throughout the reaction, unlike acetic acid, whose concentration is maintained virtually constant throughout the reaction and it is regenerated in the epoxidation step (see Figure 1.2). The evolution of the acetic acid and hydrogen peroxide concentrations are shown in Figure 5.7.

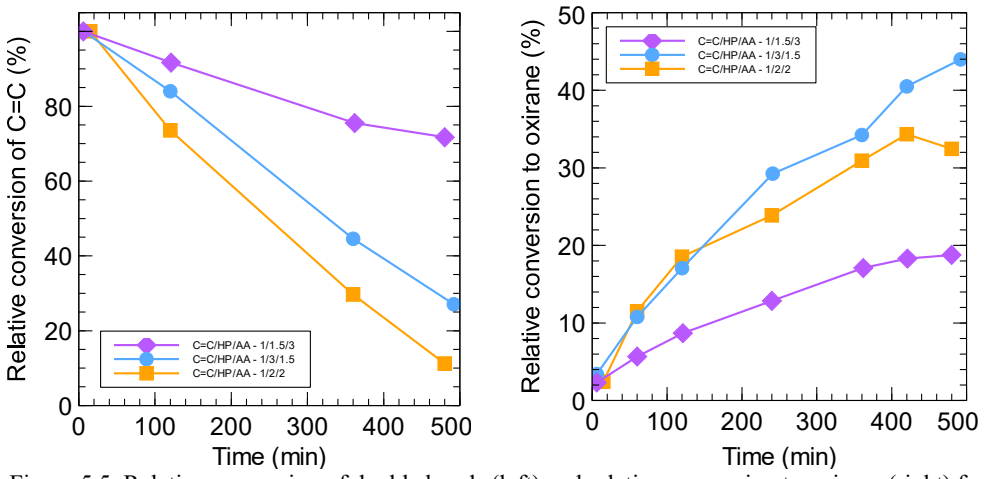

Figure 5.5. Relative conversion of double bonds (left) and relative conversion to oxirane (right) for three different DB:HP:AA molar ratios at 50°C.

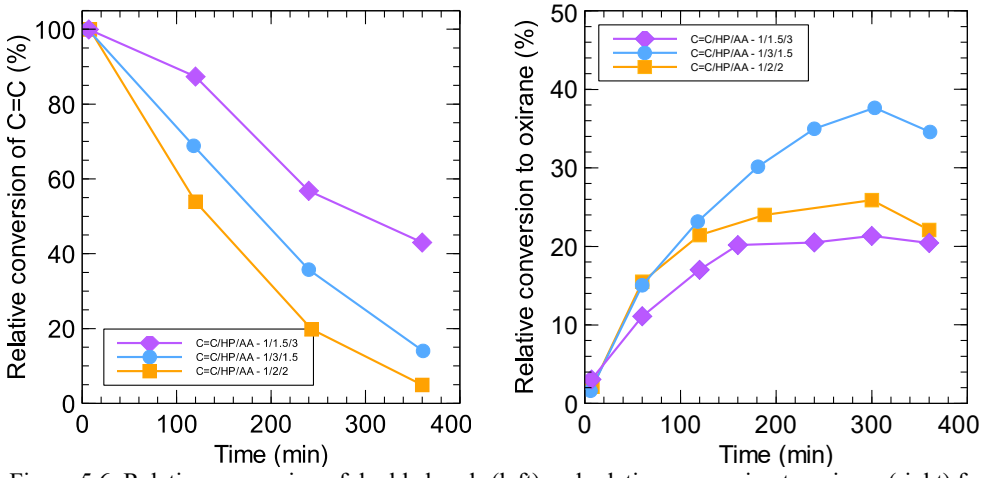

Figure 5.6. Relative conversion of double bonds (left) and relative conversion to oxirane (right) for three different DB:HP:AA molar ratios at 60°C.

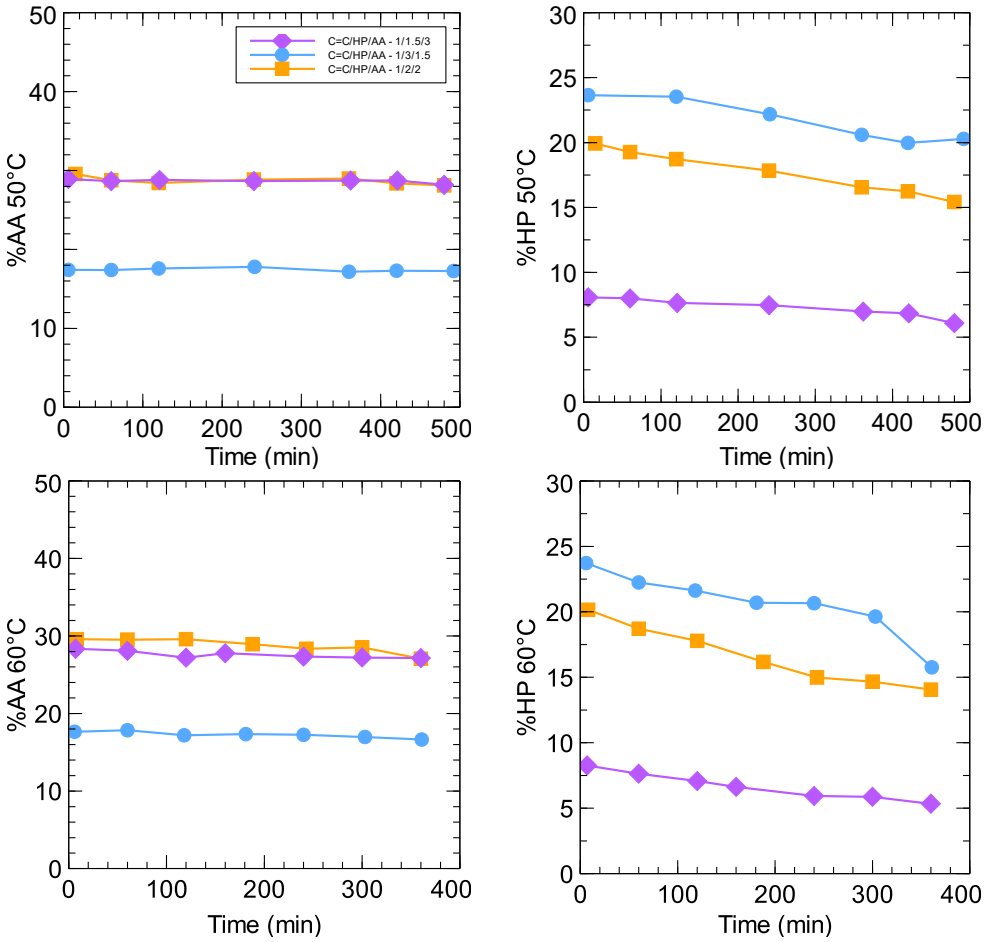

Figure 5.7. Concentrations of acetic acid (left) and hydrogen peroxide (right) over time at 50°C and 60°C. For the experimental conditions, see Figures 5 and 6.

5.2.2 Catalyst loading

Based on the catalyst screening for the epoxidation of oleic acid, Amberlite IR-120 was selected for this study as one of the best performing acidic ion exchange resins of the screening. Experiments were conducted at 50°C using the optimal molar ratios from the previous section (DB: HP:AA – 1:3:1.5). The amounts of catalysts are based on dry mass percentage w.r.t. oil mass.

The kinetic results displayed in Figure 5.8 reveal that the epoxidation of TOFA is faster in the presence of Amberlite IR-120. Evidently, higher conversions of double bonds were reached for the experiment at 7% compared to 0% Amberlite. However, experiments with 7% and 14% of catalyst showed similar rates of epoxidation. This indicates that external mass transfer limitations might be present in the system.

Only minimal mass transfer limitations were found in the experiments with oleic acid under similar conditions (same reactor setup and same conditions). However, TOFA is a mixture of fatty acids with a higher viscosity and density (Table 5.1) which can influence in the liquid-liquid-solid mass transfer.

It is also important to mention that the steric hindrance might also play a role in the reaction kinetics. In case of linolenic acid epoxidation in the presence of acidic ion exchange resins, a previous study has revealed that the reactivities of the different double bonds in the fatty acid depend on the position in the fatty acid chain. Ergo, not all the double bonds can be treated in the same way. This explains the fact that the TOFA mixture behaves differently from oleic acid [96], since linolenic acid is present in the TOFA mixture in a large quantity.

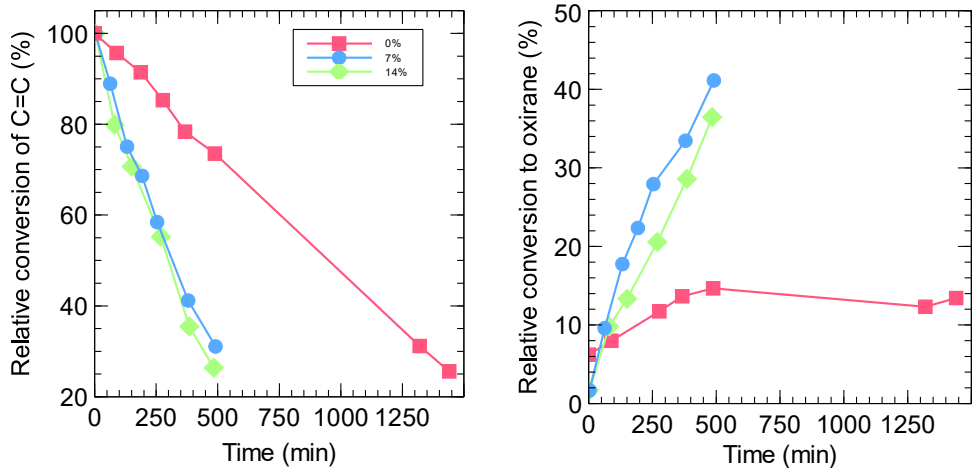

Figure 5.8 Relative conversion of double bonds (left) and relative conversion to oxirane (right) at different catalyst loadings, 50°C.

5.2.3 Temperature

Epoxidation of tall oil fatty acids was conducted at four different temperatures between 40 and 70°C. The most suitable molar ratio was selected from the results obtained with the experiments from the previous section and 7% loading of dry catalyst. The results depicted in Figure 5.9 show that the conversions of double bonds to oxirane increase proportionally with temperature. At higher temperatures, the conversion to oxirane proceeds faster at the beginning of the reaction, however, the selectivity to oxirane starts to decay after some time. This is due to the presence of ring opening reactions that convert the oxirane groups into side products. The nature of these side products was studied with NMR spectroscopy and the spectrum showed the presence of alcohols, ethers and esters, which include fatty acid esters and acetates. The experiment at 50°C produced the highest selectivity of oxirane.

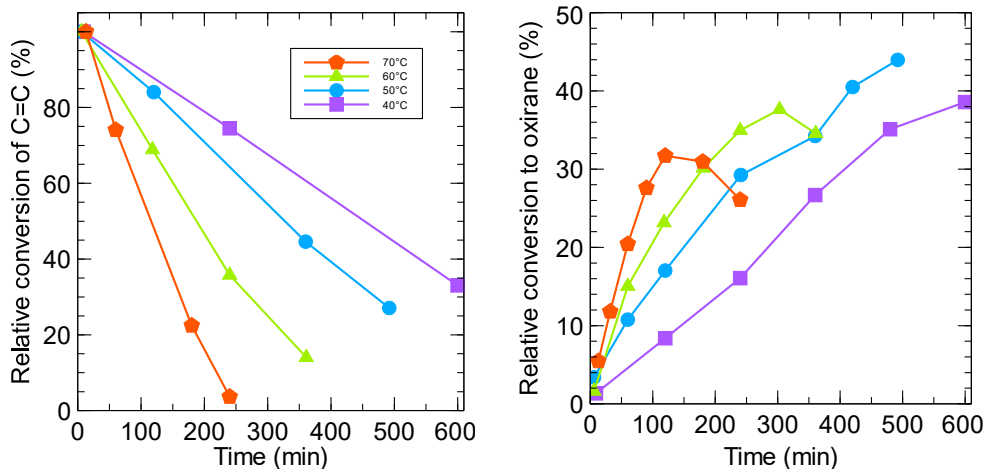

Figure 5.9. Relative conversion of double bonds (left) and relative conversion to oxirane (right) at different reaction temperatures.

5.3 Microwave heating

Up to now, the irradiation of microwaves in the epoxidation of oleic acid has shown to cause either a positive or a neutral effect on the reaction yield. Moreover, once applied to the epoxidation of tall oil mixtures, a different trend was observed. Figure 5.10 and Figure 5.11 illustrate the conversion of double bonds and the formation of oxirane with time for conventional and microwave heated experiments. The experiments carried out under microwave irradiation gave higher epoxidation rates, but the final oxirane yields were lower compared to the conventionally heated experiments. Microwave irradiation appears to have promoted the ring opening reactions. This could be attributed to the rapid nature of the microwave heating which might have unchained a series of ring opening reactions between neighboring double bonds and/or oxirane groups and with the present nucleophilic agents in the mixture. This tendency has not been observed for the studies previously mentioned with oleic acid because there is only one unsaturation per a fatty acid chain.

Selected samples of every experiment (circled in Figure 5.10, Figure 5.11, Figure 5.13 and Figure 5.14, numbered from 1 to 8) were analyzed with NMR spectroscopy and compared to confirm the composition of the mixture at a certain moment of the reaction. ^{1}H NMR spectra for TOFA and distilled tall oil epoxidation are depicted in Figure 5.12 and Figure 5.15.

According to Figure 5.10 and Figure 5.11, the experiments with TOFA under conventional heating have higher contents of the oxirane groups compared to the experiments carried out under microwave heating. The composition of the samples for microwave-heated experiments reveal the presence of ring opening products (see Figure 5.12).

Experiments performed with distilled tall oil show a similar behavior in terms the oxirane selectivity, since the presence of ring opening is evident for the experiments conducted under conventional and microwave heating in the presence and absence of the solid catalyst. Figure 5.13 and Figure 5.14 evidence that the ring opening reactions manifest earlier during the reaction process when microwave irradiation is used.

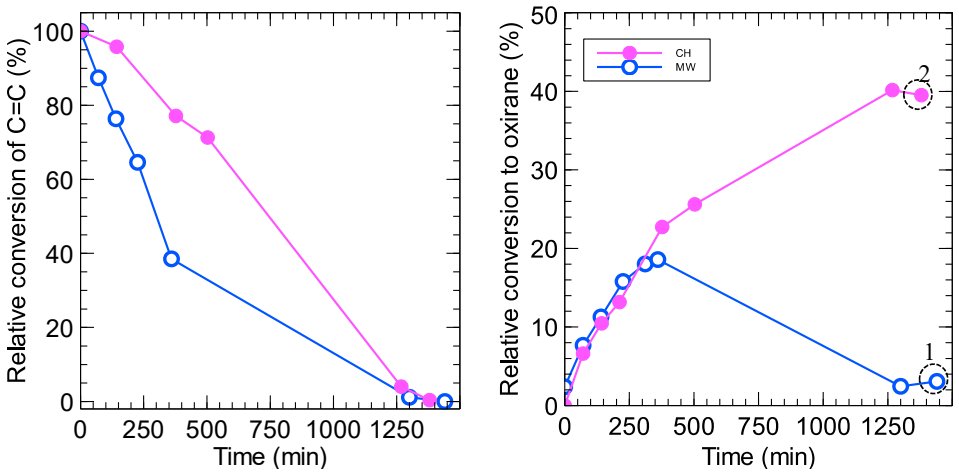

Figure 5.10. Relative conversion of double bonds (left) and relative conversion to oxirane (right) for TOFA epoxidation in the absence of a solid catalyst under microwave and conventional heating at 50°C.

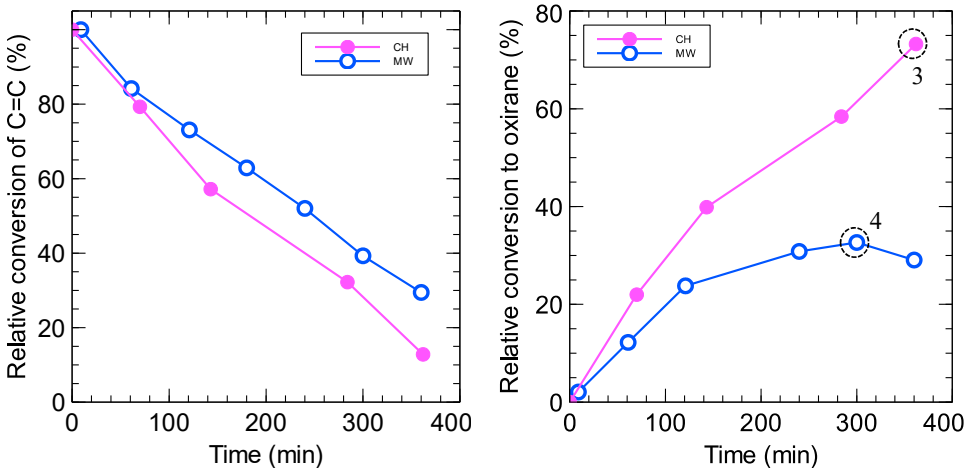

Figure 5.11. Relative conversion of double bonds (left) and relative conversion to oxirane (right) for TOFA epoxidation in the presence of the solid catalyst under microwave and conventional heating at 50°C.

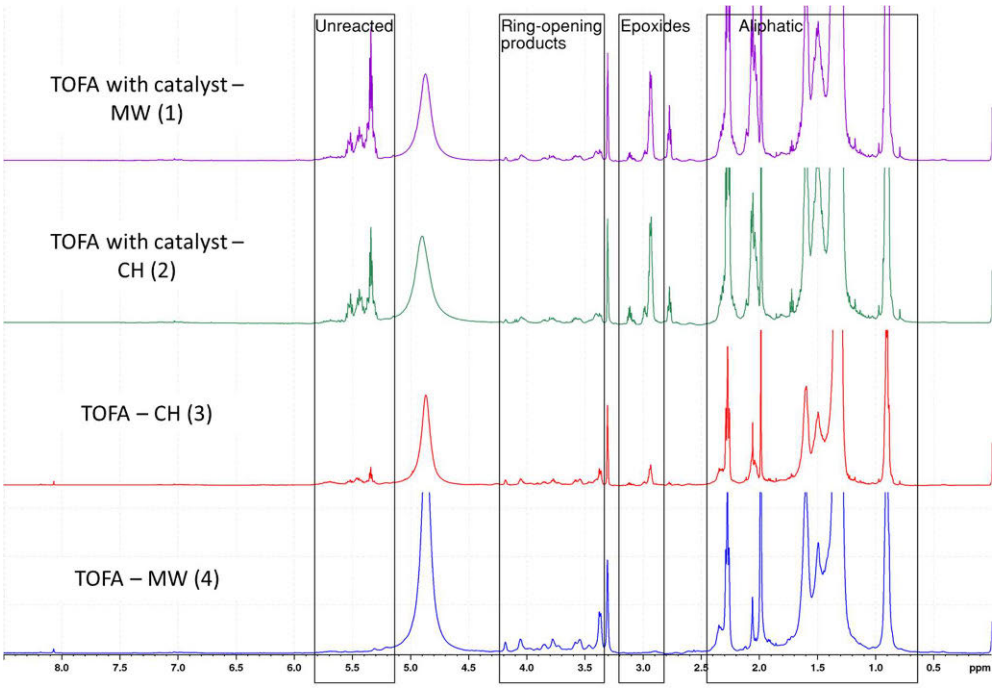

Figure 5.12. NMR spectra for epoxidized TOFA samples.

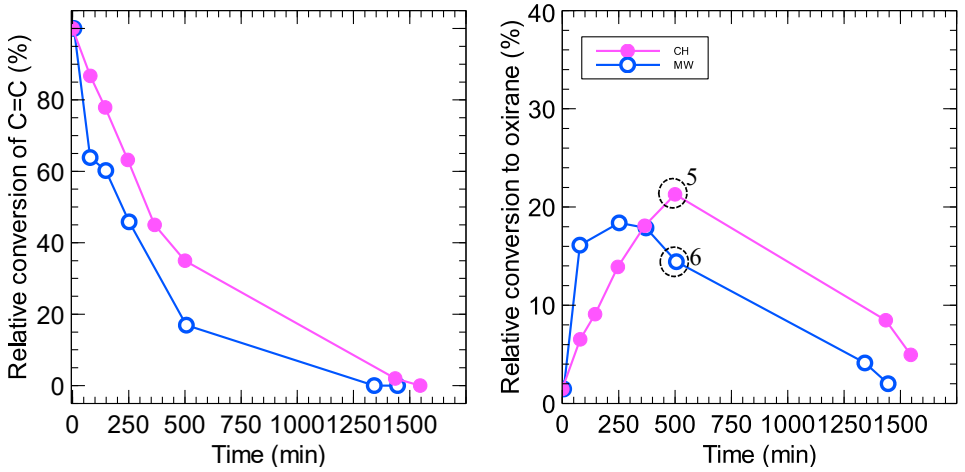

Figure 5.13. Relative conversion of double bonds (left) and relative conversion to oxirane (right) for distilled tall oil epoxidation in the absence of a solid catalyst under microwave and conventional heating at 50°C.

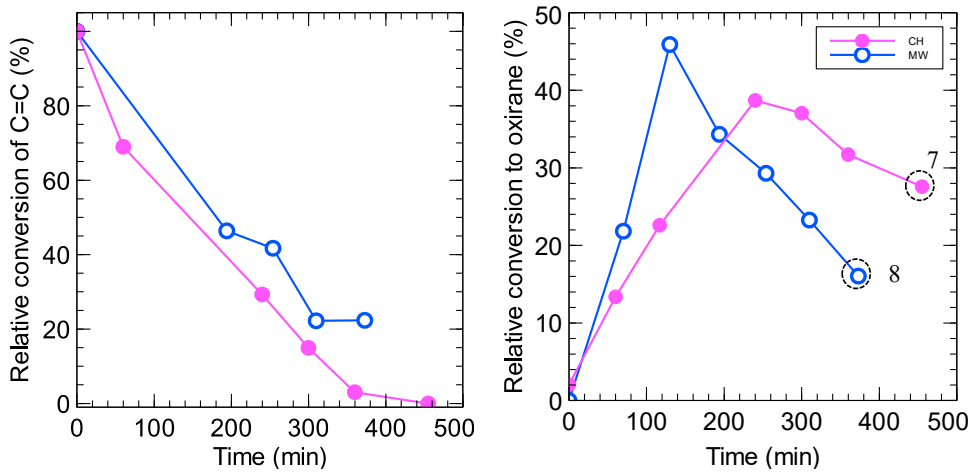

Figure 5.14. Relative conversion of double bonds (left) and relative conversion to oxirane (right) for TOFA epoxidation in the presence of the solid catalyst under microwave and conventional heating at 50°C.

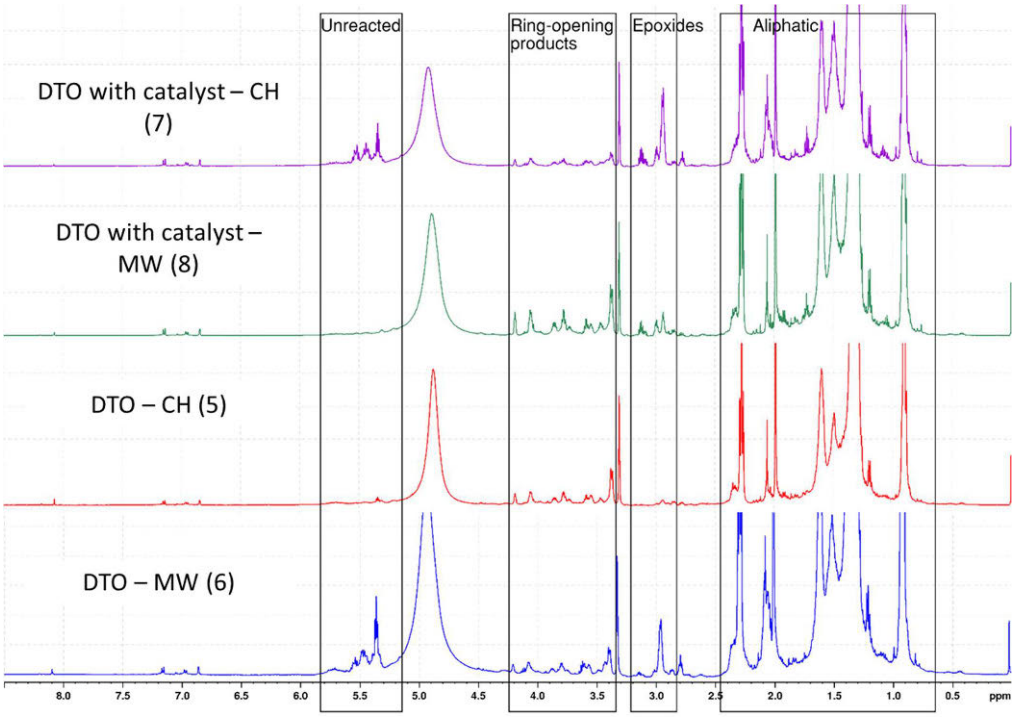

Figure 5.15. NMR spectra for epoxidized distilled tall oil samples.

6. Ring opening of epoxides (Article VIII)

6.1 Kinetic studies

In this section, the effect of sulfuric acid (as the homogeneous catalyst for perhydrolysis), hydrogen peroxide, acetic acid, and peracetic acid concentrations on the kinetics of ring opening reactions was investigated.

6.1.1 Sulfuric acid concentration

Figure 3.10 shows the influence of the sulfuric acid concentration on the ring opening of epoxide groups. In accordance to Dinda et al., the kinetics is faster as the sulfuric acid concentration increases [21]. This graph illustrates the catalytic effect of sulfuric acid on the kinetics of ring opening reactions. Moreover, the kinetic results displayed in Figure 6.1 show the presence of an induction period. As the concentration of sulfuric acid increases, the induction period diminishes and becomes negligible. Campanella and Baltanás [97] have also observed this phenomenon for the ring opening of epoxidized soybean oil at medium pH values and low temperatures. Based on their observations, this induction period seems to be linked to the polar effect of the aqueous phase. The concentration of protons can affect the value of the surface tension, which interferes with the interfacial area [98].

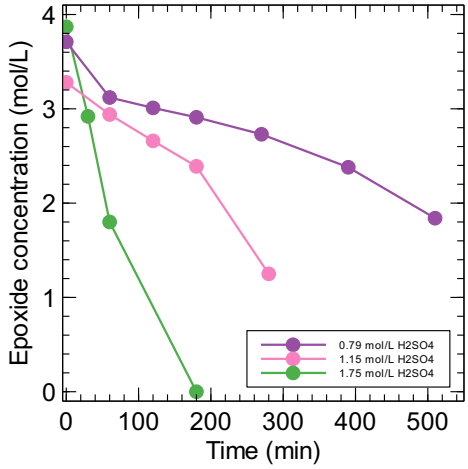

Figure 6.1. Effect of sulfuric acid concentration on the kinetics of ring opening reactions at 70°C with $[EP]_{org,initial}$=3.28-3.87 mol/L, $[AA]_{aq,initial}$=0.00 mol/L, $[HP]_{aq,initial}$ =0.00 mol/L.

6.1.2 Hydrogen peroxide

Figure 6.2 shows the influence of the hydrogen peroxide concentration on the ring opening of epoxide groups. As revealed by this figure, the rate of ring opening slightly increases with the hydrogen peroxide concentration. Hydrogen peroxide could dissociate to provide protons,

$$H_2O_2 \rightleftarrows H^+ + HO_2^-$$

and the pK_a value for this dissociation process is 11.75 at 20°C [99]. Thus, hydrogen peroxide is a very weak acid compared to acetic acid, whose pK_a is 4.73 at 20°C [100], and compared to the second dissociation of sulfuric acid, whose pK_a is 1.88 at 20°C [101]. Therefore, the enhancement of the reaction rate with hydrogen peroxide cannot be linked to the acidity of hydrogen peroxide but possibly on its nucleophilic activity.

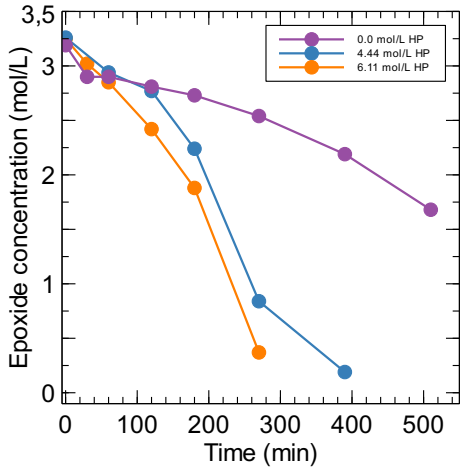

Figure 6.2. Effect of hydrogen peroxide concentration on the kinetics of ring opening reactions at 70 °C with $[EP]_{org,initial}$ =3.19-3.54 mol/L, $[AA]_{aq}$ =0.00 mol/L, $[H_2SO_4]_{aq}$=0.76-0.82 mol/L.

6.1.3 Acetic acid and peracetic acid

Figure 6.3 shows the influence of the acetic acid concentration on the ring opening of the epoxide group. The kinetics of ring opening is accelerated as the concentration of acetic acid is increased.

The rate enhancement by acetic acid can be explained by several factors:

- the nucleophilic activity of acetic acid towards ring opening,
- the increase of acetic acid concentration leads to the increase of peracetic acid production, which can cause opening of the epoxide group, and
- the catalytic effect of acetic acid on the perhydrolysis and ring opening reactions.

For this reason, the kinetic model developed in this work [Article VIII] takes into account these three factors. As experiments illustrated by Figure 3.10, when the concentration of acetic acid increases, the induction period decreases (Figure 6.3) and this induction period seems to be linked to the concentration of protons. When the concentration of protons and the reaction temperature are high, the interfacial area between the aqueous and organic phase increases leading to a shortening in the induction period.

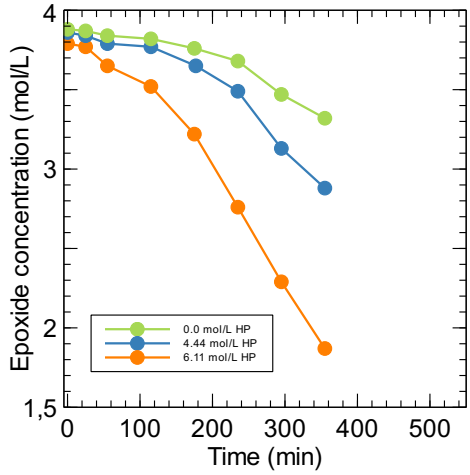

Figure 6.3. Effect of acetic acid concentration on the kinetics of ring opening reactions at 50 °C with $[EP]_{org,initial}$ =3.79-3.86 mol/L, $[H_2O_2]_{aq,initial}$ =5.95-6.07 mol/L, $[H_2SO_4]_{aq}$=0.26 mol/L.

To conclude, these experiments showed that the kinetic model should take into account the catalytic effect of sulfuric acid and acetic acid on the kinetics of perhydrolysis and ring opening reactions. The ring opening effect caused by water, hydrogen peroxide, acetic acid and peracetic acid were included in the mathematical model developed in this study.

The kinetic constants estimated from the model developed for the ring opening reactions presented standard errors less than 30%, which means that the parameter estimation was reliable [Article VIII]. The estimated constants suggested that the ring opening by peracetic and acetic acid was shown to be faster than by water and hydrogen peroxide. Additionally, the activation energy for ring opening by hydrogen peroxide is higher than for the other ring opening agents. This high value suggests that this reaction is less important than the other ring opening reactions.

In general, the correlations between the kinetic constants was negligible. Nevertheless, the correlations between the kinetic constants of ring opening by water and hydrogen peroxide were high. This high correlation might suggest that the kinetics of ring opening for these nucleophiles is more complex.

7. Conclusions and future perspectives

This work focused on the Prilezhaev epoxidation of plant oils as a green process, since it used renewable raw materials and produced biodegradable products through a non-toxic synthesis route. Experimental and modelling work was conducted in order to determine the epoxidation kinetics and the optimal operating parameters. Oleic acid was used as a model compound for plant oils and tall oil mixtures were studied further on.

This thesis emphasized the use of process intensification methods for a more energy efficient process with higher epoxide yield, compared to conventional approaches. The work included the application microwave irradiation, heterogeneous catalysis and a rotating bed reactor.

The results showed that an increased temperature, as well as higher concentrations of acetic acid and hydrogen peroxide accelerated both the epoxidation and the ring opening processes, therefore the temperature and the reactant molar ratios were experimentally optimized to maximize the yield of epoxidized oil. Moreover, a significant improvement of the epoxide yields was observed in the presence of ion exchange resin catalysts. Dowex 50-x8-50, Dowex 50Wx8-100 and Amberlite IR-120 proved to be the most active and suitable ones among the heterogeneous catalysts screened for this reaction. This observation was attributed to the high capacity, small particle size and degree of crosslinking that was high enough to reduce the probability of the epoxide making contact with the acid sites on the catalyst and triggering the ring opening reactions.

Microwaves offered many advantages in the execution of the experiments, such as safety, speed, effectiveness and selective heating. A clear enhancement of the reaction rate was accomplished with microwave heating in comparison to conventional heating for the epoxidation of oleic acid in the absence of a solid catalyst due to the selective heating effect. However, in the presence of acidic ion exchange resins, the effect of the catalyst strongly overlapped the microwave effect, which was not noticeable then. A combination of titrimetric analysis and NMR revealed that microwave irradiation induced ring opening reactions in tall oil epoxidation. The rapid nature of the microwave heating and the selective heating effect seems to be advantageous or detrimental depending on the case.

The stirring rate showed to be a crucial factor to enable an efficient mass transfer until 450rpm, because the interfacial mass transfer area was already close to optimal for higher stirring rates. The use of the special mixing device, SpinChem RBR, was beneficial in the presence of solid catalysts, in terms of suppressing the mass transfer limitations and enabling a simpler collection and recycling of the catalyst.

Mathematical modelling of the oleic acid epoxidation by peracetic acid in the recycled reactor system under conventional heating and microwave irradiation was conducted. To diminish the number of adjustable parameters in the model, the interfacial mass transfer was assumed to be rapid compared to the intrinsic reaction kinetics. Two models were developed for conventional and microwave heating separately and different energy balances and system configurations were considered. A reasonably good fit of the kinetic models to the experimental data was achieved. The estimated rate constants and activation energies for the reactions were within the same order of magnitude as the ones reported in the literature. Furthermore, a third, new mathematical model was developed for the epoxidation of oleic acid in the presence of Amberlite IR-120 as the solid catalyst. The reactor model took into account the co-existence of the oil phase, the aqueous phase and the solid catalyst phase. Non-linear regression analysis revealed that the model gave a very satisfactory description of oleic acid epoxidation in the

presence of the solid catalyst. The general principles of these models can be used for epoxidation of other components, too and the models have a potential in process design and optimization.

Epoxidation of tall oil was studied under several operating conditions and it was proven that oleic acid is a suitable model compound for the epoxidation of tall oil fatty acids. Moreover, the higher viscosity and high content of rosin acids in the distilled tall oil mixture resulted in lower oxirane yields compared to the yields obtained with oleic acid and tall oil fatty acids.

Finally, the influence of ring opening reactions during the epoxidation of cottonseed oil by peracetic acid was investigated. A kinetic study revealed that all the nucleophiles (water, hydrogen peroxide, and acetic and peracetic acids) can attack the epoxide groups. Moreover, it was found that ring opening by peracetic and acetic acid is faster than by water and hydrogen peroxide.

Some future perspectives for this research include a more detailed study on the ring opening mechanism, including possible ring opening reactions triggered by the components in the aqueous phase, the catalyst surface protons, rosin acids and the hydroxyl groups from already generated side products. An interesting approach on the domain of process intensification would be to study the influence of microwaves by irradiating directly the catalyst particles, i.e. by placing the catalyst inside the microwave chamber. Besides, using an infrared camera would allow to prove the existence of thermal gradients between the oil and aqueous phases. Additionally, the application of ultrasound on this epoxidation reaction system might generate interesting temperature peaks within the emulsion (at low frequencies) and create free radicals (at high frequencies), which could influence in the epoxide yield positively. Images recorded by a high-speed camera could allow us to determine the Sauter mean diameter of the oil droplets in the emulsion and the mass transfer coefficients could be estimated. Moreover, modelling studies on the diffusion in the oil droplets are currently in progress, taking into account intra- and interfacial mass transfer effects coupled to intrinsic reaction kinetics. Future investigations should also be done by including a cost and energy assessment for the epoxidation process in laboratory and industrial scale.

Overall, the study of the epoxidation of fatty acids and plant oils for the development of building blocks for environmentally friendly chemicals has been executed successfully applying the principles of green chemistry and utilizing green technologies.

Notation

A_{eq}	Pre-exponential factor, -
A	Interfacial area, m^2
AA	Acetic acid
C	Concentration
%C	Conversion
CH	Conventional heating
DB	Double bond
D	Microwave parameter, eq. (19)
E_a	Activation energy
EP	Epoxidized oil
ΔH	Enthalpy change
HP	Hydrogen peroxide
IV_0	Initial iodine value
IV_f	Iodine value of final sample
K	Equilibrium constant
k	Rate constant
K	Adsorption constant, -
K	Partition coefficient for the phase equilibrium
K'_{AA}	Acetic acid dissociation constant
k_0	Pre-exponential factor (unit depends on the reaction order)
k'	Merged rate constant (unit depends on the reaction order)
m	Mass, g
MCMC	Markov Chain Monte Carlo
MM	Molar mass, g/mol
MW	Microwaves
N	Interfacial flux, $kg/s/m^2$
n	Amount of substance, mol
OA	Oleic acid
OO_{expt}	Experimentally determined oxirane oxygen, mol/100 g oil
OO_{th}	Theoretical maximum oxirane oxygen content, mol/100 g oil
PA	Propionic acid
PAA	Peracetic acid
R	General gas constant (8.3143 J/molK)
R_i	Reaction rate, mol/L/min
RBR	Rotating Bed Reactor
$RCO\%$	Relative conversion to oxirane
ROP	Ring opening products
S	Speed
T	Temperature, °C
$\|u\|^2$	Microwave input power
V	Volume, L
$\dot{V}$	Volumetric flow L/min
v_{ij}	Stoichiometric coefficient, -
W	Water
wt.%	Weight percent
[ ]	Concentration, mol/L
α	Phase ratio
β	Volumetric flow ratio, -
ρ	Density g/mL

ρ_B	Bulk density, g/L
τ	Mean residence time
ω	Objective function
$*$	Acid site

Subscripts and superscripts

aq	Aqueous phase
cat	Catalytic
decom	Decomposition
epox	Epoxidation
L	Liquid
nocat	Non-catalytic
oil	Oil phase
perh	Perhydrolysis
RO	Ring opening
^	Estimated quantity form the model

Acknowledgments

The present work was carried out at the Laboratory of Industrial Chemistry and Reaction Engineering, John Gadolin Process Chemistry Centre, Faculty of Science and Engineering, Åbo Akademi University between 2016 and 2019. The main part of the work was funded by the Academy of Finland (AKA) (Grant number 320115, period 01/2019–12/2019) and with the scholarship provided by Fortum Foundation (Grant numbers 201500286, 201600224 and 201700115 period 05/2016–12/2018). This research work is a part of the activities of the Johan Gadolin Process Chemistry Centre (PCC), a centre of excellence financed by Åbo Akademi University.

FORTUMIN SÄÄTIÖ
FORTUM FOUNDATION

References

1. US Department of Agriculture, & USDA Foreign Agricultural Service. Consumption of vegetable oils worldwide from 2013/14 to 2018/2019, by oil type (in million metric tons). 2018 [cited 2019 Aug 22]. Available from: https://www.statista.com/statistics/263937/vegetable-oils-global-consumption/
[2] M. Law, Plant sterol and stanol margarines and health, BMJ. 320 (2000) 861–864.
[3] Institute of Food Science and Technology, Current Hot Topics, Phytosterols esters (plant sterol and stanol esters), (2000).
[4] E. Vanags, M. Kirpluks, U. Cabulis, Z. Walterova, Highly Functional Polyol Synthesis from Epoxidized Tall Oil Fatty Acids., J. Renew. Mater. 6 (2018) 764–771.
[5] M.R.L. Furst, T. Seidensticker, D.J. Cole-Hamilton, Polymerisable di- and triesters from Tall Oil Fatty Acids and related compounds, Green Chem. 15 (2013) 1218–1225.
[6] A. Behr, A.J. Vorholt, K.A. Ostrowski, T. Seidensticker, Towards resource efficient chemistry: tandem reactions with renewables, Green Chem. 16 (2014) 982–1006.
[7] Q. Ma, X. Liu, R. Zhang, J. Zhu, Y. Jiang, Synthesis and properties of full bio-based thermosetting resins from rosin acid and soybean oil: the role of rosin acid derivatives, Green Chem. 15 (2013) 1300–1310.
[8] H. Wang, B. Liu, X. Liu, J. Zhang, M. Xian, Synthesis of biobased epoxy and curing agents using rosin and the study of cure reactions, Green Chem. 10 (2008) 1190–1196.
[9] X. Liu, W. Xin, J. Zhang, Rosin-based acid anhydrides as alternatives to petrochemical curing agents, Green Chem. 11 (2009) 1018–1025.
[10] C. Mantzaridis, A.-L. Brocas, A. Llevot, G. Cendejas, R. Auvergne, S. Caillol, S. Carlotti, H. Cramail, Rosin acid oligomers as precursors of DGEBA-free epoxy resins, Green Chem. 15 (2013) 3091–3098.
[11] I. Hachemi, K. Jeništová, P. Mäki-Arvela, N. Kumar, K. Eränen, J. Hemming, D.Y. Murzin, Comparative study of sulfur-free nickel and palladium catalysts in hydrodeoxygenation of different fatty acid feedstocks for production of biofuels, Catal. Sci. Technol. 6 (2016) 1476–1487.
[12] P. Mäki-Arvela, B. Rozmysłowicz, S. Lestari, O. Simakova, K. Eränen, T. Salmi, D.Y. Murzin, Catalytic Deoxygenation of Tall Oil Fatty Acid over Palladium Supported on Mesoporous Carbon, Energy Fuels. 25 (2011) 2815–2825.
[13] B. Rozmysłowicz, P. Mäki-Arvela, S. Lestari, O.A. Simakova, K. Eränen, I.L. Simakova, D.Y. Murzin, T.O. Salmi, Catalytic Deoxygenation of Tall Oil Fatty Acids Over a Palladium-Mesoporous Carbon Catalyst: A New Source of Biofuels, Top. Catal. 53 (2010) 1274–1277.
[14] F. Zaccheria, R. Psaro, N. Ravasio, Selective hydrogenation of alternative oils: a useful tool for the production of biofuels, Green Chem. 11 (2009) 462–465.
[15] F.O. Michel Baumassy, The Tall oil and Resin Industry: Global overview and Trends, in: 2016.
[16] C.A. Vinay, Enhanced Advances in Epoxidation of Vegetable Oils, Int. J. Sci. Res. Sci. Technol. 2 (2018) 1048–1053.
[17] G. Sienel, R. Rieth, K.T. Rowbottom, Epoxides, in: Wiley-VCH Verlag GmbH & Co. KGaA (Ed.), Ullmanns Encycl. Ind. Chem., Wiley-VCH Verlag GmbH & Co. KGaA, Weinheim, Germany, 2000.
[18] T. Saurabh, M. Patnaik, S.L. Bhagt, V.C. Renge, Epoxidation of Vegetable oils: A review, Int. J. Adv. Eng. Technol. 2 (2011) 491–501.

[19] A. Campanella, E. Rustoy, A. Baldessari, M.A. Baltanás, Lubricants from chemically modified vegetable oils, Bioresour. Technol. 101 (2010) 245–254.
[20] J. McNutt, Q. He, Development of biolubricants from vegetable oils via chemical modification, J. Ind. Eng. Chem. 36 (2016) 1–12.
[21] S. Dinda, A.V. Patwardhan, V.V. Goud, N.C. Pradhan, Epoxidation of cottonseed oil by aqueous hydrogen peroxide catalysed by liquid inorganic acids, Bioresour. Technol. 99 (2008) 3737–3744.
[22] B.M. Abdullah, J. Salimon, Epoxidation of Vegetable Oils and Fatty Acids: Catalysts, Methods and Advantages, J. Appl. Sci. 10 (2010) 1545–1553.
[23] R. Rinaldi, J. Sepúlveda, U. Schuchardt, Cyclohexene and Cyclooctene Epoxidation with Aqueous Hydrogen Peroxide using Transition Metal-Free Sol-Gel Alumina as Catalyst, Adv. Synth. Catal. 346 (2004) 281–285.
[24] N. Wilde, C. Worch, W. Suprun, R. Gläser, Epoxidation of biodiesel with hydrogen peroxide over Ti-containing silicate catalysts, Microporous Mesoporous Mater. 164 (2012) 182–189.
[25] J. Sepulveda, S. Teixeira, U. Schuchardt, Alumina-catalyzed epoxidation of unsaturated fatty esters with hydrogen peroxide, Appl. Catal. Gen. 318 (2007) 213–217.
[26] C. Orellana-Coca, S. Camocho, D. Adlercreutz, B. Mattiasson, R. Hatti-Kaul, Chemo-enzymatic epoxidation of linoleic acid: Parameters influencing the reaction, Eur. J. Lipid Sci. Technol. 107 (2005) 864–870.
[27] R.A. Sheldon, J.A. Van Doorn, Metal-catalyzed epoxidation of olefins with organic hydroperoxides: I. A comparison of various metal catalysts, J. Catal. 31 (1973) 427–437.
[28] J.K. Satyarthi, D. Srinivas, Selective epoxidation of methyl soyate over alumina-supported group VI metal oxide catalysts, Appl. Catal. Gen. 401 (2011) 189–198.
[29] D. Kahlich, U. Wiechern, J. Lindner, Propylene Oxide, Ullmanns Encycl. Ind. Chem. (2000).
[30] T.W. Findley, D. Swern, J.T. Scanlan, Epoxidation of Unsaturated Fatty Materials with Peracetic Acid in Glacial Acetic Acid Solution, J. Am. Chem. Soc. 67 (1945) 412–414.
[31] N. Prileschajew, Oxydation ungesättigter Verbindungen mittels organischer Superoxyde, Berichte Dtsch. Chem. Ges. 42 (1909).
[31] S. Leveneur, A. Ledoux, L. Estel, B. Taouk, T. Salmi, Epoxidation of vegetable oils under microwave irradiation, Chem. Eng. Res. Des. 92 (2014) 1495–1502.
[33] S.G. Tan, W.S. Chow, Biobased Epoxidized Vegetable Oils and Its Greener Epoxy Blends: A Review, Polym.-Plast. Technol. Eng. 49 (2010) 1581–1590.
[34] S. Sinadinović-Fišer, M. Janković, Z.S. Petrović, Kinetics of in situ epoxidation of soybean oil in bulk catalyzed by ion exchange resin, J. Am. Oil Chem. Soc. 78 (2001) 725–731.
[35] M. Kurańska, H. Beneš, A. Prociak, O. Trhlíková, Z. Walterová, W. Stochlińska, Investigation of epoxidation of used cooking oils with homogeneous and heterogeneous catalysts, J. Clean. Prod. 236 (2019) 117615.
[36] S. Leveneur, Doctoral thesis: Catalytic synthesis and decomposition of peroxycarboxylic acids, Doctoral thesis:, Åbo Akademi University (2009)
[37] R. Mungroo, N.C. Pradhan, V.V. Goud, A.K. Dalai, Epoxidation of Canola Oil with Hydrogen Peroxide Catalyzed by Acidic Ion Exchange Resin, J. Am. Oil Chem. Soc. 85 (2008) 887–896.
[38] K. Dorfner, Ion exchangers, Walter de Gruyter, Berlin; New York, 1991.
[39] Z. Quian, Q. Chen, I.E. Grossmann, Optimal synthesis of rotating packed bed and packed bed: a case illustrating the integration of PI and PSE, 44 (2018) 2377–2382.
[40] P.T. Anastas, J.C. Warner, Green Chemistry: Theory and Practice, Oxford University Press, 1998.

[41] C.R. Strauss, D.W. Rooney, Accounting for clean, fast and high yielding reactions under microwave conditions, Green Chem. 12 (2010) 1340–1344.
[42] H. Mallin, J. Muschiol, E. Byström, U.T. Bornscheuer, Efficient Biocatalysis with Immobilized Enzymes or Encapsulated Whole Cell Microorganism by Using the SpinChem Reactor System, ChemCatChem. 5 (2013) 3529–3532.
[43] S. Caddick, Microwave assisted organic reactions, Tetrahedron. 51 (1995) 10403–10432.
[44] J.L. Zheng, J. Wärnå, T. Salmi, F. Burel, B. Taouk, S. Leveneur, Kinetic modeling strategy for an exothermic multiphase reactor system: Application to vegetable oils epoxidation using Prileschajew method, AIChE J. 62 (2016) 726–741.
[45] F.P. Greenspan, D.G. Mackellar, Analysis of aliphatic per acids, Anal. Chem. 20 (1948) 1061–1063.
[46] The Lubrizol Corporation, Standard test procedure for determining Iodine value. (2006).
[47] R.R. Jay, Direct Titration of Epoxy Compounds and Aziridines, Anal. Chem. 36 (1964) 667–668.
[48] Z.S. Petrović, A. Zlatanić, C.C. Lava, S. Sinadinović-Fišer, Epoxidation of soybean oil in toluene with peroxoacetic and peroxoformic acids — kinetics and side reactions, Eur. J. Lipid Sci. Technol. 104 (2002) 293–299.
[49] R. Turco, R. Vitiello, V. Russo, R. Tesser, E. Santacesaria,.M. Di Serio, Selective epoxidation of soybean oil with performic acid catalyzed by acidic ionic exchange resins, Green Process. Synth. 2 (2013) 427–434.
[50] A. Campanella, M.A. Baltanás, M.C. Capel-Sánchez, J.M. Campos-Martín, J.L.G. Fierro, Soybean oil epoxidation with hydrogen peroxide using an amorphous Ti/SiO_2 catalyst, Green Chem. 6 (2004) 330–334.
[51] A. Campanella, M.A. Baltanás, Degradation of the oxirane ring of epoxidized vegetable oils with hydrogen peroxide using an ion exchange resin, Catal. Today 107–108 (2005) 208–214.
[52] A. Campanella, M.A. Baltanás, Degradation of the oxirane ring of epoxidized vegetable oils in a liquid–liquid–solid heterogeneous reaction system, Chem. Eng. Process. Process Intensif. 46 (2007) 210–221.
[53] S.S. Block, Disinfection, sterilization, and preservation, Lea & Febiger, Philadelphia, 1991.
[54] A. Campanella, M.A. Baltanás, Degradation of the oxirane ring of epoxidized vegetable oils in a liquid–liquid–solid heterogeneous reaction system, Chem. Eng. Process. Process Intensif. 46 (2007) 210–221.
[55] M. Hosseini, N. Stiasni, V. Barbieri, C.O. Kappe, Microwave-assisted asymmetric organocatalysis. A probe for nonthermal microwave effects and the concept of simultaneous cooling, J Org Chem. 72 (2007) 1417–24.
[56] M.Z.C. Lee, T. Marchant, Semi-analytical solutions for continuous-flow microwave reactors, Semi-Anal. Solut. Contin.-Flow Microw. React. 44 (2002) 125–145.
[57] V. Casson Moreno, V. Russo, R. Tesser, M. Di Serio, E. Salzano, Thermal risk in semi-batch reactors: The epoxidation of soybean oil, Process Saf. Environ. Prot. 109 (2017) 529–537.
[58] S. Leveneur, Thermal Safety Assessment through the Concept of Structure–Reactivity: Application to Vegetable Oil Valorization, Org. Process Res. Dev. 21 (2017) 543–550.
[59] P. Patil, V.G. Gude, S. Pinappu, S. Deng, Transesterification kinetics of Camelina sativa oil on metal oxide catalysts under conventional and microwave heating conditions, Chem. Eng. J. 168 (2011) 1296–1300.
[60] S. Leveneur, N. Kumar, T. Salmi, D.Y. Murzin, Stability of hydrogen peroxide during perhydrolysis of carboxylic acids on acidic heterogeneous catalysts, Res. Chem. Intermed. 36 (2010) 389–401.

[61] S. Leveneur, L. Estel, C. Crua, Thermal risk assessment of vegetable oil epoxidation, J. Therm. Anal. Calorim. 122 (2015) 795–804.
[62] X. Cai, J.L. Zheng, A.F. Aguilera, L. Vernières-Hassimi, P. Tolvanen, T. Salmi, S. Leveneur, Influence of ring-opening reactions on the kinetics of cottonseed oil epoxidation, Int. J. Chem. Kinet. 50 (2018) 726–741.
[63] S. Leveneur, J. Wärnå, T. Salmi, D.Y. Murzin, L. Estel, Interaction of intrinsic kinetics and internal mass transfer in porous ion-exchange catalysts: Green synthesis of peroxycarboxylic acids, Chem. Eng. Sci. 64 (2009) 4101–4114.
[64] S. Leveneur, J. Zheng, B. Taouk, F. Burel, J. Wärnå, T. Salmi, Interaction of thermal and kinetic parameters for a liquid–liquid reaction system: Application to vegetable oils epoxidation by peroxycarboxylic acid, J. Taiwan Inst. Chem. Eng. 45 (2014) 1449–1458.
[65] A. Campanella, C. Fontanini, M.A. Baltanás, High yield epoxidation of fatty acid methyl esters with performic acid generated in situ, Chem. Eng. J. 144 (2008) 466–475.
[66] S. Sinadinović-Fišer, M. Janković, O. Borota, Epoxidation of castor oil with peracetic acid formed in situ in the presence of an ion exchange resin, Chem. Eng. Process. Process Intensif. 62 (2012) 106–113.
[67] V.V. Goud, A.V. Patwardhan, S. Dinda, N.C. Pradhan, Kinetics of epoxidation of jatropha oil with peroxyacetic and peroxyformic acid catalysed by acidic ion exchange resin, Chem. Eng. Sci. 62 (2007) 4065–4076.
[68] T.-C. Chou, J.-Y. Chang, Acetic acid as an oxygen carrier between two phases for epoxidation of oleic acid., Chem. Eng. Commun. 41 (1986) 253–266.
[69] L.A. Rios, D. Echeverri, A. Franco, Epoxidation of jatropha oil using heterogeneous catalysts suitable for the Prileschajew reaction: Acidic resins and immobilized lipase, Appl. Catal. Gen. 394 (2011) 132–137.
[70] S. Leveneur, D.Y. Murzin, T. Salmi, J.-P. Mikkola, N. Kumar, K. Eränen, L. Estel, Synthesis of peroxypropionic acid from propionic acid and hydrogen peroxide over heterogeneous catalysts, Chem. Eng. J. 147 (2009) 323–329.
[71] X.X. Zhu, K. Banana, R. Yen, Pore Size Control in Cross-Linked Polymer Resins by Reverse Micellar Imprinting, Macromolecules. 30 (1997) 3031–3035.
[72] E. Monono, D.M. Haagenson, D.P. Wiesenborn, Characterizing the epoxidation process conditions of canola oil for reactor scale-up, Ind. Crops Prod. 67 (2015) 364–372.
[73] S. Miao, P. Wang, Z. Su, S. Zhangad, Vegetable-oil-based polymers as future polymeric biomaterials, Acta Biomater. 10 (2014) 1692–1704.
[74] A.S.A. Hazmi, M.M. Aung, L.C. Abdullah, M.Z. Salleh, M.H. Mahmood, Producing Jatropha oil-based polyol via epoxidation and ring opening, Ind. Crops Prod. 50 (2013) 563–567.
[75] J.C. de Haro, I. Izarra, J.F. Rodríguez, Á. Pérez, M. Carmona, Modelling the epoxidation reaction of grape seed oil by peracetic acid, J. Clean. Prod. 138 (2016) 70–76.
[76] A.P. Chavan, P.R. Gogate, Ultrasound assisted synthesis of epoxidized sunflower oil and application as plasticizer, J. Ind. Eng. Chem. 21 (2015) 842–850.
[77] N. Kim, Y. Li, X.S. Sun, Epoxidation of Camelina sativa oil and peel adhesion properties, Ind. Crops Prod. 64 (2015) 1–8.
[78] W. Li, M. Tian, H. Du, Z. Liang, A new approach for epoxidation of fatty acids by a paired electrosynthesis, Electrochem. Commun. 54 (2015) 46–50.
[79] S. Leveneur, D.Y. Murzin, T. Salmi, Application of linear free-energy relationships to perhydrolysis of different carboxylic acids over homogeneous and heterogeneous catalysts, J. Mol. Catal. Chem. 303 (2009) 148–155.
[80] S. Leveneur, J. Wärnå, T. Salmi, D.Y. Murzin, A review: catalytic synthesis and decomposition of peroxycarboxylic acids, Trends Chem Eng. 13 (2010) 17–52.

[81] M.S. Saha, Y. Nishiki, T. Furuta, A. Denggerile, T. Ohsaka, A new method for the preparation of peroxyacetic acid using solid superacid catalysts, Tetrahedron Lett. 44 (2003) 5535–5537.
[82] S. Leveneur, T. Salmi, D.Y. Murzin, L. Estel, J. Wärnå, N. Musakka, Kinetic Study and Modeling of Peroxypropionic Acid Synthesis from Propionic Acid and Hydrogen Peroxide Using Homogeneous Catalysts, Ind. Eng. Chem. Res. 47 (2008) 656–664.
[83] J.R. Leis, M.A. Kramer, Algorithm 658: ODESSA–an Ordinary Differential Equation Solver with Explicit Simultaneous Sensitivity Analysis, ACM Trans Math Softw. 14 (1988) 61–67.
[84] D.W. Marquardt, An Algorithm for Least-Squares Estimation of Nonlinear Parameters, J. Soc. Ind. Appl. Math. 11 (1963) 431–441.
[85] Handbook of Markov Chain Monte Carlo, CRC Press. (n.d.). https://www.crcpress.com/Handbook-of-Markov-Chain-Monte-Carlo/Brooks-Gelman-Jones-Meng/p/book/9781420079418 (accessed November 1, 2019).
[86] L. Kunigk, D.R. Gomes, F. Forte, K.P. Vidal, L.F. Gomes, P.F. Sousa, The influence of temperature on the decomposition kinetics of peracetic acid in solutions, Braz. J. Chem. Eng. 18 (2001) 217–220.
[87] J. La Scala, R.P. Wool, Effect of FA composition on epoxidation kinetics of TAG, J. Am. Oil Chem. Soc. 79 (2002) 373–378.
[88] Manar El-Sayed Abdel-Raouf; Abdul-Raheim Mahmoud Abdul-Raheim, Rosin: Chemistry, Derivatives, and Applications: a review, BAOJ Chem. 4 (2018) 39.
[89] D.S. McLean, D. Vercoe, K.R. Stack, D.E. Richardson, The colloidal pKa of lipophilic extractives commonly found in Pinus radiata, Appita J. 58 (2005) 362–366.
[90] A.-L. Brocas, A. Llevot, C. Mantzaridis, G. Cendejas, R. Auvergne, S. Caillol, S. Carlotti, H. Cramail, Epoxidized rosin acids as co-precursors for epoxy resins, Des. Monomers Polym. 17 (2014) 301–310.
[91] M. Shiraiwa, U. Pöschl, D.A. Knopf, Multiphase Chemical Kinetics of NO3 Radicals Reacting with Organic Aerosol Components from Biomass Burning, Environ. Sci. Technol. 46 (2012) 6630–6636.
[92] P. Chauhan, H. Chen, S. Roy Goswami, N. Yan, Improved mechanical properties of flexible bio-based polymeric materials derived from epoxy mono/di-abietic acid and soyabean oil, Ind. Crops Prod. 138 (2019) 111437.
[93] P. Gamage, M. O'Brien, L. Karunanayake, Epoxidation of some vegetable oils and their hydrolysed products with peroxyformic acid - Optimised to industrial scale, J. Natl. Sci. Found. Sri Lanka. 37 (2009) 229–240.
[94] T.T. Kouroosh Saremi, Epoxidation of Soybean Oil, Sch. Res. Libr. 3 (2012) 4254–4258.
[95] D. Favero, V.R.R. Marcon, T. Barcellos, C.M. Gómez, M.J. Sanchis, M. Carsí, C.A. Figueroa, O. Bianchi, Renewable polyol obtained by microwave-assisted alcoholysis of epoxidized soybean oil: Preparation, thermal properties and relaxation process, J. Mol. Liq. 285 (2019) 136–145.
[96] A.B. Kousaalya, S.D. Beyene, B. Ayalew, S. Pilla, Epoxidation Kinetics of High-Linolenic Triglyceride Catalyzed by Solid Acidic-Ion Exchange Resin, Sci. Rep. 9 (2019) 8987.
[97] A. Campanella, M.A. Baltanás, Degradation of the oxirane ring of epoxidized vegetable oils in liquid-liquid systems: I. Hydrolysis and attack by H2O2., Lat. Am. Appl. Res. 35 (2005) 205–210.
[98] S. Leveneur, C.A. de Araujo Filho, L. Estel, T. Salmi, Modeling of a Liquid–Liquid–Solid Heterogeneous Reaction System: Model System and Peroxyvaleric Acid, Ind. Eng. Chem. Res. 51 (2012) 189–201.

[99] M.G. Evans, N. Uri, The dissociation constant of hydrogen peroxide and the electron affinity of the HO_2 radical, Trans. Faraday Soc. 45 (1949) 224–230.
[100] K. Sue, F. Ouchi, K. Minami, K. Arai, Determination of Carboxylic Acid Dissociation Constants to 350 °C at 23 MPa by Potentiometric pH Measurements, J. Chem. Eng. Data. 49 (2004) 1359–1363.
[101] D.A. Knopf, B.P. Luo, U.K. Krieger, T. Koop, Thermodynamic Dissociation Constant of the Bisulfate Ion from Raman and Ion Interaction Modeling Studies of Aqueous Sulfuric Acid at Low Temperatures, J. Phys. Chem. A. 107 (2003) 4322–4332.

ISBN 978-952-12-3894-9 (printed version)
ISBN 978-952-12-3895-6 (electronic version)
ISSN 2669-8315 (*Acta technologiae chemicae Aboensia 2019 A/2*)

Painosalama Oy Turku/Åbo 2019